Max-Planck-Institut für Kolloid- und Grenzflächenforschung

Multi-Component Protein Films by Layer-by-Layer: Assembly and Electron Transfer

Dissertation
zur Erlangung des akademischen Grades
"doctor rerum naturalium"
(Dr. rer. nat.)
in der Wissenschaftsdisziplin "Physik"

eingereicht an der
Mathematisch-Naturwissenschaftlichen Fakultät
der Universität Potsdam

von
Roman Dronov

Potsdam, den 28 November 2007

"As a rule, what is out of sight disturbs men's minds more seriously than what they see"

Julius Caesar

Acknowledgements

This project would have been impossible without the advice, support and criticism from a broad group of people. First of all, I am grateful for having Profs. Helmuth Möhwald, Fred Lisdat, Frieder Scheller and Dr. Dirk G. Kurth as my advisors. Co-advised projects can easily become a nightmare, swamped in conflicts and with the student struggling in the middle. Helmuth Möhwald, Fred Lisdat and Frieder Scheller have an exceptional working relationship, which allowed me to gain a lot from the interplay between the different research programs. I appreciate the freedom and space they gave me and their tolerance in my effort to pursue the thesis both during the times when the research was in its difficult stages and when it was going smoothly. I thank Frieder Scheller for his inestimable constant support and good nature, which helped he throughout the whole project and, especially in its final stage. I thank Helmuth Möhwald for his invaluable advice, especially in the beginning of this Ph.D project, for the opportunity to work at the MPI of Colloids and Interfaces, and his enthusiasm and clear vision. He always managed to see through my sometimes convoluted thinking. I thank Dirk Kurth for his immense help in seeing new perspectives in my "very ordinary" data, as well as in scientific writing and handling public talks. It has always been effective keeping me working on my "B-Game"! I thank Fred Lisdat for the immense professional guidance he offered throughout the whole course of my Ph.D project, his extensive support and valuable advice. He has always been an inexhaustible source of ideas. It is impossible to overrate the value of our short and not-so-short discussions in order to advance a little bit further in untangling the mysteries of the lab research.

I also thank the members of my thesis committee and the referees of my thesis for critical reading of my work.

I thank my former and current lab mates in the AG-Kurth at the MPI and AG-Scheller at the Uni-Potsdam whom I learned a great deal from and who made the routine of the lab work much fun. From the AG-Lisdat: Franziska Wegerich, Dr. Thomas Balkenhohl, Dr. Andrey Krylov, Jan Kafka, Dr. Oliver Pänke, Daniel Schäfer, Andreas Kapp, Dr. Martin Weigel, Dr. Moritz Beissenhirtz, and all the colleagues from the department of Analytical Biochemistry. From the AG-Kurth: Naoko Miyashita, Guntram Schwarz, Torsten Sievers, Annika Vergin, Viviane Friese, Dr. Sabine Fuchs, Dr. Yves Bodenthin, Dr. Jesus Pitarch Lopez, Dr. Matthias Beinhoff, Dr. Hongwei Duan, Anne Lindner, and all my colleagues and friends from the MPI. In particular, I want to thank Dr. Moritz Beissenhirtz for giving me a smooth start on my way to protein multilayers at the time when it was really necessary, Dr. Jiří Žeravic for a practical crash-course on QCM, Carsten Teller for occasionally lending me QCM crystals, Dr. Walter Stöcklein for help with SPR, Dr. Jan Halamek and Raj Kumar for laboratory philosophy. I also would like to acknowledge a considerate assistance of Anneliese Heilig in AFM, as well as evaporation

of tremendous amounts of gold on numerous silicon wafers to take the ultra flat Au electrodes to the next level of perfection.
Due to the interdisciplinary nature of the project, I benefited to a large extent from the International Max Planck Research School on Biomimetic Systems (IMPRS) offering essential specialized training given by the best scientists in the field, coordinated by Dr. Angelo Valleriani.
I thank the European taxpayers for financial support via the Marie Curie program "Early Stage Training on Biomimetic Systems" MEST-CT-2004-504465, which I gratefully acknowledge. This project has been more than just a group of people working on similar topics. It helped most of us to feel a spirit of collaboration and establish first scientific connections. In particular, I would like to thank Dr. Kirstine Berg-Sørensen of the Technical University of Denmark for accommodating me at her group during my short visit within "Marie Curie Stay Abroad".

I also thank a former scientific officer of the European Commission Carmela Di Santo who was responsible for the Marie Curie program "Early Stage Training on Biomimetic Systems" specifically for allowing me to have a part of the "Marie Curie Stay Abroad" at the University of Natural Resources and Applied Life Sciences, Vienna, in the Nanobiotechnology group. I thank all members of the group of Prof. Uwe B. Sleytr for being wonderful hosts and making everything to make my stay as fruitful and unforgettable as it was. During this time I learned a lot about S-layers and AFM measurements in liquid from Jacqueline Friedmann, whom I also would like to thank for a great time at "Lange Nacht der Musik"!

A part of the project was carried out in collaboration with Prof. Peter Hildebrandt at the Max-Volmer-Laboratorium of the Technical University of Berlin. This part would have been impossible without a practical expertise in Raman spectroscopy of Dr. Daniel H. Murgida and Jana Grochol.

In addition, I would like to acknowledge Profs. Silke Leimkühler, Ulla Wollenberger and my good friend Roberto Spricigo for support and very stimulating in-house collaboration, which made it possible to give more answers to open questions on inter-protein electron transfer.

No matter that the research here was as good as it gets, it was the group of people that I met along the way who made MPI, Potsdam University, and Golm a second home.

I also thank my undergraduate mentor Dr. Larisa A. Bityutskaya and my friends from her group at the University of Voronezh. Besides their support and friendship, they set an important example for me early in my research career by their work ethics and the supportive environment they created in this group.

Finally, I'd like to thank my parents Vasily Dronov and Liubov Dronova, and my sister, Natalia for their support and love. I dedicate this thesis to my parents who have always believed in me and instilled in me a great confidence.

List of Abbreviations

DET	Direct electron transfer
SAM	Self-assembled monolayer

Proteins

Cyt.c	Cytochrome c
XOD	Xanthine oxidase
BOD	Bilirubin oxidase
SOx	Sulfite oxidase

Chemicals

MUA	11-Mercaptoundecanoic acid
MU	11-Mercaptoundecanol
PASA	Poly(anilinesulfonic acid)
PSS	Poly(styrenesulfonic acid)
PAH	Poly(allylamine hydrochloride)
PEI	Poly(ethyleneimine)

Methods

CV	Cyclic voltammetry
AFM	Atomic force microscopy
QCM	Quartz crystal microbalance
SPR	Surface plasmon resonance
LbL	Layer-by-Layer
LB	Langmuir-Blodgett

Units

Da	Dalton
M	Molar
A	Ampere
V	Volt
k	kilo- (10^{3})
m	mili- (10^{-3})
μ	micro- (10^{-6})
n	nano- (10^{-9})

Table of Contents

2. Introduction

2.1. State of the art

Electron transfer phenomena in proteins represent one of the most common types of biochemical reactions. They play a central role in energy conversion pathways in living cells, primarily in respiration and photosynthesis. These complex biochemical reaction cascades consist of a series of proteins and protein complexes that couple a charge transfer to other forms of chemical energy. The efficiency and sophisticated optimisation of signal transfer in these natural redox chains has inspired engineering of artificial architectures mimicking essential properties of their natural analogues.

Such protein assemblies with the ability to perform selective signal transduction have application potential in biosensors, bioelectronics and biofuel cells. Confinement of the biological catalytic reactions to electrode surfaces has been a central paradigm for the development of enzyme electrodes and biosensors.

Implementation of direct electron transfer (DET) in protein assemblies was a breakthrough in bioelectronics, providing a simple and efficient way of coupling biological recognition events to a signal transducer. DET avoids the use of redox mediators, reducing potential interferences and side reactions, as well as being more compatible with in vivo conditions. However, only a few haem proteins, including the redox protein cytochrome c (cyt.c), and blue copper enzymes show efficient DET on different kinds of electrodes, including gold, highly oriented pyrolytic graphite, and glassy carbon electrodes.

Many studies report on arrangement of cyt.c at different electrode surfaces. Considerable efforts were done towards investigations of heterogeneous electron transfer processes between monolayers of this redox protein and gold electrodes. Cyt.c immobilized in a monolayer film on a surface of a promoter gold electrode shows a quasi-reversible one electron transfer. It was also found that a cyt.c monolayer can efficiently oxidize superoxide radicals and, thus, serve as a third generation biosensor.

An important advance was made by going beyond the monolayer coverage by electrostatic layer-by-layer self-assembly, leading to an extensive increase in the surface protein density. A number of protein multilayer designs have been reported, all of which are stabilized by a polyelectrolyte matrix. Usually the scaffolding matrix is composed of an electrochemically inert polymer which keeps the arrangement together.

The layer-by-layer approach is suitable for precise tuning of the protein concentration on the electrode, while the polyelectrolyte provides a bio-compatible matrix maintaining the activity of the biomolecules. The ease of fabrication, the stability, and the controllable permeability of the polyelectrolyte multilayers make them particularly attractive for electroanalytical applications.

For a multilayer arrangement combining cyt.c and sulfonated polyaniline as a counter polyelectrolyte it was for the first time shown that electroactive multilayers of a redox protein could be prepared. These multilayers containing up to 15 protein layers showed a quasi-reversible electron transfer with a formal potential corresponding to a value found for a cyt.c monolayer.

The mechanism behind the electron transport over long distances in cyt.c/PASA multilayers has been an intriguing question. Electron exchange between the cyt.c molecules was proposed as a dominating mechanism, however, the role of the polymer in the electron transfer process has not been solved completely.

2.2. Aim of this study

The aim of this work was to

● establish and characterize surface-confined inter-protein electron transfer reactions in novel protein multilayer electrodes combining cyt.c with enzymes;

● develop the protocol for the construction of the multilayer assemblies integrating two different protein species;

● design, implement and characterize the "analyte-enzyme-protein-electrode" redox cascades mimicking natural protein interaction via mediated and direct electron transfer;

● elucidate the electron transfer mechanisms through protein multilayer films and verify the role of the polyelectrolyte in this process;

● combine the protein multilayer assembly approach with the S-layer protein recrystallization technique as a complex 'molecular construction kit'.

In the first part of the work the cyt.c/PASA multilayer assembly – used in this thesis as a basic system – shall be characterized with respect to the electron transfer mechanism and the redox behavior of the polyelectrolyte by SERRS. The formation of the cyt.c/PASA multilayer shall be investigated on ultra-flat gold surfaces throughout the intermediate assembly stages by AFM.

In the second part of the work the concept of inter-molecular electron exchange shall be employed for protein/polyelectrolyte multilayers integrating cyt.c with enzymes, demonstrating two principle ways for the design of coupled redox cascades: via mediated and direct electron exchange between two surface-confined proteins.

The third part of the work would demonstrate a new, original method for the layer-by-layer assembly of counter-charged proteins avoiding the use of a polyelectrolyte. This approach is expected to shed more light on the electron transfer phenomena between surface-confined proteins, and should verify the role of the polyelectrolyte matrix in the basic cyt.c/PASA system.

Finally, the technique of the S-layer recrystallization shall be combined in a complementary way with the protein layer-by-layer assembly. These hybrid multilayer systems shall be characterized with respect to the topology of the surface layer and electroactivity of the encaged protein multilayer.

2. Literature Digest

The current chapter gives a brief overview of the modern understanding of the biosensor approach, with an emphasis on electrochemical biosensors and third generation devices based on direct electron transfer provided along with an essential information about the proteins used in this work. Special attention is paid to layer-by-layer self assembly and its application in design of electrochemical biosensors, summarizing recent developments in this leading edge approach. Finally, an introduction on bacterial surface layer proteins and its recrystallyzation technique shall provide the reader with the basics of an alternative approach for design of protein layers, which was also employed in the current study.

2.1. Biosensors

Bioelectronics is an interdisciplinary science based on interplay of electronics and biochemistry as well as physical chemistry and electrochemistry. The first step in this direction has been the development of biosensors. The concept of biosensors, formulated in the sixth decade of the twentieth century has constantly been evolving, employing new concurrently developing techniques and approaches, broadening its frameworks and establishing new paradigms. Nowdays this field is rapidly expanding with a global biosensor market value of some $5 billion in 2003, which has increased from around $2 billion in 2000 (Bogue 2005).

The primary demands are coming from the health-care, including medical diagnostics, but also from the other areas, such as food quality control, environmental monitoring and bio-defense applications. There is a vast market expansion potential with suggested annual growth rate of 10% (MindBranch 2004).

2.1.1. Biosensors' ABC

A biosensor[i] is an analytical device integrating a biological recognition element with a suitable transducer, translating a chemical signal of a recognition reaction into a measurable electronic response (Thevenot, Toth et al. 2001). A large variety of biological

[i] Due to discrepancy in definition, sometimes this term is assigned for the sensor devices used to determine the concentration of biologically relevant substances, even if they don't directly utilize a biological system. This definition will not be used in this work.

entities can be used as a recognition element, including enzymes, antibodies, receptors, nucleic acids and cells. A signal transducer is a crucial part of a biosensor design, converting a physical magnitude, changing during the biological recognition process, into an electronic signal.

Along with electrochemical transducers, which are currently among the most popular ones, many types of gravimetric, optical, calorimetric devices have been employed. Recognition elements of different kinds can be combined with various types of transducers resulting in a wide variety of possible biosensor designs. In Table 2.1 typical transducers are given which can be used with corresponding recognition elements.

Table 2.1. Common biological recognition elements, type of interaction with an analyte, and possible trasducers (Scheller, Wollenberger et al. 2001)

Recognition element	**Interaction with analyte**	**Type of transducer**
Enzyme	catalysis	electrochemical, optical, calorimetric
Antibody	binding	direct: gravimetric, optical, calorimetric; indirect: via electrochemical or optical marker
Nucleic acid	hybridization	direct: electrochemical, gravimetric, optical,; indirect via marker
Receptor	binding	optical, conductometric

One of the most widely used ways for the signal readout is via an optical transducer. Most often an optical fiber or optical fiber bundles are used as a platform for the recognition element, and as a conduit for excitation light and the resultant signal. The detection methods include absorbance, reflectance, fluorescence, chemiluminescence, evanescent wave, and surface plasmon resonance.

Optical immunosensors have been the subject of detailed research, ranging from detection of specific analytes to broad immunoassay systems for general use (Wolfbeis 2002; Monk and Walt 2004). Four kinds of immunoassays can be employed: direct,

competitive, binding inhibition and sandwich (Marazuela and Moreno-Bondi 2002). These methods would typically require the immobilization of the primary antibody to the surface and the use of an optical label.

Enzyme based optical fiber biosensors represent the most common type of optical fiber biosensors (Kuswandi, Andres et al. 2001; Wolfbeis 2002; Epstein and Walt 2003) due to inherited selectivity that enzymes have for a specific analyte. Most common detection methods for the enzyme fiber biosensors are absorbance and reflectance, while the fluorescent detection is not often used (Monk and Walt 2004). At the same time, chemiluminescence is used for detection of H_2O_2 formed by an enzymatic process, which has an advantage, since no excitation light source is required.

A nucleic acid optical fiber biosensor requires immobilization of a single stranded probe sequence on the surface of the optical substrate. This probe sequence is allowed to bind a fluorescently labeled target sequence of interest. Label-free detection, however, is also possible (Marazuela and Moreno-Bondi 2002; Wolfbeis 2002; Epstein and Walt 2003).

Optical transducers have also been used for simultaneous detection of analytes in microarray biosensing of DNA or proteins. Microarrays are made by immobilization of a high density of biologically relevant moieties into discrete spatial arrangements (with a spot size from 10 to 500 μm). The probe molecules are used to trap target molecules through specific interactions (Bally, Halter et al. 2006).

The most straightforward method to characterize a binding process is registering a mass change by a piezoelectric microbalance. Here quartz crystals are used as oscillators vibrating under the influence of an electric field. Each crystal has a characteristic resonance frequency, which depends on its geometry, and changes upon binding of molecules at the surface of the crystal (proportionally to the mass loading up to about a 2% of mass change). A review by P. Skladal, focusing on piezoelectric biosensors, demonstrates that a large variety of analytes can be measured by this technique, including viruses, bacteria, proteins, nucleic acids and small molecules. The author also discusses the influence of additional effects introduced by conformational changes of attached biolayers in contact with solution (Skladal 2003).

A novel mechanical transduction mechanism is represented by microcantilevers. This approach is based on the AFM technique, providing an extremely versatile method

e.g. for measuring directly avidin-biotin binding (Florin, Moy et al. 1994; Lee, Kidwell et al. 1994), antigen-antibody interaction (Dammer, Hegner et al. 1996; Hinterdorfer, Baumgartner et al. 1996; BrowningKelley, WaduMesthrige et al. 1997), and hybridization of complementary DNA strands (Lee, Kidwell et al. 1994). Microcantilevers transduce a number of different kinds of physical signal: mass, temperature, heat, electromagnetic field, stress into mechanical deformation with sub-angstrom resolution (Raiteri, Grattarola et al. 2001). As force sensors they allow measurements at the single molecule level (Florin, Moy et al. 1994; Ros, Schwesinger et al. 1998).

Many enzyme-catalyzed reactions occur with concurrent evolution of heat (Spink and Wadso 1976), offering a convenient basis for measuring the reaction rate, which has been widely used in design of biosensors (Xie, Ramanathan et al. 2000; Ramanathan, Jonsson et al. 2001). The heat change is usually measured by a thermistor at the inlet and the outlet of the reactor with immobilized enzyme. In table 2.2. typical values of the enthalpy change are given for some enzyme reactions.

Table 2.2. Molar enthalpies of enzyme catalyzed reactions (NIST).

Analyte	**Enzyme**	**ΔH, kJ mol^{-1}**
H_2O_2	Catalase	-(207..223)
Glucose	Glucose oxidase	-(125..233)
Urea	Urease	-(16..61)
Cholesterol	Cholesterol oxidase	-(114..214)
Peptides	Trypsin	-(1..47)
Starch	Amylase	-4.5

Another well implemented approach for construction of biosensors, is to use potentiometric transducers to correlate a biological reaction with an electrical signal. Usually these sensors use ion-selective (e.g. pH-) electrodes with an immobilized enzyme (Pranitis, Teltingdiaz et al. 1992). The catalyzed reaction generates or absorbs hydrogen ions, whose concentration is monitored by an ion-sensitive probe. In order not to interfere with the reaction, the electrical potential is determined at devices with very high impedance allowing effectively zero current flow. The response of an ion-selective electrode is given by equation 2.1.

$$E=E_k+RT/zF \cdot \ln([i]) \quad (2.1)$$

where E is the measured potential (in volts), E_k is a characteristic constant for the ion-selective/reference electrode system, R is the gas constant, T is the absolute temperature (K), z is the signed ionic charge, F is the Faraday constant, and [i] is the concentration of the free uncomplexed ionic species.

A special class of ion-selective electrodes are ion-selective field effect transistors (ISFETs), which found application in biosensors as enzyme-linked field effect transistors (ENFETs) (Barbaro, Colapicchioni et al. 1992; Colapicchioni, Barbaro et al. 1992; Shulga, Koudelkahep et al. 1995; Sandifer and Voycheck 1999; Dzyadevych, Soldatkin et al. 2003). Enzyme membranes are coated on the ion-selective gates of these electronic devices. Such a biosensor responds to the electrical potential change via the current output. The main advantage of such devices is their extremely small size and integrated circuit technology allowing cheap mass-production. Recently, a new type of field effect transducer based on carbon nanotubes (Allen, Kichambare et al. 2007), silicon and conducting polymer nanowires (Wanekaya, Chen et al. 2006) has been employed for construction of potentiometric biosensors.

Amperometric biosensors are based on another class of electrochemical transducers, which generate current when a constant potential is applied. Simple amperometric biosensors are based on the Clark oxygen electrode, consisting of a platinum cathode at which oxygen is reduced and a Ag/AgCl reference electrode. At a potential of -0.6 V (vs. the Ag/AgCl) applied to the platinum cathode, a current proportional to the oxygen concentration is produced. After a pioneering suggestion by Clark and Lyons (Clark and Lyons 1962) of using enzyme-containing membranes coupled to these electrodes, Updike and Hicks (Updike and Hicks 1967; Updike and Hicks 1967) made a further development by using two oxygen electrodes, one of which coupled with an enzyme (glucose oxidase, GOx) and measuring the differential current, thus eliminating oxygen background variation. An enzyme electrode for determination of blood glucose described by Guilbault and Lubrano in 1973 was based on anodic monitoring of liberated hydrogen peroxide (Guilbaul.Gg and Lubrano 1973).

$$\text{glucose} + O2 \rightarrow \text{gluconic acid} + H_2O_2 \quad (2.2)$$

$$H_2O_2 \rightarrow O_2 + 2H^+ + 2e^- \quad (2.3)$$

A large number of amperometric enzyme electrodes, differing in design, material, membrane composition, or immobilization procedures have since been described. Further developments have been achieved by replacing the oxygen with a synthetic electron acceptor (a redox mediator), performing electron transfer from the redox center of the enzyme to the electrode surface. This approach received particular attention for construction of glucose biosensors, where the compounds, such as ferrocene derivatives, ferricyanide, conducting organic salts or quinone, have been employed to shuttle the electrons between the FAD center and the surface according to eq. 2.4-6:

$$\text{glucose} + GOx_{(ox)} \rightarrow \text{gluconic acid} + GOx_{(red)} \quad (2.4)$$

$$GOx_{(red)} + 2M_{(ox)} \rightarrow GOx_{(ox)} + 2M_{(red)} + 2H^+ \quad (2.5)$$

$$2M_{(red)} \rightarrow 2M_{(ox)} + 2e- \quad (2.6)$$

where M (ox) and M (red) are the oxidized and reduced forms of the mediator. The current produced in such a mediation cycle is proportional to the glucose concentration. However, a more advanced method to measure an amperometric signal is to have no mediator, but an electrode with which an enzyme is able to exchange electrons directly. These three approaches represent three generations of biosensors.

Generally, first generation biosensors rely on diffusion of the normal product of the reaction towards the transducer, where it generates the response current by undergoing redox transformations. Second generation biosensors use artificial redox mediators to transfer electrons between the main catalytic reaction and the transducer, while third generation biosensors represent a class of devices where the response current is generated by direct electron transfer (DET) between the enzyme and the electrode, without direct involvement of any diffusive product or a mediator.

2.1.2. Biosensors Based on Direct Electron Transfer of Redox Proteins

The most promising approach in development of electrochemical biosensors is to establish a direct electron communication between the biomolecules and the electrode surface (Freire, Pessoa et al. 2003; Murphy 2006). Despite some fundamental restrictions in establishing DET, this type of biosensors has a great potential for the development of new approaches and devices. The principle advantage offered by the third generation biosensors is the development of simple analytical tools (reagentless sensors) with high sensitivity, due to a close integration of the biological recognition element to a signal transducer, and high selectivity due to specificity of interaction between the biomolecules and their substrates.

In addition, under such conditions the electrode operates in a potential window closer to the redox potential of the enzyme, thus reducing possible interference (Gorton 1995).

The main limiting factor for the development of the third generation biosensors is the inability for many proteins to establish direct electrical communication with electrodes, or special conditions have to be fulfilled, e.g. modification of the electrode. Therefore designing new electrode surface functionalization, searching for new proteins with direct electron transfer properties, and genetic modification have been the strategies, extensively explored in recent decades. According to the Marcus theory, the electron transfer rate between the two redox sites depends on the potential difference and the distance between these centers (Marcus and Sutin 1985; Marcus 1993).

$$k_{ET} = 2\pi/h \mid H_{DA}\mid^2 FC \qquad (2.7a)$$

$$FC = 1/(4\ \pi\lambda k_b T)^{1/2} \exp[-(\Delta G_0+\lambda)^2/4\ \lambda k_B T] \qquad (2.7b)$$

$\mid H_{DA}\mid^2$ decreases exponentially with separation distance for many systems, therefore

$$k(r)\nu = 2\pi/h \cdot 1/(4\ \pi\lambda k_B T)^{1/2} \mid H_{DA}\mid^2 \qquad (2.7c)$$

$$k(r)\nu = 10^{13} \exp\ [-\beta(r-r_0)]\ s^{-1} \qquad (2.7d)$$

here k_{ET} is the direct electron transfer rate, FC – Franck-Condon factor, r_0 and r are the minimal and actual electron donor-acceptor distance, respectively. β is a decay parameter depending on the molecular structure, λ is reorganization free energy, and ΔG_0 is the reaction free energy.

In the case when $\lambda = -\Delta G_0$ the reaction proceeds with its maximal rate, with a maximal rate constant k_s. Values for k_s can be found experimentally by measuring the rate constant for a reaction under different conditions.

In the case, when the prosthetic group of the protein molecule is well insulated by the protein shell, DET with a high electron transfer rate is unlikely due to the exponential decrease of the tunneling probability with the increase of distance between the redox centers. Hence, the probability of DET between protein and the electrode surface depends on their relative spatial orientation, and, in turn, on the immobilization protocol. Voltammetry of surface-confined proteins (protein film voltammetry, PFV) is a recognized way to investigate the coupling of protein electron transfer to chemical reactions (Armstrong, Heering et al. 1997). Usually, the proteins are adsorbed on the electrode surface with similar orientation, guided by the surface properties of the electrode. In this case the diffusion restriction and slow kinetics of protein-surface interaction at the electrode are eliminated.

One of the most commonly used materials for establishing DET of proteins and enzymes is carbon. Many attempts of protein DET at carbon electrodes, including glassy carbon, spectroscopic graphite, and highly oriented pyrolytic graphite electrodes have been successful. Coupling of the redox protein to carbon electrodes usually does not induce adsorptive denaturation in contrast to metal electrodes. DET of haem proteins, such as myoglobin, hemoglobin, cytochrome c and copper enzymes have been extensively studied on carbon electrodes (Freire, Pessoa et al. 2003; Christenson, Dimcheva et al. 2004; Shleev, El Kasmi et al. 2004; Shleev, Tkac et al. 2005).

Self-assembled monolayers (SAMs) also represent a suitable system for mimicking biointerfaces (Ulman 1996; Wink, vanZuilen et al. 1997). Redox proteins immobilized on SAMs by physisorption or covalent immobilization display difusionless electron transfer processes. The distance between the protein active site and the electrode can be regulated by varying the chain length of self-assembling molecules. Moreover, this method allows

easy tuning of the surface charge by mixing molecules with different moieties at the terminus. First reports on surface modification with organic adsorbents to promote diffusion-controlled electrochemistry of cytochrome c (cyt.c) (Taniguchi, Toyosawa et al. 1982; Taniguchi, Toyosawa et al. 1982; Allen, Hill et al. 1984) stimulated further efforts in investigation of SAMs. Some blue copper enzymes were demonstrated to have DET on gold electrodes modified with animo- and carboxy-terminated alkanethiols (Shleev, Tkac et al. 2005).

Many proteins function in nature while being bound to membranes. For over four decades the approach of protein immobilization into surfactant or lipid bilayer films has been in practice, providing conditions for membrane proteins close to natural environment. However, this approach has been also used to immobilize non-membrane proteins. Bayachou et al. reported direct electrochemistry of myoglobin in films of dimethyldidodecylammonium bromide (DDAB) on graphite electrodes, catalyzing electrochemical reduction of nitrous oxide (N_2O) and azide (N_3^-) in aqueous solutions (Bayachou, Elkbir et al. 2000). In addition, reversible direct electron transfer of the photosystem I (PS I) reaction center has been established in lipid films for the first time: two reversible redox couples were observed for native PS I in dimyristoylphosphatidylcholine films (Munge, Das et al. 2003).

A simple way to study direct protein electrochemistry is via its entrapment in a sol-gel matrix. Under such conditions the protein is hydrated in the bathing buffer in a macroscopic environment similar to the protein aqueous solution. Rusling et al. reported a study on electrochemistry of hemoglobin and myoglobin in a composite sol-gel matrix with template additives (surfactants, Nafion, PSS) (Nadzhafova, Zaitsev et al. 2004; Lu, Yang et al. 2006). Ray et al. reported direct electrochemistry and the determination of the redox potential of myoglobin in a pure sol-gel matrix. It was shown by UV-vis and Raman spectroscopy (Ray, Feng et al. 2005) that the protein remained in the native form. This approach was also adopted in the biosensor designs (Nocek, Hatch et al. 2002; Samuni, Dantsker et al. 2002; Navati, Ray et al. 2004).

Conductive and non-conductive nanoscale materials, such as carbon nanotubes, Au, SiO_2, TiO_2 colloids have been co-immobilized with proteins in order to establish DET reactions (Lvov, Munge et al. 2000; Li, Luo et al. 2001; Topoglidis, Campbell et al. 2001; Willner 2002; Zhou, Hu et al. 2002). Au nanoparticles have been shown to facilitate

favorable orientation of the protein and to establish conducting channels between active site of the protein and the electrode (Zhao, Henkens et al. 1992). Carbon nanotubes, characterized by high conductivity, stability and mechanical strength, have been widely explored as an electrode material in electrochemical reactions due to their ability to promote electron transfer reactions. Since the first attempts to use multi-wall carbon nanotubes (MWNT) to realize direct electrochemistry of proteins by Hill and co-workers (Davis, Coles et al. 1997), carbon nanotubes have been extensively investigated (Wang, Xu et al. 2002; Wang, Li et al. 2002; Wang, Zhang et al. 2003). Direct electrochemistry of the microperoxidase MP-11 redox center has been shown on gold electrodes modified with single wall carbon nanotubes (SWNT) by Gooding et al. (Gooding, Wibowo et al. 2003). SWNTs were fixed at the surface by forming amide bonds with a cysteamine promoter. The authors show, that shortened SWNTs aligned normally to the electrode surface. Microperoxidase MP-11 was adsorbed to the free ends of the SWNTs by incubation in HEPES buffer.

In addition to conductive nanomaterials, non-conductive metal oxides (Xu, Wang et al. 2002; Zhang, He et al. 2004), SiO_2, NiO (Salimi, Sharifi et al. 2007) and other metal oxide colloids have been extensively employed to enhance the electron transfer properties between the electrodes and enzymes. However, the DET enhancement mechanism for such materials is still not completely understood.

Recently, a novel approach to establish DET of redox proteins and enzymes has been proposed, using DNA as a promoter or as a matrix. It can be considered that DNA provides biocompatible microenvironments for the immobilized enzyme molecules, prevents its denaturation, and amplifies the surface coverage, acting as a charge carrier thus facilitating electron transfer. Several groups reported on DNA-facilitated immobilization of HRP for H_2O_2 biosensor design (Song, Wang et al. 2006; Wang, Yuan et al. 2007). Fan et al reported a third generation biosensor for nitric oxide based on hemoglobin-DNA films on pyrolytic graphite electrodes with detection limit of 2.9 μM (Fan, Li et al. 2000). In addition, Li et al. for the first time report on establishing direct conversion of the Mo-center of xanthine oxidase on DNA-modified pyrolytic graphite electrodes (Liu, Peng et al. 2005).

2.2. Electrochemistry of Proteins and Enzymes

2.2.l. Cytochrome c

A heme protein Cytochrome c (cyt.c), found in the inner mitochondria membrane, is responsible for electron transfer from cytochrome c reductase (complex III) to cytochrome c oxidase (complex IV) and is an essential component of the mitochondrial respiratory chain. This water soluble protein has a molecular mass of about 12 kDa and is composed of a single polypeptide chain of 104 amino acid residues with an iron-containing haem prosthetic group. The iron ion can be in the oxidized (ferric, Fe^{3+}) or the reduced (ferrous, Fe^{2+}) form and is the actual electron carrier. The binding mechanism of cyt.c to its reaction partners has been studied by mutating the protein (Dopner, Hildebrandt et al. 1999). The crucial role in the electron transfer between cyt.c and its reaction partners within the respiratory chain is assigned to its asymmetric spatial charge distribution (Brautigan, Fergusonmiller et al. 1978; Brautigan, Fergusonmiller et al. 1978; Fergusonmiller, Brautigan et al. 1978; Kang, Brautigan et al. 1978). The lysine residues located in the haem vicinity introduce positive charge into this part of the protein, which determines its binding affinity towards the reaction partners. Substitution of these lysine residues by other amino acids weakens the binding between cyt.c and cytochrome c oxidase. Apart from its main physiological function, cyt.c can catalyze several reactions, (hydroxylation and aromatic oxidation), has a peroxidase activity (oxidation of 2,2-azino-bis(3-ethylbenzthiazoline-6-sulphonic acid) (ABTS), 2-keto-4-thiomethyl butyric acid and 4-aminoantipyrine), and is able to exchange electrons with other cyt.c molecules with a self-exchange rate in the order of 10^3 $M^{-1}s^{-1}$ (Gupta 1973; Dryhurst and Kadish 1982).

Being in focus of electrochemical research for decades, cyt.c is now one of the most characterized redox proteins. It has been often used as a model system for experiments on protein electrochemistry due to its moderate molecular weight, good water solubility, relatively low cost, and, most importantly, the electron transfer properties, determined by a partially-exposed haem moiety (Stellwagen and Cass 1975).

It was shown that cyt.c strongly adsorbs to Pt, Hg, Au, Ag electrodes, however, this adsorption entails significant conformation changes of the protein and often leads to denaturation (Hinnen, Parsons et al. 1983; Reed and Hawkridge 1987). The effect of denaturating adsorption can be avoided by using promoter modification of the electrode surfaces. Many examples of horse heart cyt.c votammetric studies on chemically modified

electrodes have been described (Eddowes and Hill 1977; Taniguchi, Murakami et al. 1982; Taniguchi, Toyosawa et al. 1982; Armstrong, Bond et al. 1989; Xie and Dong 1992; Wei, Liu et al. 2002). Over 50 different kinds of promoter layers have been successfully used for establishing DET between cyt.c and gold electrodes (Allen, Hill et al. 1984).

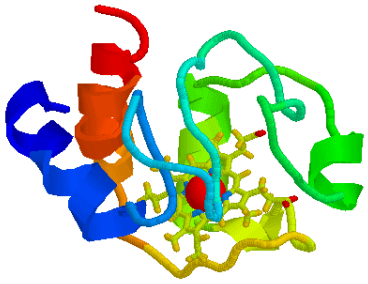

Figure 2.1.Schematic representation of the spatial structure of cyt.c (Banci, Bertini et al. 1997)

Modification of the electrode surface with carboxy-terminated alkanethiols has been one of the advantageous strategies to facilitate immobilization of cyt.c by electrostatic attraction between the negatively charged promoter and cationic lysine residues around the haem group (Frew and Hill 1988; Tarlov and Bowden 1991; Song, Clark et al. 1993; Avila, Gregory et al. 2000). In this way a highly oriented binding of the protein to the surface is achieved, similar to the mechanism of cyt.c – cytochrome c oxidase interaction in the respiratory chain.

The electron transfer properties of cyt.c electrodes based on coupling to alkanethiol promoter layers are determined by several factors, among them the chain length of the promoter molecules. For short molecules, i.e. containing up to 8 CH_2 groups, the electron transfer rate doesn't show any dependence on the chain length, however, this factor becomes most important for longer chains. In this case the heterogeneous electron transfer rate constant (k_s) decreases exponentially as a function of the chain length in accordance with the Marcus theory (Feng, Imabayashi et al. 1997). On the other hand, use of longer alkanethiols yields more homogenous layers due to stabilization via hydrophobic

interactions between the promoter molecules (Frew and Hill 1988). Modification of gold electrodes with mercaptoundecanoic acid (MUA) has been shown to provide an electron transfer rate large enough for biosensor application, and at the same time to protect the electrode surface from diffusion of interfering substances (Shen, Mark et al. 1997; Lisdat, Ge et al. 1999).

Cyt.c molecules remain stable and electroactive after adsorption onto a self-assembled monolayer (SAM) of MUA (Scheller, Jin et al. 1999). The surface concentration of the adsorbed electroactive cyt.c reaches a value of 10-15 pmol cm^{-2}, which corresponds to a coverage close to a monolayer. Covalent immobilization causes a decrease in the amount of electroactive protein by a factor of 1/3 (Ge and Lisdat 2002), which is explained by unfavorable orientation and structural rearrangement of the protein layer. This system showed a relatively low electron transfer rate (k_s of about 4±1 s^{-1}), which can be improved by using a promoter layer where MUA is mixed with mercaptoundecanol (MU) in a ratio of 1:3. In this case the formal potential of the cyt.c redox conversion was -13±5 mV for adsorbed, and 3±5 mV for covalently immobilized protein (Ge and Lisdat 2002) measured vs. Ag/AgCl (1M KCl) reference electrode. The electron transfer rate for the covalently fixed cyt.c layer was 40±6 s^{-1} with a surface coverage close to 9.2 pmol cm^{-1}, which is very close to the value reported for the adsorbed cyt.c monolayer.

The rate of DET of surface-confined cyt.c electrostatically adsorbed at carboxilate-terminated alkanethiol SAMs was investigated by Niki et al. with respect to the lysine residues in vicinity of the heme (Niki, Hardy et al. 2003). The authors showed that substitution of a lysine at the position 13 with alanine in the recombinant rat cyt.c lowered the heterogeneous electron transfer rate by over 5 orders of magnitude, whereas electron transfer was only slightly affected by the exchange of lysine-72 or lysine-79 by alanine, thus demonstrating that lysine-13 is directly involved in coupling of the protein to the SAM carboxilate terminus.

Wei et al. Proposed a new strategy for immobilization of cyt.c onto mixed SAMs. Thiol SAMs with an addition of ω-terminated alkanethiols (pyridine, imidazole, nitrile groups) are able to coordinate the haem of cyt.c, Figure 2.2 (Wei, Liu et al. 2002; Wei, Liu et al. 2004). In this way it was possible to achieve fast electron transfer up to 850 s^{-1} for imidazole-terminated C11 chains, and 780 s^{-1} for C-12 chains.

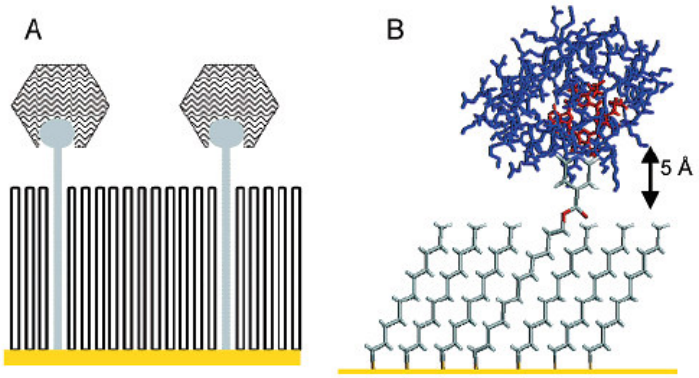

Figure 2.2. Schematic illustration of a strategy for immobilizing a molecule on the monolayer surface through a specific binding event, ***A****, and realization of this approach for cyt.c immobilization,* ***B (Wei, Liu et al. 2002)****.*

2.2.2. Xanthine Oxidase

The enzyme xanthine oxidase (XOD, EC. 1.17.3.2.) is a 290 kDa homodimer, and is a part of the xanthine oxidase family also including xanthine dehydrogenase (XDH) and aldehyde oxidase. Each monomer is organised into several domains. The first two domains each coordinate a [Fe_2S_2] cluster; they are followed by a flavin domain, and finally by two domains which bind one molybdenum cofactor (Hille 1996). The enzyme catalyzes oxidation of purines, pteridines, heterocyclic molecules and aldehydes (Fried 1971; Pick, Mcgartol.Ma et al. 1971). The oxidation of xanthine takes place at the molybdenum center and the electrons are distributed to other redox centers. The reoxidation of the reduced enzyme occurs through FAD (Rodrigues, Wedd et al. 1991).

Xanthine and hypoxanthine are products of the adenine nucleotide metabolism (Heptinstall, Johnson et al. 2005). In blood adenosine triphosphate (ATP) is degraded to adenosine diphosphate (ADP), which is quickly transformed to adenosine monophosphate (AMP) and inosine monophosphate (S. Heptinstall, A. Johnson, J Thromb Haemost 2005, 3, 2331-9). These compounds can be dephosphorylated and deaminated to adenosine and inosine, which are degraded to xanthine or hypoxanthine.

The mammalian enzyme originally exists in the cell in the form of XDH (Dellacorte and Stirpe 1968). In contrast to XOD, it has a high xanthine/NAD and very low xanthine/O_2 activity. XDH can be converted to XOD form either by oxidation of sulfhydryl residues or irreversibly by proteolysis (Waud and Rajagopalan 1976). In contrast to

mammalian XDH, chicken liver XDH is not converted to XOD form (Massey, Schopfer et al. 1989; Nishino, Nishino et al. 1989).

Figure 2.3.Schematic representation of the spatial structure of XOD (Eger, Okamoto et al. 2000).

When the fully reduced enzyme is in the oxygen environment, two molecules of H_2O_2 are produced rapidly, after which two superoxide radicals are liberated sequentially according to the reaction scheme shown in Figure 2.4 (Porras, Olson et al. 1981). Every oxidative step is initiated by rapid and reversible formation of oxygen·$FADH_2$ complex. In the case of 6- and 4-electron-reduced enzyme, two electrons per step are transferred rapidly (k_e=60 s^{-1}) generating hydrogen peroxide molecules and partially oxidized XOD. This two-electron oxidation process carries on until XOD(2) is produced. At this stage oxygen again binds to the FAD site, but in the resulting complex fully reduced flavin cannot be regenerated after the first electron transfer to oxygen. Thus, at this step only one electron is transferred rapidly and superoxide radical is produced. The remaining electron remains in the iron-sulfur center and is removed slowly in a second-order process (k=1·10^4 $M^{-1}s^{-1}$), which leads to liberation of superoxide as well. Olsen et al. proposed that the reaction sequence can also start at the phase when the enzyme has 5 electrons in order to explain

the 5:1 ratio of the fast and slow phase as measured by absorbance at 450 nm (Olson, Ballou et al. 1974; Olson, Ballou et al. 1974).

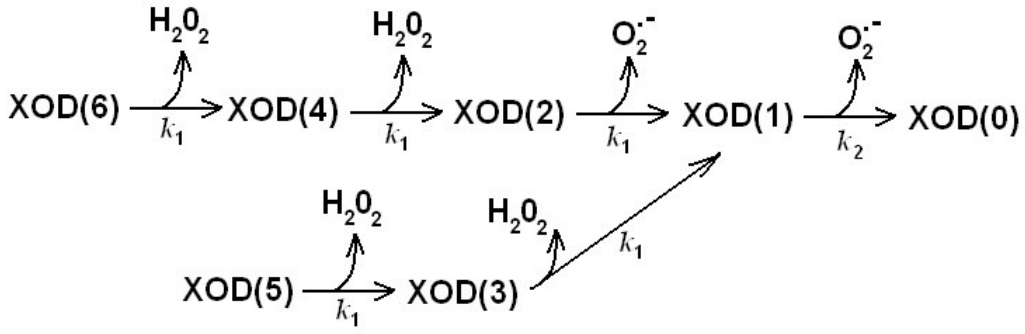

Figure 2.4. Reaction scheme showing consecutive XOD oxidation steps with concurrent generation of hydrogen peroxide and superoxide molecules. XOD(n) represents a reduced enzyme species containing n electrons (Porras, Olson et al. 1981).

Electrochemical studies of XOD are still rather limited. Electron transfer of XOD has been examined at glassy carbon, mercury electrodes (Rodrigues, Wedd et al. 1991) and carbon nanotube-modified gold electrodes (Wang and Yuan 2004), however, only FAD response was detected and no electrochemistry of molybdenum or iron-sulfur sites was observed. Liu et al. applied an alternative approach of embedding XOD into a DNA matrix. The authors found that DNA can facilitate electron communication both to FAD and molybdenum centers, while XOD retained its catalytic activity towards hypoxanthine, a catalytic current could be observed in the presence of the enzyme substrate (Liu, Peng et al. 2005). Zhou et al. were also successful in obtaining DET of FAD and [Fe_2S_2] centers of XOD with the help of nanocrystalline TiO_2 (Zhou, Xu et al. 2006). Furthermore, the authors reported on the interaction between XOD and NO, which was studied with electrochemical techniques.

Catalytic activity of XOD towards xanthine and hypoxanthine has been employed in construction of biosensors (Yao 1993; Nakatani, Vieira dos Santos et al. 2005). Usually, the design relies on detection of H_2O_2, produced during the catalytic reaction, by an electrochemical electrode polarized at a potential of +600 mV (vs. Ag/AgCl). Hypoxanthine concentration in fish is relevant to its freshness, therefore most of the developed biosensors based on immobilized xanthine oxidase can be employed in food quality control (Tarr 1966; Venugopal 2002). Reported biosensors have response times in

the order of 30 seconds, lower detection limit in the μmolar range and sensitivity in the order of $2 \cdot 10^{-2}$ A· $M^{-1} \cdot cm^{-2}$.

2.2.3. Bilirubin Oxidase

Bilirubin oxidase (bilirubin: oxygen oxidoreductase, EC 1.3.3.5) is a multicopper enzyme catalyzing oxidation of bilirubin to biliverdin with concurrent reduction of molecular oxygen to water. This monomeric enzyme has a molecular weight of about 64 kDa (Guo, Liang et al. 1991; Xu, Shin et al. 1996).

Similar to other enzymes of the "blue" copper oxidase family, the catalytic site of BOD consists of four copper ions: one type 1 (T1), one type 2 (T2), and two type 3 (T3) (Xu, Shin et al. 1996; Shimizu, Kwon et al. 1999). The T1 center has been shown to be responsible for accepting electrons from the enzyme substrate, and the T2 and T3 ions form a trinuclear cluster, which plays a central role in 4-electron oxygen reduction (Xu, Shin et al. 1996; Shimizu, Kwon et al. 1999; Tsujimura, Kano et al. 2005).

Mediated electrochemistry of the enzyme has been reported with such compounds as $Fe(CN)_6^{3-/4-}$, $W(CN)_8^{3-/4-}$, $Os(CN)_6^{3-/4-}$, and $Mo(CN)_8^{3-/4-}$ in addition to redox polymers (Nakagawa, Tsujimura et al. 2003; Tsujimura, Kawaharada et al. 2003). These experiments show that the starting potential of catalytic oxygen reduction, as well as the magnitude of the catalytic current, depend on the formal potential of a redox mediator (Tsujimura, Wadano et al. 2001; Mano, Mao et al. 2003).

Direct electrochemistry of BOD has been reported in recent years mainly for different kinds of carbon electrodes, i.e. glassy carbon electrodes (GCE), spectroscopic graphite electrodes (SPGE), highly oriented pyrolytic graphite electrodes (HOPGE) and plastic formed carbon electrodes (PFCE) (Shleev, El Kasmi et al. 2004; Tsujimura, Nakagawa et al. 2004). However, up till the year 2007 there have been no reports on DET of BOD on any kind of metal electrodes. It has been shown that under aerobic conditions BOD generates electrocatalytic current not only when the enzyme is suspended under a membrane, but also in the case of adsorbed BOD. For SPGE BOD-modified electrodes electrocataytic oxygen reduction started around a potential of +800 mV (vs. NHE) with a half-wave potential of +700 mV as measured at pH 4.0, whereas at a higher pH the starting potential for O_2 reduction showed a negative shift, e.g. +700 mV as measured at pH 7.4.

Attempts to study DET of the enzyme at anaerobic conditions have also been reported for MWCNT-modified glassy carbon electrodes and SPGE electrodes (Shleev, El Kasmi et al. 2004; Weigel, Tritscher et al. 2007). There is a discrepancy in reported values of formal potential. In the case of MWCNT electrodes, a pair of peaks was found under anaerobic conditions at pH 7.4 with a formal potential of 450±15 mV vs. Ag/AgCl, 1M KCl (=685 mV vs. NHE). This value is more positive than the T1 site redox potential determined by redox titration by Xu et al. (490 mV vs NHE) (Xu, Shin et al. 1996) and Shleev et al (515 mV vs NHE) (Shleev, El Kasmi et al. 2004). The formal potential found for the MWCNT-modified electrodes, however, correspond very well to the half-wave potential of O_2 reduction found for SPGE (605 mV vs. NHE, pH 7.4) (Xu, Shin et al. 1996) and HOPG electrodes (597 mV vs. NHE, pH 7) (Tsujimura, Nakagawa et al. 2004) and is in a good agreement with the redox potential recently found by redox titration by Christenson et al. (Christenson, Shleev et al. 2006). The authors suggest, that these results may indicate that the heterogeneous electron transfer of BOD at carbon electrodes follows a different mechanism than catalysis in solution. In this case the electrons may be transferred to the T2/T3 cluster directly without involvement of the T1 center, and subsequently transferred to O_2. However, this assumption needs to be verified by additional experiments.

2.2.4. Sulfite Oxidase

Sulfite oxidase (sulfite: oxygen oxidoreductase, EC 1.8.3.1, SOx) is a 110 kDa homodimer enzyme containing a molybdopterin and haem cofactors. It belongs to a family of molybdo-enzymes, which includes DMSO reductase, xanthine oxidase, and nitrite reductase. Each subunit of the enzyme contains a molybdopterin binding domain connected to a haem-containing domain (cytochrome b_5 type) via a flexible loop. SOx catalyzes a two-electron oxidation of sulfite to sulfate with ferric cytochrome c as a natural electron acceptor (Kisker, Schindelin et al. 1997).

$$SO_3^{2-} + H_2O \rightarrow SO_4^{2-} + 2H^+ + 2e^- \qquad (2.8)$$

It has been shown that oxidation of sulfite occurs at the molybdenum center of the enzyme with reduction of the Mo(VI) to Mo(IV). This process is followed by oxidation of the

molybdenum cofactor by the b_5 haem with subsequent electron transfer to cyt.c (in natural reaction) or any other suitable electron acceptor, e.g. electrode (Ferapontova, Ruzgas et al. 2003).

Most of the reports on electrochemical behavior of the enzyme focus on the mechanism of intramolecular electron transfer from the molybdenum to the haem b_5 center (Kisker, Schindelin et al. 1997; Elliott, McElhaney et al. 2002). According to the crystallographic data reported by Kisker et al. (Kisker, Schindelin et al. 1997) the two domains are separated by approx. 30 Å, which is a prohibitively large distance for the electron transfer. The authors suggest that the electron transfer to the haem occurs after a change of the enzyme conformation (due to a flexible loop) in such a way that the ET distance decreases. This conformational change is thought to be induced by a cyt.c binding event and can be largely affected by the composition, ionic strength, viscosity and pH of the solution (Sullivan, Hazzard et al. 1993; Kisker, Schindelin et al. 1997; Feng, Kedia et al. 2002).

Figure 2.5.Schematic representation of the spatial structure of SOx (Karakas, Wilson et al. 2005).

Electrochemical coupling of SOx to electrodes modified with promoters mimicking the natural partner of the enzyme (cyt.c) has been recently demonstrated (Elliott, McElhaney et al. 2002; Ferapontova, Ruzgas et al. 2003). Elliot and co-workers showed

that the enzyme can partially retain its activity after immobilization onto a pyrolytic graphite edge or Au electrodes modified with mercapto-6-hexanol SAM. In the absence of sulfite a single pair of peaks were observed with a formal potential of +90 mV (vs. SHE). Upon addition of 1 mM Na_2SO_3 the CV transformed into an oxidative catalytic wave. However, in comparison with the case of homogenous catalysis with cyt.c, the immobilized SOx showed a more than 25-fold decrease in the catalytic turnover number (2-4 s^{-1} for immobilized enzyme, and 100 s^{-1} for reaction in solution (Brody and Hille 1999). While most of the immobilized enzyme was electroactive without the substrate in solution and gave rise to a quasi-reversible electrochemical response (calculated surface concentration Γ_{total} = 4.3 pmol/cm^2), it showed a very small catalytic efficiency upon addition of sulfite. The authors conclude that most of the enzyme had an unfavorable conformation prohibiting electron transfer from the reduced molybdenum to the haem domain.

Later, Ferapontova et al. realized a faster heterogeneous electron transfer of SOx immobilized on Au electrodes modified with 11-mercapto-1-undecanol and 11-mercapto-1-undecanamine. The heterogeneous ET rate constant k_s determined for this system was in the order of 15 s^{-1}, and the catalytic turnover number for immobilized enzyme to oxidation of sulfite was comparable with the efficiency of enzymatic oxidation in solution with cyt.c as electron acceptor (Ferapontova, Ruzgas et al. 2003).

The specificity of SOx towards sulfite has been practically employed in the design of biosensors. First reports relied on amperometric detection using a mediator (Nader, Vives et al. 1990), or reducing H_2O_2, by-product of the enzymatic conversion, at carbon electrodes (Mulchandani, Groom et al. 1991). These biosensors showed a comparable linear response range and a lower detection limit of several μM. In 1992 Korell and Lennox reported a sulfite biosensor based on SOx directly adsorbed onto the conducting salt electrode material tetrathiafulvalene tetracyanoquinodimethane (TTFTCNQ) (Korell and Lennox 1993). In CV these electrodes showed a catalytic behavior in the presence of sulfite ions. Rather recent designs employ screen-printed carbon electrodes integrating SOx and cyt.c, with the possibility to operate at rather low potential of +0.3 V (Abass, Hart et al. 2000; Hart, Abass et al. 2002).

2.3. Layer-by-Layer self-assembly

Recently layer-by-layer (LbL) assembly has been demonstrated to be a simple yet versatile method to prepare thin films of polymeric materials (Decher 1997; Hammond 1999). Polyelectrolytes are polymers with ionizable groups on each monomer repeat unit. Some common polyelectrolytes and the ones used in this thesis are shown in Figure 2.6.

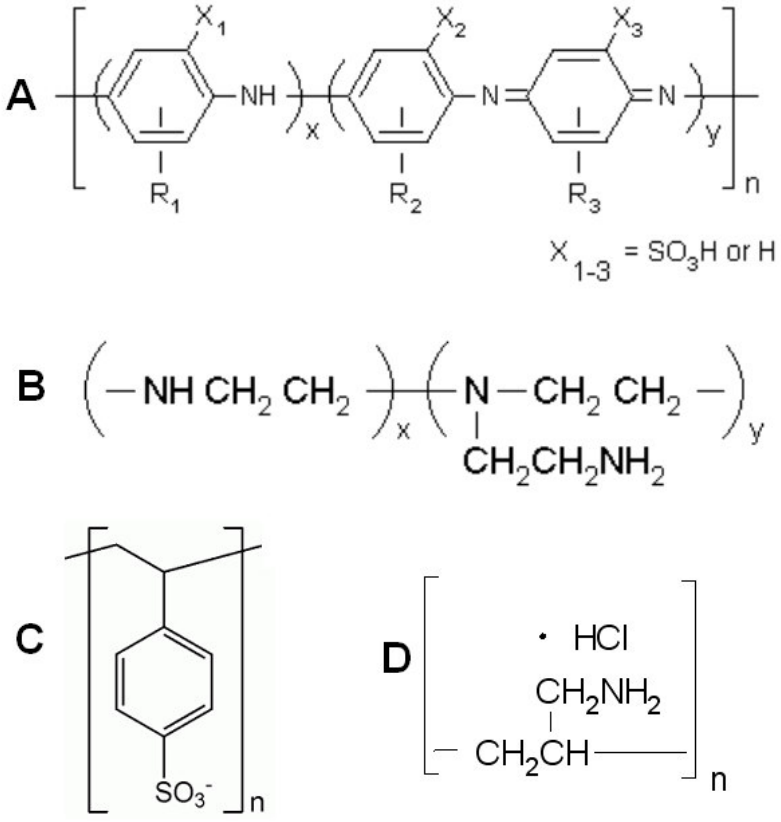

*Figure 2.6.Chemical formulae of **A** poly(anilinesulfonic acid), **B** poly(ethylene imine), **C** Poly(styrenesulfonate), **D** Poly(allylamine hydrochloride).*

They are categorized as strong if the degree of ionization is independent of solution pH (i.e., fully ionized over all pH ranges) and weak if the degree of ionization is pH dependent. Typically, the multilayer is formed by adsorbing a polyelectrolyte of one charge from solution onto an immersed substrate. A polyelectrolyte of the opposite charge from another solution is then adsorbed onto the same substrate. The multilayer assembly is driven by electrostatic interactions between the oppositely charged polyelectrolytes. This process is repeated, alternating between the two polyelectrolyte solutions until the desired

thickness or number of layers is achieved. Thicknesses from nanometers, with a monolayer adsorbed, to micrometers can be obtained while still maintaining a uniform structure. The covered area is limited only by the substrate size and polyelectrolyte solution volume. Many different variations on the LbL process are possible. For example, one may use not only one set of polyelectrolytes but also two or three to create different "blocks". Three-dimensional heterostructures may be created in combination with photolithography, soft lithography, and inkjet printing techniques.

The LbL assembly has distinct advantages over traditional ultrathin film fabrication techniques like LB. Although the LB technique produces highly oriented films, it requires specialized preparation equipment and specific substrate surface properties. In contrast, PM films can be prepared on a wide range of surface materials and geometries (Chen and McCarthy 1997; Delcorte, Bertrand et al. 1997; Phuvanartnuruks and McCarthy 1998; Elbert, Herbert et al. 1999; Graul and Schlenoff 1999; Caruso and Schuler 2000). In addition, the alternating immersion can be automated. Besides dipping into baths, the polyelectrolyte solutions can be applied by spraying (Schlenoff, Dubas et al. 2000) and spin-coating (Chiarelli, Johal et al. 2001; Lee, Hong et al. 2001).

2.3.1. Polyelectrolyte Multilayers: How Polyelectrolytes stick together

The pioneering work to demonstrate that multiple layers of polyelectrolytes can be sequentially adsorbed onto a substrate with controlled morphology was purely based on using electrostatic interactions between fully-ionized polyelectrolytes and a substrate with a charged surface (Decher, Hong et al. 1992; Lvov, Decher et al. 1993). Poly(vinylsulfate) (PVS), potassium salt, or poly(sodium 4-styrenesulfonate) (PSS) were used as polyanion and poly(allylamine hydrochloride) (PAH) or poly(-4-vinylbenzyl-(N,N-diethyl-N-methyl-)ammonium iodide) as polycation. The polyanion was adsorbed first onto a cationic surface, either treated silicon, glass, or quartz. Repeated, alternating immersions of the substrate into the polycation and the polyanion solutions formed uniform, smooth films. Although the first few adsorbed layers were thinner, the layer thickness reached equilibrium quickly. The film growth was linear in thickness over at least hundred layers. Depending on the salt concentration of the polyelectrolyte solutions, the thickness ranged from 1 to 4 nm per layer. The added salt, typically NaCl, shields the charges on the polyelectrolyte in solution, reduces the screening length between charged groups on the

polymer chain, and allows the polyelectrolyte to attain a more randomly coiled conformation. Rather than adsorbing in a thinner, distended conformation, the salt-shielded polyelectrolyte adsorbs in a thicker, coiled conformation.

While the layer structure of PMs prepared with strong polyelectrolytes is principally influenced by the solution ionic strength, the solution pH during assembly can be used to manipulate the structure of multilayers composed of weak polyelectrolytes. Because weak polyelectrolytes contain ionizable functional groups, the multilayer structure is sensitive to assembly pH conditions. In addition, the assembly pH is a more flexible parameter for controlling molecular architecture than ionic strength because the solubilities of high molecular weight polyelectrolytes become poorer at high ionic strength (Chan, Craig et al. 1992). The linear charge density of weak polyelectrolytes like poly(acrylic acid) (PAA) can substantially vary in the pH region near its pI. Moreover, unlike ionic strength, which affects all parts of the polyelectrolyte equally, the pH modifies a predictable and controllable fraction of the functional groups.

Using multilayers composed of PAA and PAH adsorbed on hydrophilic glass and silicon, the effect of assembly pH on molecular organization has been investigated (Yoo, Shiratori et al. 1998; Shiratori and Rubner 2000). The polyelectrolyte solution pH sets the linear charge density of the polyelectrolyte and hence also the polymer conformation. In addition, the solution pH affects the charge of the surface on which the polyelectrolyte adsorbs. At high pH relative to its pK_a (between 5 and 6 for PAA depending on ionic strength (Nagasawa, Murase et al. 1965), the polyanion is almost completely ionized. Conversely, the polyanion becomes more neutral at low pH relative to its pK_a. The polycation exhibits the opposite ionization behavior (pI between 7 and 9 for PAH depending on ionic strength (Choi and Rubner 2005).

The incremental thickness of adsorbed PAH and PAA as a function of assembly pH, with both polyelectrolyte solutions having the same pH, can be characterized by three regimes over most of the pH range. In the high pH regime ($6 <$ assembly pH < 8), PAH/PAA layers are molecularly thin. Both polyelectrolytes are almost completely ionized in solution and hence adsorb onto the surfaces, in a distended manner. This regime is similar to the case of strong polyelectrolytes discussed above where the polyelectrolytes adsorb flat forming many ionic bonds with the highly charged surface. In the low pH regime ($2 <$ assembly pH < 5), PAH (Chan, Schrock et al. 1992) is fully ionized while

PAA is only partially ionized. The PAH/PAA thickness increases with decreasing assembly pH in this regime. The PAA is only partially charged, with its degree of ionization decreasing with lower pH, and adopts a more random coil conformation in solution. At lower assembly pH, more PAA molecules need to be adsorbed onto the fully charged PAH surface to neutralize the surface charge. The PAA adsorption appears to dominate over the counter effect of fewer fully charged PAH molecules adsorbing onto the less charged PAA surface at lower pH. Between an assembly pH of 5 and 6, a transition regime exists where large changes in layer thicknesses are obtained (Park, Barrett et al. 2001). As with strong polyelectrolytes, film growth is uniform and linear after the first few layers.

The surface properties of these PAH/PAA multilayers have been shown to be strongly controlled by the outer-most adsorbed layer. For example, the advancing contact angle can alternate between 10^{o} and 40^{o} when the outer-most layer alternates between PAA and PAH, respectively (Shiratori and Rubner 2000).

The primary mechanism for multilayer formation is the electrostatic interaction between the oppositely charged polyelectrolytes (Hoogeveen, Stuart et al. 1996; Dubas and Schlenoff 1999). Charge overcompensation occurs after every adsorption step to facilitate the adsorption of the oppositely charged polyelectrolyte in the following step. This has been observed by the sign alternation of the zeta potential of the surface after each polyelectrolyte layer is adsorbed. However, electrostatic interactions between the adsorbing polyelectrolytes and the oppositely charged surface polyelectrolytes are not the only way of LbL self-assembly. Non-electrostatic interactions, e.g. hydrophobic interactions, hydrogen bonding, or bio-affinity can also play important roles.

Even though the polyelectrolytes are adsorbed sequentially in LbL assembly, the internal structure of the assembled multilayer can be highly interpenetrated. The internal structure has primarily been studied using neutron and x-ray reflectivity (Schmitt, Grunewald et al. 1993; Tarabia, Hong et al. 1998), though nuclear magnetic resonance (NMR) (Rodriguez, Gomez et al. 2000) has also been employed. Using neutron and x-ray reflectivity, PAH/PSS multilayers deposited from salt-containing solutions showed interpenetration between polymer layers on the same order as the individual layer thicknesses (Schmitt, Grunewald et al. 1993). PAH/sulfonated polyaniline multilayers show even greater interfacial widths (Kellogg, Mayes et al. 1996). These multilayers

formed from one pair of polyelectrolytes have been described as "fuzzy" (Decher 1997), with their internal structure similar to that of "scrambled salt" bulk polyelectrolyte complexes (Michaels and Miekka 1961; Farhat, Yassin et al. 1999; Arys, Laschewsky et al. 2001). However, in multilayers comprising different pairs of polyelectrolytes, so called heterostructures, stratification of these layers was observed (Baur, Rubner et al. 1999). This stratification is consistent with the evidence of interpenetration on the order of an individual layer thickness but not more.

The LbL assembly of polyelectrolytes has been shown to be a versatile process for forming multilayer films. This sequential adsorption process facilitates fine control over film structure through adsorption conditions and the ability to choose and mix polyelectrolytes with desired properties. As will be described in the following paragraphs, these two aspects are essential for the design of functional multilayers.

2.3.2. Biomimetics by Layer-by-Layer technique

The technique of LbL self-assembly has been used in development of biomimetic[i] materials with superior mechanical, optical, electrical and biological properties compared with synthetic composites. Lotus leaf, a classical example of a system with natural superhydrophobicity, which is believed to arise from micro- and nanostructures, has inspired nanoscale design of artificial materials by LbL assembly. Soeno et al. were the first to report superhydrophobic surfaces by LbL by alternating assembly of anionic silica nanoparticles with cationic PAH. After thermal (70˚C, 1 h) and hydrophobic (with dichlorodimethylsilane) treatment the assembly showed water contact angles larger than 160˚ (Soeno, Inokuchi et al. 2004). Later, similar structures were built by incorporating Ag and Au and polystyrene nanoparticles into LbL templates (Zhang, Shi et al. 2004; Sangribsub, Tangboriboonrat et al. 2005; Zhao, Shi et al. 2005). Besides nanoparticles clay nanorods assembled with perfluorinated polyelectrolytes also were reported to yield superhydrophobicity (Jisr, Rmaile et al. 2005).

LbL films offer a good environment for mimicking biomechanical systems. Jaber et al. investigated myosin motility on PAH/PSS films with a PAH-terminating surface layer. The authors show that myosin-driven motion of actin filaments rises with increasing ionic

[i] Biomimetics or "The mimicry of Nature" is the term introduced by Otto Schmitt signifying a new field of science operating with artificial (engineered) systems resembling natural structure and/or function. It is also known as bionics (a term by Jack E. Steele), biognosis, or bionical creativity engineering.

strength of the motility buffer with concurrent elongation of the filaments' length (Jaber, Chase et al. 2003).

Incorporation of proteins and enzymes into LbL films represents an elegant way for design of functional multilayers. Photosynthesis has been one of the most attractive biological processes to mimic, a source of energy to sustain cellular life. He et al. reported on photosynthetic membranes by LbL assembly of a photochromic protein bacteriorhodopsin (bR) and PDDA. The films consisting of 8 wild-type bR/PDDA layers showed a maximum light-on current of 52 nA/cm^2, while the films containing D96N mutant were even more efficient. Besides bR, other molecules, such as thylakoids, porphyrins, and cyt.c were used to design photosynthetic films by LbL (Kaschak, Johnson et al. 1999; Balbinot, Atalick et al. 2003; Zilbermann, Lin et al. 2004; Dementiev, Baikov et al. 2005).

High efficiency and selectivity of enzymes are advantageous for construction of catalytic bioreactors, where multiple enzymes can be immobilized by LbL assembly without significant loss of activity. These enzyme biosensors are described in the following chapter.

2.3.3. Biosensors based on Layer-by-Layer sssembly

Immobilization of functional biomaterials on electrodes is an essential step in biosensor design. Generally, special immobilization conditions have to be fulfilled in order to maintain biological activity of a recognition component, and LbL assemblies provide a strategy to tailor specific properties of the immobilized films and in this way to enhance the biosensor performance. Biological materials can be assembled in multilayer films using LbL assembly based on electrostatic interactions, as well as bioaffinity, cross-linking, or covalent binding. Table 2.3. summarizes some of the electrochemical biosensors prepared by different LbL assembly methods.

Table 2.3. Electrochemical biosensors based on various LbL assembly methods (Zhao, Xu et al. 2006).

LBL assembly methods	Biorecognition molecules in multilayer films	Analyte	References
Electrostatic force	Glucose oxidase	Glucose	(Mizutani, Sato et al. 1996; Hodak, Etchenique et al. 1997; Hou, Fang et al. 1997; Calvo, Etchenique et al. 2001; Trau and Renneberg 2003)
	Cytochrome oxidase	Cyt.c	(Lindholm-Sethson, Gonzalez et al. 1998)
	Horseradish peroxidase	H_2O_2	(Sun, Li et al. 1999; Li, Wang et al. 2000; Rosca and Popescu 2002)
	Polyphenol oxidase	Dopamine Catechol	(Forzani, Solis et al. 2000) (Coche-Guerente, Desbrieres et al. 2005)
	Uricase	Uric acid	(Hoshi, Saiki et al. 2003)
	Catalase	H_2O_2	(Yu and Caruso 2003)
	Cholesterol oxidase	Cholesterol	(Gobi and Mizutani 2001)
	Lactate oxidase	Lactic acid	(We, Zhang et al. 2003; Xu, Zhao et al. 2005)
	Diaphorase/glucose-6-phosphate dehydrogenase	Glucose-6-phosphate	(Zheng, Okada et al. 2004)
	Fructose dehydrogenase/horseradish peroxidase/HRP-alcohol oxidase	Fructose/H2O2/ methanol	(Narvaez, Suarez et al. 2000)
	Myoglobin/horseradish peroxidase	Trichloroacetic acid/O_2/H_2O_2	(Zhou, Li et al. 2002; Li and Hu 2003)
	Glucose oxidase/catalase	Glucose/H_2O_2	(Shi, Lu et al. 2003)
	Glucose oxidase/glucoamylase	Glucose/maltose	(Nguyen, Ping et al. 2003)
	Cholesterol oxidase/ cholesterol esterase	Cholesterol	(Ram, Bertoncello et al. 2001)
	Hepatitis B surface antibody	Hepatitis B surface antigen	(Tang, Yuan et al. 2005)
	ds-DNA	Damaged DNA Oxidized DNA 8-Oxoguanine/ oxidized nucleobases	(Wang and Rusling 2003) (Mugweru, Wang et al. 2004) (Ropp and Thorp 1999)

Avidin-biotin interaction	Glucose oxidase	Glucose	(Hoshi, Anzai et al. 1995; Chen, Kobayashi et al. 1998)
	Alcohol oxidase	Alcohol	(Du, Anzai et al. 1996)
	Glucose oxidase/ lactate oxidase *(biotinilated enzyme vs. avidin)*	Glucose/lactic acid	(Anzai, Takeshita et al. 1998; Suzuki, Murakami et al. 1998)
Lectin – sugar interaction	Glucose oxidase	Glucose	(Farooqi, Saleemuddin et al. 1997)
	Glucose oxidase/horseradish peroxidase/lactate oxidase	Glucose	(Anzai and Kobayashi 2000)
	Glucose oxidase/horseradish peroxidase *(glycoenzyme vs. concanavalin A)*	Glucose/H2O2	(Kobayashi and Anzai 2001)
Antibody – antigen interaction	Glucose oxidase	Glucose	(Bourdillon, Demaille et al. 1996)
Cross-linking	Glucose oxidase	Glucose	(Willner, Katz et al. 1992; Willner, Liondagan et al. 1995)
	Bilirubin oxidase	Bilirubin	(Shoham, Migron et al. 1995)
	Glucose oxidase/choline oxidase/acetylcholine esterase	Glucose/ acetycholine	(Riklin and Willner 1995)
	Glucose oxidase/lactate oxidase	Glucose, lactic acid	(Sirkar, Revzin et al. 2000)
Covalent binding	Glucose oxidase	Glucose	(Yoon, Hong et al. 2000; Zhang, Yang et al. 2004)
	Quinoprotein glucose dehydrogenase	p-Aminophenol	(Jin, Bier et al. 1995)

Almost all types of oxyreductases have been shown to form electroactive multilayer films on electrodes, including those employed in this work, e.g. glucose oxidase (Hodak, Etchenique et al. 1997; Calvo, Etchenique et al. 2001; Calvo, Danilowicz et al. 2002; Calvo and Wolosiuk 2004; Zhang, Yang et al. 2004), glucose dehydrogenase (Loew, Scheller et al. 2004; Suye, Zheng et al. 2005), lactate oxidase (Sirkar, Revzin et al. 2000; Xu, Zhao et al. 2005), pyruvate oxidase (Simonian, Revzin et al. 2002), horseradish peroxidase (Sun, Li et al. 1999; Anzai and Kobayashi 2000; Rosca and Popescu 2002), fructose dehydrogenase (Narvaez, Suarez et al. 2000), polyphenol oxidase (Forzani, Solis et al. 2000; Coche-Guerente, Desbrieres et al. 2005), choline oxidase (Qu, Yang et al. 2005; Shi, Song et al. 2005), cholesterol oxidase (Ram, Bertoncello et al. 2001; Yang, Yang et al. 2006), uricase (Hoshi, Saiki et al. 2003), xanthine oxidase (Hoshi, Noguchi et al. 2006), etc. In most cases, the multilayer films containing enzymes undergo electrochemical conversion using electrochemical mediators, which can be diffusible e.g.

ferrocene (Zhang, Yang et al. 2004), osmium compounds (Calvo JACS 2002), NAD (Suye, Zheng et al. 2005), H_2O_2 (Yang, Yang et al. 2006), or fixed onto a polyelectrolyte chain (Li, Wang et al. 2000; Calvo, Danilowicz et al. 2005).

As an alternative, to produce mediator-free multilayer films, redox active enzymes can be co-immobilized with conducting polymers (Ram, Adami et al. 2000). In this case the polymer is solely responsible for the protein-electrode electron transfer and plays a role of a molecular wire. Interesting are reports on electroactive multilayers assembled using non-conductive polylectrolytes. Hu et al. demonstrated that LbL films of myoglobin (Mb) and PSS on pyrolytic graphite electrodes show an increase in electroactive Mb up to 7 PSS/Mb layers (Ma, Hu et al. 2000). At the same time, similar assemblies on Au electrodes showed no increase in loading of electroactive Mb after two PSS/Mb layers. The authors explain this effect by the influence of the surface roughness, which was greater in the case of the pyrolytic graphite electrodes. This assumption was also confirmed by using graphite electrodes with different roughness factors. Increase of the ionic strength of the assembly buffer caused a slight rise in the amount of electroactive surface-confined Mb, which the authors attribute to PSS adopting a more coiled conformation, thus allowing more protein to have a direct contact with the electrode. Therefore, here the electron transfer between the electrode and Mb was still realized via a tunneling mechanism requiring localization of the protein molecules in close proximity to the electrode surface in order to be electroactive.

Later, Beissenhirtz et al. showed that cyt.c co-immobilized with poly(anilinesulfonic acid)(PASA) leads to electroactive multilayer films, where the amount of electroactive protein shows a linear dependence on the number of deposited layers up to 15 (Beissenhirtz, Scheller et al. 2004). Upon adddition of the cross-linking agent 1-ethyl-3(-3-dimethyl-aminopropyl)carbodiimide (EDC) to a multilayer electrode, the amount of electrode-addressable cyt.c decreased with increasing peak separation in CVs, which allows the authors to conclude that the flexibility of the protein molecules plays a crucial role for an efficient electron transfer within the multilayer.

The cyt.c monolayer electrode is able to exchange electrons with cyt.c molecules in solution at lower scan rates. An increase in the scan rate, surpassing the rate of electron transfer between the cyt.c monolayer and cyt.c in solution (at about 1 V/s) eliminated this effect. A similar behavior can be observed for the multilayer assembly. While the amount

of electroactive cyt.c for a monolayer electrode is independent of the scan rate, the multilayer assemblies show a drastic decrease in the amount of electrode-addressable protein upon increasing the scan rate. The electron transfer rate between cyt.c molecules within the polyelectrolyte matrix is significantly lower (k_s=1.5±0.3 s^{-1}) than that between the cyt.c monolayer and the electrode surface (k_s=75±5 s^{-1}).

In order to clarify the role of the polyelectrolyte, the authors exchanged PASA by a strong polyelectrolyte (PSS), which also led to multilayer formation, although it hindered the electron transfer (Beissenhirtz, Kafka et al. 2005). PASA showed no redox activity in the range between –0.5 .. +0.5 Volt (vs. Ag/AgCl/1M KCl) at a cyt.c monolayer electrode at a scan rate of 100 mVs^{-1} . Here the authors suggest the role of the polyelectrolyte in the protein multilayer system stabilizing the structure rather than electrochemical wiring of the protein to the electrode. However, the possibility that PASA is involved in the electron transfer process could not be excluded, since this polyaniline form (emeraldine salt) can be conductive under certain conditions. This question will be addressed in the experimental part of this thesis.

2.4. S-layer Rescrystallization Approach

Monocrystalline S-layers (bacterial surface layers) are (glyco)protein arrays commonly found in eubacteria and archaea and represent one of the most simple cell envelopes. S-layer protein subunits non-covalently interacting with each other and underlying cell-envelope components form a two-dimensional crystalline protein layer. In the last decades the technique of S-layer recrystallization has become a popular approach to assemble molecularly ordered self-assembled protein films with prominent mechanical properties, and has found a broad range of applications, discussed in section 2.4.2.

2.4.1. S-layer proteins

The evolution of prokaryotes has led to a diversity of the outermost boundary as a result of adaptation to environmental conditions (Sleytr, Egelseer et al. 2007). Hence, the S-layer proteins are poorly conserved and can profoundly differ even between related species. The S-layer lattices can have oblique, square, or hexagonal symmetry. Depending on species the S-layers have a thickness between 5 and 25 nm and possess identical pores with 2-8 nm in diameter and center-to-center spacing of approximately 2.5 to 35 nm.

Isolated S-layer proteins are able to assemble into two-dimensional monocrystalline arrays, Figure 2.7, in suspension and at a large variety of supports (Schuster, Pum et al. 2006). Thus, plenty of studies reported recrystallization of S-layer proteins at lipid membranes, liposomes, air-water interface, and a number of solid materials, including silicon, gold, silanized glass and plastic (Kupcu, Sara et al. 1995; Wetzer, Pfandler et al. 1998; Schuster, Pum et al. 2001; Gyorvary, Stein et al. 2003; Gufler, Pum et al. 2004; Schuster, Gufler et al. 2004; Vadillo-Rodriguez, Busscher et al. 2005; Schuster, Pum et al. 2006).

Chemical analysis of isolated S-layer subunits showed that most of them consist of a single protein or glycoprotein species with a molecular weight of 40 – 200 kDa. Amino acid analysis revealed that S-layer proteins from different organisms are rather similar in overall composition (Sleytr and Messner 1983; Sara and Sleytr 1996). As a rule, these proteins contain predominantly acidic and hydrophobic amino acids. From the basic amino acids lysine is observed most frequently, while the arginine, histidine and methionine content is generally very low, and cysteine was only detected in a few S-layer proteins (Sara and Sleytr 1996). Isoelectric points of most S-layer proteins are in the weakly acidic

pH range. According to CD data, approximately 20% of the amino acid residues form α-helices, and about 40% occur as β-sheets.

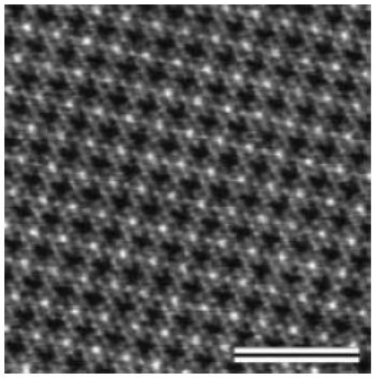

Figure 2.7. Scanning force microscopy image of an S-layer with square lattice symmetry recrystallized on a silicone wafer. Image was recorded in contact mode in a liquid cell; bar 50 nm (Sleytr 2004).

Despite considerable data on the structure, assembly, biochemistry, and genetics of S-layers, relatively little information is available about their specific tasks (Beveridge 1994; Sleytr and Beveridge 1999). A closed, isoporous and crystalline protein layer has the potential to fulfill a broad spectrum of functions in S-layer-carrying organisms. Due to a precise pore size, the S-layers work as molecular sieves, providing sharp cut-off for the bacterial cells, thus serving as a barrier against high molecular weight substances, e.g. enzymes (Sara and Sleytr 1987). In addition, S-layers facilitate cell adhesion (in case of glycosylated S-layers), stabilize the cell membrane and provide adhesion sites for exoproteins.

The S-layer protein SbpA of *Bacillus sphaericus* CCM2177, discussed later in the current thesis, has a molecular mass of 132 kDa and a calculated isoelectric point of 4.69. The S-layer lattice of *Bacillus sphaericus* shows square symmetry with a center-to-center spacing of 13.1 nm (Ilk, Vollenkle et al. 2002).

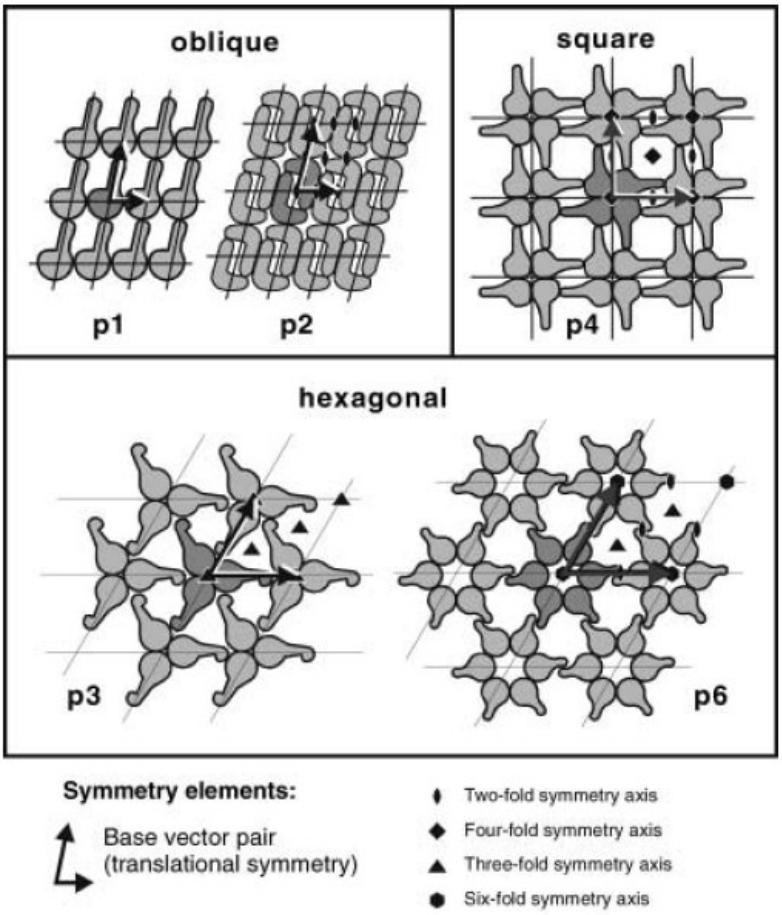

Figure 2.8. Schematic representation of S-layer lattice types grouped according to the possible two-dimensional space group symmetries. Morphological units were chosen arbitrarily and are shown in dark gray. Symmetry axes are shown for a single unit cell only.(Sleytr 2004).

2.4.2. S-layers in technology

Recrystallization of S-layers is an appealing approach for the bottom-up self-assembly and is of practical significance for nanobiotechnology. Due to its unique, compared to the majority of biological systems, structural organization, symmetry, and mechanical properties, the S-layers are of high interest for design of ultrafiltration membranes, nanocontainers, drugs, biocompatible templates, and matrices for inorganic nanostructures (Sara and Sleytr 1987; Neubauer, Pum et al. 1993; Neubauer, Hodl et al. 1994; Sleytr, Bayley et al. 1997). While in conventional membranes the pore size fluctuates around a mean value, the S-layers have been used in construction of ultrafiltration membranes with a highly uniform pore size in the rage from 2 to 8 nm and

very sharp cut-off. Pores of such membranes show very low unspecific sorption of various proteins (Sara and Sleytr 1987). Yet, up till now, S-layer ultrafiltration membranes have found very limited industrial relevance due to a strong competition with other materials, and are, therefore, used predominantly for R&D purpose.

Chemical attachment of low molecular weight haptens to S-layers has been shown to stimulate the immune response, and, thus, can be employed as vaccines (Sleytr, Bayley et al. 1997). Regular arrangement of the S-layer protein units shall, in turn, yield an ordered haptene pattern. Such vaccines caused no visible adverse effects after intramuscular and subcutaneous injections and are effective as well upon oral or nasal administering.

S-layers are advantageous materials as biosensor matrices providing a high packing density monolayer arrangement of attached functional biomolecules. However, chemical attachment of biologically active molecules to S-layer proteins has a drawback: the binding of target molecules to S-layer proteins does not reach 100%, hence the surface density of the bioactive molecules may be low, and their arrangement irregular. This effect can be overcome by synthesizing a fusion protein having a target protein incorporated into the S-layer unit (Ilk, Vollenkle et al. 2002).

Recrystallization of the S-layer subunits at lipid bilayers, phospholipid monolayers, and liposomes has been a method for stabilization of these fragile structures without total restriction of the membrane fluidity (Kupcu, Sara et al. 1995; Schuster, Pum et al. 1998; Wetzer, Pfandler et al. 1998). This approach mimics an archaea envelope, which commonly exists under extreme conditions. S-layer supported liposomes are of medical importance, as liposomes are exposed to a mechanical stress when injected with a syringe or during the vascular transportation (Mader, Kupcu et al. 1999).

S-layers have been shown to serve as templates for construction of two-dimensional arrays of inorganic material. In natural environment, calcium sulfate and calcium carbonate crystallization occurs in pores of cyanobacterial S-layers (Schultze-Lam, Harauz et al. 1992). In a similar way, regular superlattices of cadmiun silfide and gold have been obtained using S-layers in vitro (Shenton, Pum et al. 1997; Dieluweit, Pum et al. 1998).

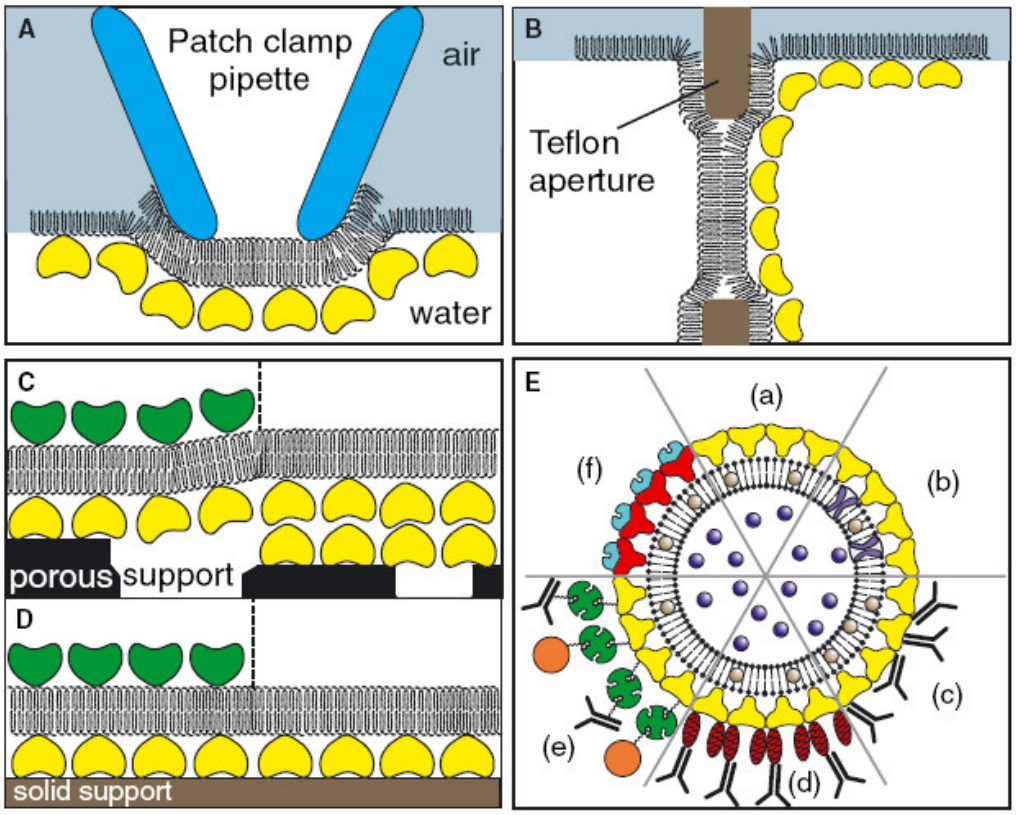

Figure 2.9. Schematic illustrations of various S-layer-supported lipid membranes. (A) bilayer lipid membranes have been generated across an aperture of a patch clamp pipette by the tip-dip method, and a closed S-layer has been recrystallized from the aqueous subphase. In (B), a folded or painted membrane has been generated to span a Teflon aperture. Subsequently S-layer protein can be injected into one or both compartments (not shown) whereby the protein self-assembles to form closely attached S-layer lattices on the lipid membranes. (C) On an S-layer ultrafiltration membrane (SUM), a lipid membrane can be generated by a modified Langmuir–Blodgett (LB) technique. As a further option, a closed S-layer lattice can be attached on the external side of the SUM-supported lipid membrane (left part). (D) Solid supports can be covered by a closed S-layer lattice, and subsequently lipid membranes can be generated using combinations of the LB and Langmuir–Schaefer technique, and vesicle fusion. As shown in (C), a closed S-layer lattice can be recrystallized on the external side of the solid-supported lipid membrane (left part). (E) Schematic drawing of (a) an S-liposome with entrapped water-soluble (blue) or lipid-soluble (brown) functional molecules and (b) functionalized by reconstituted integral proteins. S-Liposomes can be used as immobilization matrix for functional molecules (e.g. IgG) by direct binding (c) or immobilization via the Fc-specific ligand protein A (d), or biotinylated ligands can be bound to the S-liposome via the biotin–streptavidin system (e). (f) Alternatively, liposomes can be coated with genetically modified S-layer proteins incorporating functional domains (Sleytr, Egelseer et al. 2007).

3. Materials and Methods

3.1. Materials

3.1.1. Buffers

Phosphate buffers were prepared with potassium di-hydrogen phosphate and di-potassium hydrogen phosphate and pH adjusted with potassium hydroxide or phosphoric acid. Citrate-phosphate buffers were prepared with potassium di-hydrogen phosphate and citric acid and pH adjusted with potassium hydroxide or citric acid.

Buffer 1 (5 mM phosphate pH 7.0) was used for cytochrome c monolayer preparation, recording of cyclic voltammograms, AFM scans, and during SERRS measurements.

Buffer 2 (0.5 mM phosphate pH 5.0) was used for preparation, thermal treatment and storage of the cytochrome c multilayer electrodes, preparation of cytc/BOD and cyt.c/SOx multilayer electrodes.

Buffer 3 (0.5 mM phosphate pH 6.0) was used for preparation of mulilayers with xanthine oxidase.

Buffer 4 (5 mM phosphate pH 7.5) was used for amperometric experiments as well as for preparation of the stock solutions of hypoxanthine and superoxide dismutase.

Buffer 5 (5 mM citrate-phosphate) with various pH values was used for electrochemical investigation of cyt-BOD interaction.

Buffer 6 (10 mM CaCl, 0.5mM Tris, pH 9.0) was used for recrystallization of SbpA.

3.1.2. Chemicals

Horse-heart cytochrome c, Bovine Erythrocyte Superoxide Dismutase (EC 1.15.1.1) (SOD), Bilirubin oxidase from *Myrothecium verrucaria* (EC 1.3.3.5), (-)-epigallocatechin gallate, and rutin hydrate were purchased from Sigma (Steinheim, Germany). Xanthine oxidase (XOD) (EC 1.1.3.22) from cow milk was purchased from Roche (Mannheim, Germany) and purified by overnight dialysis against buffer 3 in a tubular 14kDa cut-off membrane provided by Carl Roth GmbH (Karlsruhe, Germany). 11-mercapto-1-undecanoic acid (MUA), 11-mercapto-1-undecanol (MU), poly(anilinesulfonic acid) (PASA), poly(allylamine) (PAA) 20 wt. % solution in water, poly(ethylenimin) (PEI), 50 wt. % solution in water, and poly(styrenesulfonic acid) (PSS) were provided by Aldrich (Taufkirchen, Germany). Sulfuric acid, potassium phosphate, potassium dihydrogen phosphate, sodium sulfite, and calcium chloride-dihydrate were provided by

Merck (Darmstadt, Germany). Gold wire with a diameter of 0.5 mm was purchased from Goodfellow (Bad Nauheim, Germany). Silver ring electrodes were machined from 99.99 % Ag rods from GoodFellow (Bad Nauheim, Germany). 99.9% gold used for evaporation was provided by Fluka (Taufkirchen, Germany). Glass slides were purchased from Plano (Wetzlar, Germany). Silicon wafers were purchased from Wacker Chemie AG (Munich, Germany). Human SOx (EC 1.8.3.1) was produced by expression in *E.coli* cells and purified by affinity chromatography (Temple, Graf et al. 2000). The bacterial cell surface layer protein SbpA was isolated from *B. sphaericus* CCM2177 (Czech Collection of Microorganisms, Brno, Czech Republic). Growth of the organism, cell wall preparation, and extraction of the protein with guanidine hydrochloride, dialyzation and further centrifugation were carried out as previously described (Pum, Stangl et al. 1997). All solutions were prepared in 18 MΩ Millipore water (Eschborn, Germany)

3.1.3. Apparatus

All cyclic voltammetric experiments were performed with the Autolab System (Metrohm, Netherlands) in a 1 ml measuring cell using Ag/AgCl/1M KCl reference electrode (Biometra, Germany) with an exception for the experiments with assemblies on roughened Ag electrodes, where an EG&G potentiostat (Princeton Applied Research) with a 10 ml electrochemical cell with optical window (for spectroscopic measurements) and an Ag/AgCl (sat. KCl) reference electrode were used.

SERR measurements were performed with the 413 nm line of a Kr^+ laser (Innova 300, Coherent) using a confocal Raman microscope (LabRam HR-800, Jobin Yvon) equipped with a N_2(l)-cooled back-illuminated CCD detector.

An Edwards FL 400 vacuum chamber (BOC Edwards, UK) was used to evaporate Au onto a silicon wafer. All AFM studies were carried out in contact mode in liquid using Nanoscope III (Veeco instruments, Santa Barbara), a standard cell for liquid measurements and silicon nitride NP-S tips (Veeco instruments, Santa Barbara) with a nominal spring constant of 0.06 N/m.

All amperometric measurements were made using a Model 720 A Electrochemical Analyzer (CH Instruments, UK).

The photometric experiments were conducted at a Beckman DU 7400 UV-vis spectrophotometer (Fullerton, CA, USA).

A Biacore 2000 (Biacore AB, Sweden) was used for SPR experiments. QCM experiments were performed at the piezoelectric detector Multilab 3900 obtained from J. Kitlička (Brno, Czech Republic) using gold covered (5 mm in diameter) quartz crystals (ICMFG Oklahoma, USA).

3.2. Methods and Protocols

3.2.1. Cyt.c/XOD multilayers

At a first step, fabrication of cyt.c multilayer electrodes was performed by alternating incubation of cyt.c monolayer electrodes in 0.2 mg/ml PASA and 20 μM cyt. c solutions in buffer 2 for 10 minutes per each incubation step as reported in literature (Beissenhirtz, Scheller et al. 2004). Cyt.c monolayer was produced by adsorption of cyt.c on gold wire electrodes previously modified with 5 mM MUA/MU (1:3) solution in ethanol. The quality of the cyt.c multilayer was controlled by cyclic voltammetry.

After immobilization of the necessary number of (PASA-cyt.c) layers the electrodes were incubated again in PASA solution in order to obtain a negatively charged surface. For immobilization of XOD in a multilayer assembly PEI was used as a polycationic electrolyte. The electrodes were rinsed with buffer 2 and buffer 3 with subsequent alternating incubations in 0.2 mg/ml PEI and 3.5 μM XOD solutions in buffer 3 for 10 minutes. Where specifically mentioned an additional polyelectrolyte membrane was produced by adsorption of two double layers of PEI/PASA or PAA/PASA on top of the last layer of XOD. 0.2 mg/ml PAA solution was made in buffer 3. After the preparation, the electrodes were stored in buffer 3 at +4 ºC. Cyt.c monolayer ITO electrodes were prepared by overnight incubation in 20 μM cyt.c solution in buffer 1 at +4 ºC. Multilayers of PASA/cyt.c were assembled on ITO surface following the same procedure as for the gold electrodes.

The amperometric sensor response curves were recorded under constant stirring in buffer 4. The working electrode was polarized at a potential of + 150 mV. The recording was started after 100-120 s of equilibration in order to obtain a stable background current. Once the stable baseline was established, 2-10 μl aliquots of the hypoxanthine stock solution were added into the cell resulting in 0.25 - 100 μM final concentration. In the experiments aimed at investigation of the role of superoxide scavengers 10 μl of SOD stock solution (0.83 mM) was added into the cell after addition of HX at the time when the

response current reached a plateau. In addition, 5 µl ethanolic aliquots of epigallocatechin gallate (16 µM), rutin (480 µM) and luteolin (300 mM) were used to test the effects of possible interference. The resulting current was measured as a function of time.

3.2.2. Cyt.c-BOD interaction

Reaction between cyt.c and BOD was investigated at Au-MUA/MU electrodes, prepared as reported in literature (Beissenhirtz, Scheller et al. 2004). Modification of the wire electrodes with carboxy- and hydroxy-terminated alkane thiols was carried out by 48 hour incubation in 5 mM MUA/MU (1:3) ethanolic solution. A cyt.c monolayer was prepared on top of the MU/MUA layer by two hour adsorption from a 20 µM cyt.c solution in buffer 1.

The photometric experiments were conducted at a Beckman DU 7400 UV-vis spectrophotometer (Fullerton, CA, USA). Here an initial concentration of reduced cyt.c of 35 µM in air-saturated buffer 1 was used. Reduction of cyt.c was carried out in excess of sodium dithionite with subsequent gel filtration (Creutz and Sutin 1973). The kinetics of the reaction with different BOD concentrations (62.5, 100, 125, 150, 187.5, 225, 250 312.5 nM) was followed at a wavelength 550 nm for one minute after addition of the enzyme.

3.2.3. Cyt.c/BOD multilayers

Cyt.c/BOD multilayer was assembled at the surface of a cyt.c monolayer electrode, produced by adsorption of 20 µM cyt.c solution in buffer 1 on gold wire electrodes previously modified with 5 mM MUA/MU (1:3) solution in ethanol.). After formation of the cyt.c monolayer, the protein surface concentration was checked by CV.

The multilayer assembly was carried out by sequential incubations of a cyt.c monolayer electrode into PASA and a cyt.c/BOD mixture. The protein mixture solution was made in buffer 2 and contained 20 uM cyt.c and 200 nM BOD. Each of the 10-minute-long adsorption steps of PASA (2 mg/ml) and a premixed protein solution was followed by rinsing in buffer 2. The electrodes were further investigated by CV both in air-saturated and N_2-purged buffer 1.

Monitoring of the multilayer formation was carried out by SPR using clean Biacore PIONEER Sensor chips. The chip was incubated in MUA/MU (1:3) ethanolic solution for 48 hours, and subsequently washed with Millipore water and installed into the Biacore

flow system. The following solutions were injected subsequently with a flow rate of 2 µl/min: buffer 1, cyt.c (20 min), PASA (10 min), and cyt.c/BOD mixture (10 min). The two latter steps were repeated three times.

3.2.4. Cyt.c/SOx multilayers

SOx/cyt.*c* arrangement was prepared by alternating incubation of a cyt.c monolayer electrode into (i) a solution containing 10 µM SOx and 1µM cyt.c for 15 min, followed by a washing step in buffer 2, and (ii) a pure 20 µM cyt.*c* solution for 10 min. The cyt.*c* monolayer was produced by 2h adsorption of cyt.c (in buffer 1) onto a MUA/MU (1:3) pre-modified electrodes.

Electrochemical response of the electrodes was controlled by recording cyclic voltammograms (CV). After formation of the cyt.c monolayer, the protein surface concentration was checked by CV. During SOx/cyt.c assembly stages no CV measurements were performed. After the final assembly step the electrode was rinsed subsequently in buffer 2, buffer 1, and placed into the measuring cell with immersion depth of 5 mm. In the case of catalytic current recording, 10 µl of sodium sulfite stock solution was added into the measuring cell and mixed with a pipette.

Sequential deposition cycles of cyt.c and SOx/cyt.c were monitored by QCM. First, a MUA/MU modified QCM chip was washed with buffer 1 until a stable baseline signal was obtained. This step was followed by pumping a cyt.c solution for 10 min, resulting in a cyt.c monolayer formation, with subsequent washing with buffer 2. At a further step a SOx/cyt.c mixture was pumped through the cell until saturation was observed. After washing with buffer 2, a pure cyt.c solution was injected until an equilibrium signal was reached, followed by a washing step with buffer 2. These steps were repeated until a desired number of layers were deposited. All injections were carried out at a flow rate of 20 µl/min.

3.2.5. Raman spectroscopy

SERR measurements were performed with the 413 nm line of a Kr^+ laser (Innova 300, Coherent) using a confocal Raman microscope (LabRam HR-800, Jobin Yvon) equipped with a N_2(l)-cooled back-illuminated CCD detector. The laser beam was focused on the surface of the working electrode by means of a long working distance

objective (20x; N.A. 0.35). SERR spectra were acquired with laser powers of 2.5 mW or 1.4 mW, accumulation times of 4 - 8 s, spectral resolution of 2 cm^{-1} and an increment per data point of 0.57 cm^{-1}. All spectra were normalized to the power of 1 mW and accumulation time of 1 s.

For time-resolved (TR) SERR experiments, potential jumps of variable duration and size were applied to trigger the redox reaction. The relaxation process was probed by measuring the SERR spectra at variable delay times δ after each jump. Synchronization of potential jumps and measuring laser pulses was achieved with a home made four channel pulse-delay generator. The measuring laser pulses were generated by passing the laser beam through two consecutive laser intensity modulators (Linos) which give a total extinction better than 1:25000 and a time response of ca. 20 ns. The real spectra acquisition time, corresponding to the product of the measuring laser pulse length Δ and the number of cycles, was 1 to 2 s. The time-dependent spectroscopic results are displayed as a function of the delay time δ defined as $\delta = \delta^{'} + \Delta/2$. The working electrode was rotated at ca. 5 Hz to avoid laser induced sample degradation. After polynomial baseline subtraction, the measured SERR spectra were treated with a home-made component analysis software.

3.2.6. Preparation of apo-cyt.c

Apo-cyt.c was prepared by chemical removal of the haem group following the protocol of Stellwagen und Rysavy (Stellwagen, Rysavy et al. 1972). A solution of 80 mg cyt.c in 10 ml Millipore water was mixed with 2 ml acetic acid and 15 ml of 0.8% silver sulfate, and incubated for 4 hours at 44°C in dark. At a further step, the mixture was dialyzed against 0.2 M acetic acid

The apo-protein was precipitated in 10 volumes of acid acetone (100 ml of acetone and 1 ml of 5N sulfuric acid) and collected after centrifugation. After washing several times in acetone, the precipitate was dissolved in 4 ml of 0.2 M acetic acid by addition of solid urea until clarification of the solution. Silver was removed by an addition of 25 molar excess of 2-Mercaptoethanol and 20 min incubation at room temperature. Finally, the protein solution was dialyzed against buffer 2 in order to remove all low molecular weight species. Concentration of apo-cyt.c in the final solution was determined spectrophotometrically. Successful removal of the haem group was confirmed spectroscopically (no haem band at 350-450 nm) and electrochemically (no peaks in CV).

3.2.7. Preparation of ultra flat Au electrodes

Template-stripped gold foil-covered glass slides were obtained by Au evaporation onto the Si-SiO_2 template wafer. Glass slides (5x30x2 mm) were glued onto the gold layer using 301-28OZ kit (Epoxy Technology, USA). The slides with Au film were separated from the Si-SiO_2 template shortly before use. Modification of the electrodes with self-assembled alkane thiol monolayer was performed in 5 mM ethanol solution of MUA/MU (1:3) by 48 h incubation. The cyt.c multilayer electrodes on ultra flat Au were assembled following the protocol published previously for gold needle electrodes (Beissenhirtz, Scheller et al. 2004).

3.2.8. S-layer recrystallization

S-layer protein SbpA was recrystallized at PSS-terminated multilayer flat Au electrodes. Recrystallization of SbpA was carried out by 3 h incubation (if not mentioned specifically) of an electrode in crystallization solution of 0.1 mg/ml SbpA in buffer 6. Adsorption of PSS was accomplished by an electrode incubation in 10 mM PSS solution (buffer 2) for 10 minutes. After recrystallization the electrodes were rinsed sequentially with buffer 6 and buffer 1 and subjected to AFM or electrochemical measurements.

3.2.9. AFM measurements in liquid media

Topography studies were performed with ultra flat Au electrodes with freshly prepared polyelectrolyte multilayer films of desired composition. The sample was glued to the magnetic sample holder with a double-adhesive tape and placed onto the scanning stage. A few drops of buffer 1 were placed upon the sample until it was covered. The scanning head (multimode) with an installed tip was subsequently fixed

Force-distance curves were measured by approaching and retracting the AFM tip to and from the surface while monitoring the deflection of the cantilever spring.

4. Results and discussion

This chapter is divided into two main parts: 4.1 describing results on protein multilayer architectures by co-immobilization with polyelectrolytes, and 4.2 showing an alternative approach for multi-protein assembly without the use of synthetic polymers. In addition, section 4.3 demonstrates a combined approach for assembly of protein layered architectures taking advantage of both LbL self-assembly and S-layer recrystallization techniques.

4.1. Single protein multilayer

The part of the work described in the current chapter was focusing on the development and characterization of electroactive protein multilayers on electrodes using cyt.c as a basic component. Based on the previously reported multilayer assembly of cyt.c with sulfonated polyaniline, where cyt.c could exchange electrons with the neighboring cyt.c molecules, this approach was extended to polyelectrolyte protein multilayers containing two functionally linked proteins.

4.1.1. Cyt.c multilayer

Assembly of cyt.c multilayer LbL films with sulfonated polaniline has been shown to be an efficient strategy to increase the surface concentration of the electroactive protein at a promoter-modified electrode (Beissenhirtz, Scheller et al. 2004). A schematic representation of the cyt.c/PASA multilayer is shown in Figure 4.1 (left). Formation of the cyt.c/PASA multilayer was verified by surface plasmon resonance and QCM experiments. Investigation of the assembly by cyclic voltammetry showed an increase in the surface concentration of the electrode-addressable protein upon each immobilization cycle (Figure 4.1, right). Multilayers consisting of up to 15 cyt.c/PASA layers showed a quasi-reversible electron transfer with a linear increase in the amount of electroactive protein.

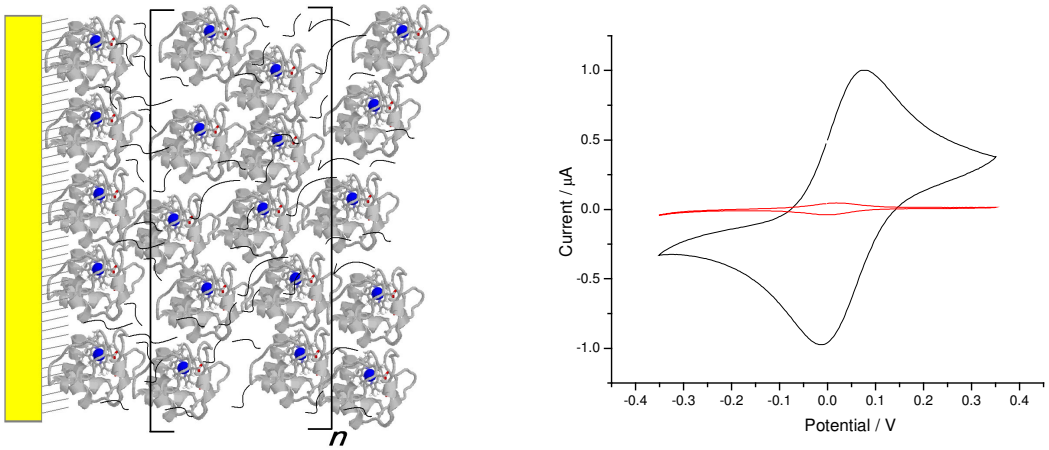

Figure 4.1. Schematic image of the cyt.c/PASA multilayer electrode (left) and cyclic voltammograms of a cyt.c monolayer (red) and multilayer (black) electrodes, scan rate 100 mVs^{-1} (right).

4.1.1.1. Assembly and its characteristics

A striking effect of the long-distance electron transfer shown by these assemblies indicated that not only cyt.c molecules located in close proximity to the electrode surface contribute to a net response current, but also those at the outer parts of the multilayer. Since such films revealed an electron transfer over a distance of several nanometers, two hypothetical mechanisms should be considered: (i) the electrons are transferred by a conducting form of sulfonated polyaniline from one cyt.c molecule to another cyt.c and then to the electrode surface, and (ii) cyt.c molecules immobilized in the polyelectrolyte matrix are themselves responsible for a long-range electron transfer, occurring via face-to-face electron hopping, while the polyelectrolyte only stabilizes the arrangement, not being involved in the electron transfer process.

Evidence that PASA undergoes redox transformations in the potential range from –350 to +350 mV was obtained in this study by CV of a cyt.c/PASA multilayer electrode at low scan rates (Figure 4.2), showing a redox activity of PASA with a formal potential of about 200 mV. Therefore, this result shows a possibility that the electron transfer in the multilayer may happen via PASA acting as a molecular wire.

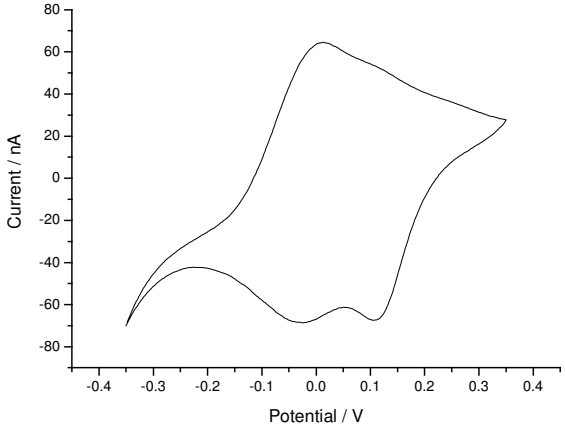

Figure 4.2. Cyclic voltammograms of Au-MUA/MU-cyt.c-(PASA-cyt.c)$_6$ electrode measured in 5 mM phosphate buffer pH 7; scan rate 5 mVs^{-1}

At the same time, several experiments reported in literature show that the protein-protein electron transfer mechanism can be a dominating mechanism (see the literature digest, chapter 2.3.3.). Therefore, an additional method is necessary to clarify the role of both assembly components in the electron transfer process.

Co-immobilization of proteins with polyelectrolytes may induce conformational changes of the protein structure. Such changes were reported for cyt.c bound to a PSS terminating layer of the PAH/PSS multilayer, or embedded into a PSS matrix (Weidinger, Murgida et al. 2006). In the case of a cyt.c/PASA multilayer a slight difference in the formal potential of the multilayer electrode and the monolayer electrode suggests a distribution of the cyt.c states within the multilayer. These questions will be discussed in detail in the following chapter.

4.1.1.2. Surface-enhanced resonance Raman spectroscopy of cyt.c/PASA films

The stationary and time-resolved surface-enhanced Raman (SERR) spectroelectrochemistry technique was used for simultaneous monitoring of the two main components of the assemblies (cyt.c and PASA). In order to obtain the effect of surface enhancement, roughened Ag electrodes were used instead of gold wires. First, cyt.c electrostatically adsorbed onto MUA/MU-modified Ag electrodes was investigated by potential-dependent SERR. Spectra of the adsorbed protein recorded at potentials sufficiently negative or positive with respect to the formal potential were identical to the

resonance Raman (RR) spectra of the ferrous and ferric cyt.c in solution, respectively. RR and SERR spectra of heme proteins measured under Soret band excitation (ca. 410 nm) are dominated by the totally symmetric modes of the porphyrin ring. The so-called marker band region (ca. 1300-1700 cm^{-1}) includes a number of bands that are particularly sensitive to electronic and structural properties of the heme iron, such as ligation pattern, spin and oxidation state (Scott and Mauk 1995). Thus, it can be concluded that the protein native structure is preserved in the electrostatic complex, at least at the level of the heme pocket. Accordingly, a series of SERR spectra measured at various potentials from -0.2 V to +0.14 V could be consistently described on the basis of only two spectral components, i.e. the ferrous and ferric native cyt.c, using only their relative contributions as adjustable parameters (Hu, Morris et al. 1993). The results were quantitatively treated in terms of the Nernst equation expressed as:

$$E = E^0 - \frac{RT}{zF}\ln\frac{f_{\mathrm{Re}d}}{f_{Ox}} - \frac{RT}{zF}\ln\frac{I_{\mathrm{Re}d}}{I_{Ox}} \qquad (4.1)$$

where I_i is the relative intensity of an individual spectral component and f_i is a factor proportional to the reciprocal SERR cross section of the species. The factors $f_{Red} = 0.28$ and $f_{Ox} = 1.00$ were estimated from the relative RR intensities of the fully reduced and fully oxidized cyt.c measured in solution under, otherwise, identical conditions.

This procedure yields nearly ideal Nernstian plots for a one-electron process with $E_0 = 20 \pm 10$ mV (vs. Ag/AgCl/ sat. KCl) and $z = 0.9 \pm 0.1$. The formal potential obtained by SERR is in excellent agreement with the results of CV measurements and with literature data for cyt.c immobilized on SAM-coated electrodes (Dopner, Hildebrandt et al. 1996; Lisdat, Ge et al. 1999; Lisdat, Ge et al. 1999; Beissenhirtz, Scheller et al. 2004).

Using the Ag-MUA/MU-cyt.c protein films as a template, multilayer assemblies of the type Ag-MUA/MU-cyt.c-(PASA-cyt.c)$_n$ were constructed by successive layer-by-layer deposition of PASA and cyt.c and characterized by CV. As shown in Figure 4.3, the loading of electrochemically addressable protein multiplies upon increasing n from 1 to 10, in agreement with previous results using Au needle electrodes (Beissenhirtz, Scheller et al. 2004; Beissenhirtz, Scheller et al. 2004). However, in contrast to these studies, the upper layers are significantly less stable on roughened Ag electrodes as indicated by a steady

decrease of the electrochemical signal during the first minutes after preparation. Presumably, the different stability behavior on the two metals is related to differences in the local electrostatics due to very different potentials of zero charge (Valincius 1998; Murgida and Hildebrandt 2001). In addition the surface roughness at the silver electrodes used within this study is much higher than at the gold needle electrodes. Therefore, SERR investigations were restricted to the stable Ag-MUA/MU-cyt.c-PASA-cyt.c assemblies (n = 1).

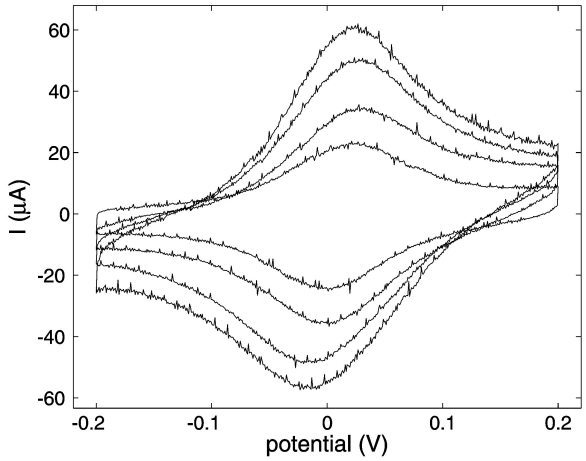

Figure 4.3. Cyclic voltammograms of Ag-MUA/MU-cyt.c-(PASA-cyt.c)$_n$ electrodes with n = 1, 3, 6 and 10, measured immediately after preparation. Scan rate: 100 mV s^{-1}.

SERR spectra of these assemblies exhibit the typical bands of native reduced and oxidized cyt.c. In addition, a relatively strong band at ca. 1620 cm^{-1} is observed (Figure 4.4), which is assigned to the C=C and C-C stretching vibrations of the quinoid and benzenoic rings of the co-adsorbed PASA polyelectrolyte (Valette and Hamelin 1973; Boyer, Quillard et al. 1997). Here, the spectral contribution of the polyelectrolyte in Figure 2 is divided in two components (PASA1 and PASA2, as described further), while cyt.c components are adopted from RR measurements in solution of the native ferrous and ferric species.

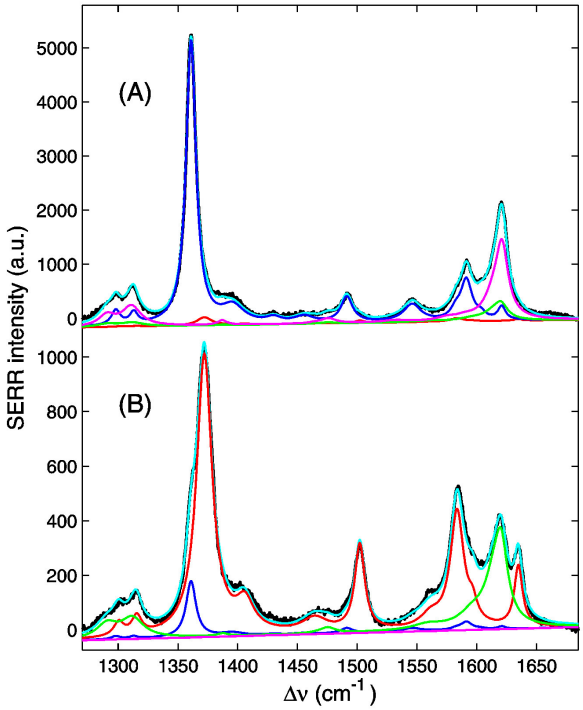

Figure 4.4. Measured SERR spectra and component analysis of the Ag-MUA/MU-cyt.c-PASA-cyt.c electrode at two different potentials: -0.1 V (A) and +0.12 V (B). Black: experimental spectra, cyan: overall fit, red: cyt.c oxidized, blue: cyt.c reduced, magenta: PASA1, green: PASA2.

Nernst analysis of potential-dependent SERR spectra of cyt.c from several electrodes yields an average value E_0 = 28 ± 10 mV (vs. Ag/AgCl/ sat. KCl) for the formal potential of cyt.c, which is in agreement with the value determined by CV and very close to the value observed for Au-MUA/MU-cyt.c assemblies. In addition, CV experiments show a linear relationship between peak currents and scan rates, indicating that the electrochemically addressable protein is actually immobilized.

4.1.1.3. Redox behavior of PASA by SERR

Direct adsorption of PASA on the Ag-MUA/MU electrodes is very poor, as judged from the lack of a SERR signal. This can be explained by electrostatic repulsion of the polyelectrolyte, since the surface layer bears the charge of the same sign. In contrast, assemblies, where cyt.c is replaced by the spectroscopically and electrochemically inert apo-protein (apo.cyt.c), consisting of apo.cyt.c/PASA/apo.cyt.c, show strong characteristic PASA signals. Representative spectra recorded at two extreme potentials are shown in Figure 4.5. The affinity of PASA for the apo-protein reflects the opposite charge of the

polyelectrolyte and the protein at pH 5 and is in agreement with previously reported QCM experiments (Beissenhirtz, Kafka et al. 2005).

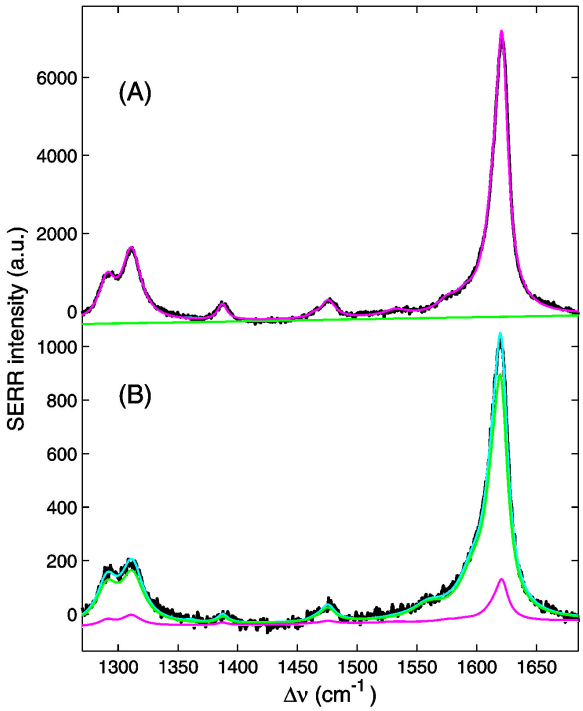

Figure 4.5. Measured SERR spectra and component analysis of the Ag-MUA/MU-apo.cyt.c-PASA-apo.cyt.c electrode at two different potentials: -0.4 V (A) and +0.25 V (B). Black: experimental spectra, cyan: overall fit, magenta: PASA1, green: PASA2.

Notably, upon raising the electrode potential from -0.40 to +0.25 V (vs. Ag/AgCl/ sat. KCl), the SERR intensity decreases by about a factor of 7. This intensity change is fully reversible and, therefore, cannot be ascribed to a partial desorption of the polyelectrolyte.

Polyanilines are known to undergo redox transitions between the oxidized pernigraniline form through the emeraldine base to the reduced leucoemeraldine form (Gruger, Novak et al. 1994). In addition, protonation of the emeraldine base gives rise to the emeraldine salt, which can be conducting under certain conditions (Huang, Humphrey et al. 1986). All these different polyaniline forms differ in color and thus in the absorption spectra (Macdiarmid, Yang et al. 1987; Hugotlegoff and Bernard 1993). The very strong PASA intensity at negative potentials can, therefore, be explained in terms of a strong resonance enhancement at the excitation wavelength of 413 nm. For different kinds of

sulfonated polyanilines, an absorption band at ca. 420 nm was assigned to emeraldine salt form, which is responsible for the conducting properties of the polyelectrolyte (Saricifti and Kuzmany 1987).

Thus, the SERR spectra recorded at the two extreme potentials most likely refer to different redox and protonation states of PASA. These states exhibit different absorption properties and SERR cross sections at the excitation wavelength; however, an unambiguous identification of these species is not possible on the basis of the present results. The interpretation is supported by the fact that the potential-dependent intensity drop is accompanied by small but distinct spectral changes that are indicative of chemically different species. Specifically, the most prominent PASA band at 1620 cm^{-1} is downshifted by ca. 1 cm^{-1} at positive potentials. This shift is accompanied by a broadening and the appearance of a more pronounced shoulder on the low frequency side. In addition, a potential-dependent change in relative intensities of the two bands at 1290 and 1311 cm^{-1} is observed.

The spectra obtained at -0.40 V and 0.25 V, denoted as PASA1 and PASA2 correspondingly, were then used as components for simulating the spectra recorded at the intermediate potential values. A consistent description of the experimental spectra was obtained in the entire potential range by solely varying the relative contributions of the spectral components PASA1 and PASA2.

Unlike cyt.c, the relative cross sections for the two PASA components are unknown and, therefore their intensities cannot be converted to relative concentrations. Alternatively, the PASA1 intensity at the most negative electrode potential is arbitrarily defined as equal to 1.0 in order to illustrate the potential-dependent variation of the relative contribution of PASA1.

Figure 4.6 compares the potential dependence of the PASA1 component for the electrodes containing cyt.c and apo.cyt.c.

Notably, for Ag-MUA/MU-apo.cyt.c-PASA-apo.cyt.c electrodes the decrease of the PASA1 contribution occurs over a very broad potential range. In contrast, Ag-MUA/MU-cyt.c-PASA-cyt.c electrodes show a better defined (reversible) transition at ca. 0 mV (vs. Ag/AgCl/ sat. KCl), which is very close to the formal potential of the immobilized cyt.c. This observation suggests, although does not prove, an electron exchange between cyt.c and PASA.

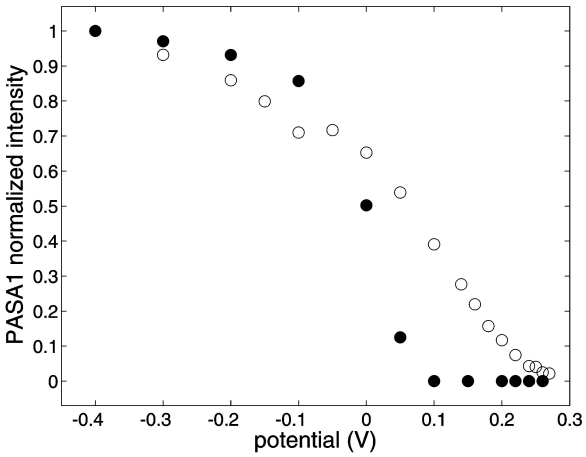

Figure 4.6. Normalized intensity of the PASA1 spectral component as a function of the electrode potential. Solid circles: Ag-MUA/MU-cyt.c-PASA-cyt.c electrode. Hollow circles: Ag-MUA/MU-apo.cyt.c-PASA-apo.cyt.c electrode.

4.1.1.4. Electron transfer dynamics and mechanism

The time response of Ag-MUA/MU-cyt.c-PASA-cyt.c electrodes to changes of the poised potential was investigated by time–resolved (TR) SERR. Spectra were measured at variable delay times δ after a potential jump from an initial value E_i to a final potential E_f. TR-SERR spectra were submitted to the same kind of component analysis as used for stationary measurements. For all TR-SERR experiments E_i = -80 mV (vs. Ag/AgCl/ sat. KCl) was selected. At this potential, cyt.c is nearly fully reduced and the polyelectrolyte signal is largely dominated by the intense PASA1 component, such that the spectral changes resulting from potential jumps in the positive direction can be easily followed (Figure 4.7).

Assuming a one step relaxation process, the time-evolution of the relative concentrations for ferric and ferrous cyt.c can be described according to equation 4.2

$$\frac{\Delta c_\delta}{\Delta c_0} = \frac{c_{red}(t=\delta) - c_{red}(t=\infty)}{c_{red}(t=0) - c_{red}(t=\infty)} = \exp\left(-\left(k_{ox} + k_{red}\right) t\right) \quad (4.2)$$

where $c_{red}(t=\delta)$ denotes the concentration of reduced cyt.c at delay time δ, $c_{red}(t=\infty)$ and $c_{red}(t=0)$ refer to the equilibrium concentrations at the final potential E_f and at the

initial potential E_i, respectively. The oxidation and reduction rate constants k_{ox} and k_{red} are linked through the equilibrium constant $K = k_{ox}/k_{red}$, which is determined from the stationary potential-dependent SERR experiments. The one step relaxation model appears to be justified since logarithmic plots according to equation 4.2 yield straight lines with intercept values very close to zero.

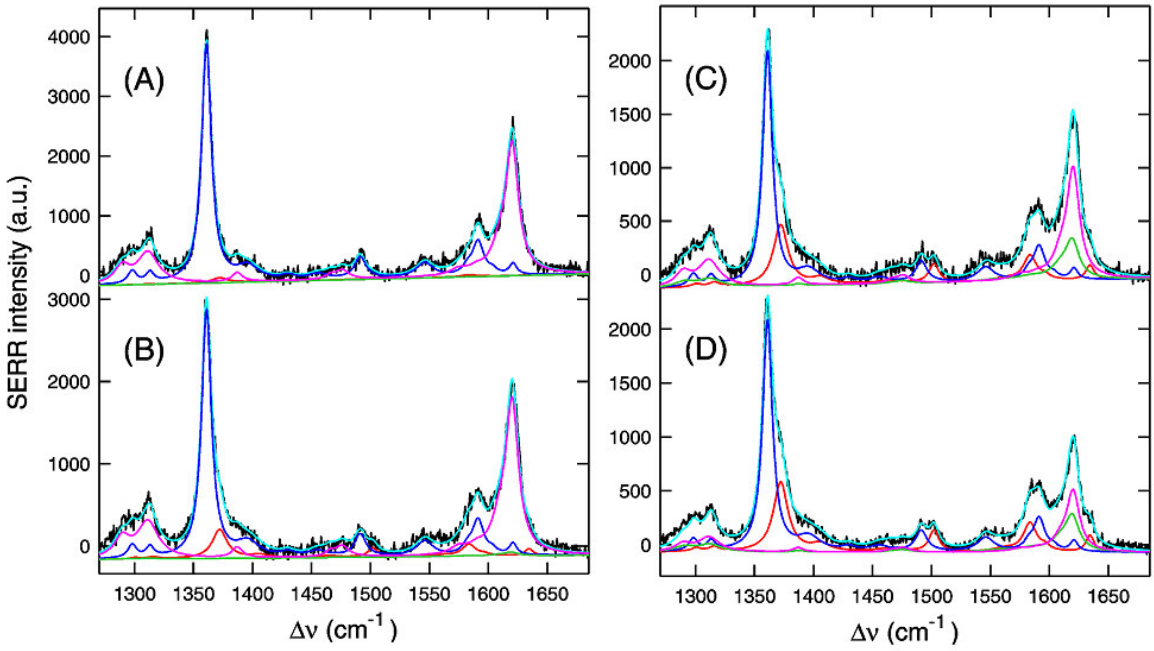

Figure 4.7. TR-SERR spectra of an Ag-MUA/MU-cyt.c PASA-cyt.c electrode at different delay times after a potential jump from E_i = -80 mV to E_f = 25 mV. (A) δ = 0; (B) δ = 21 ms; (C) δ = 210 ms and (D) δ = ∞. Black: experimental spectra, cyan: overall fit, red: cyt.c oxidized, blue: cyt.c reduced, magenta: PASA1, green: PASA2.

For potential jumps to the redox potential of cyt.c, i.e. E_f = 25 mV (vs. Ag/AgCl/ sat. KCl), the average value for $k_{ox}^0 \left(= k_{red}^0\right)$, obtained for several Ag-MUA/MU-cyt.c-PASA-cyt.c electrodes, was found to be $17 \pm 7\ s^{-1}$, which is very close to the value determined for Ag-MUA/MU-cyt.c assemblies, i.e., in the absence of PASA ($k_{ox}^0 = k_{red}^0 = 22 \pm 8\ s^{-1}$).

As shown in Figure 4.8, the polyelectrolyte undergoes spectral changes on a similar time scale. The intensity decay of the PASA1 component, however, cannot be satisfactorily treated as a single exponential and instead a minimum of two exponentials is required. This, however, does not rule out an even more complex kinetics, as one might expect from the structural complexity of the assemblies.

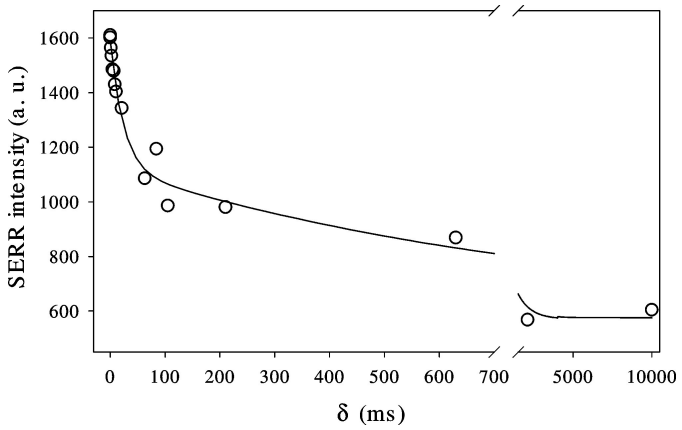

Figure 4.8. Absolute SERR intensity of the PASA1 spectral contribution as a function of the delay time δ after a potential jump from -80 mV to 25 mV for an Ag-MUA/MU-cyt.c-PASA-cyt.c electrode.

The average values of the two decay constants for the PASA1 component of several Ag-MUA/MU-cyt.c-PASA-cyt.c assemlies are $k_1^{app} = 35 \pm 15\,\mathbf{s}^{-1}$ and $k_2^{app} = 1 \pm 1\,\mathrm{s}^{-1}$ (Figure 4.8). Within the experimental error, the value of the first decay constant is similar to the electron transfer rate constant of cyt.c.

Potential jumps to E_f = 140 mV (vs. Ag/AgCl/ sat. KCl), which correspond to an overpotential of about 115 mV for cyt.c oxidation, produce an acceleration of the apparent rate constant of oxidation of cyt.c ($k_{ox} = 120 \pm 30\,\mathbf{s}^{-1}$) as well as of the first PASA decay constant ($k_1^{app} = 135 \pm 30\,\mathbf{s}^{-1}$), while the second PASA decay constant remains unaltered within the experimental error ($k_2^{app} = 3 \pm 2\,\mathrm{s}^{-1}$). Control experiments with Ag-MUA/MU-apo.cyt.c-PASA-apo.cyt.c assemblies yield $k_1^{app} = 2 \pm 1\,\mathrm{s}^{-1}$ and $k_2^{app} = 0.01 \pm 0.01\,\mathrm{s}^{-1}$ for jumps to E_f = 25 mV (vs. Ag/AgCl/ sat. KCl) and nearly no acceleration is observed for E_f = 140 mV. Consistently, the apparent formal potential of PASA immobilised with the help of cyt.c on a MU/MUA coated electrode is about +140 mV (the PASA signal can be only observed at small scan rates). SPR measurements indicate that apo.cyt.c possesses a stronger binding affinity to the surface than cyt.c. Therefore, the presence of apo.cyt.c strongly bound to the MU/MUA SAM is expected to slow down the direct electron transfer from PASA to the electrode.

The results clearly show that in the Ag-MUA/MU-cyt.c-PASA-cyt.c system a fraction of PASA is oxidized with the same rate as cyt.c (k_1^{app}). This observation is

consistent with a mechanism in which the heterogeneous electron transfer is limited by electron tunneling between the electrode and the first cyt.c layer electrostatically adsorbed to the MUA/MU SAM. These cyt.c molecules then undergo a rapid electron exchange with the nearby redox centers of the PASA molecules. The remaining fraction of PASA redox sites may be oxidized/reduced via direct electron transfer to/from the electrode (k_2^{app}).

Thus, it can be concluded that in a simple cyt.c-PASA-cyt.c system assembled on promoter-modified silver, PASA undergoes redox conversion both by a direct electron exchange with the surface (slow process) and via cyt.c as a redox mediator (rapid process). It can be expected that similar phenomena also take place in the PASA/cyt.c multilayer assembled on gold, however the results obtained with the Ag-MUA/MU-cyt.c-PASA-cyt.c electrodes do not allow to make this conclusion.

4.1.1.5. Multilayer surface properties by AFM

Since one of the assembly components of Au-MUA/MU-cyt.c-(PASA/cyt.c)$_n$ assemblies is a globular protein one can expect a difference in binding behavior and hence different layer properties, compared to pure polymer-based systems. Here the topography of the multilayer surface was analyzed throughout the assembly steps by AFM in liquid. Additional information about the tip-surface interactions was acquired by measuring force-distance curves.

Use of flat gold provides an opportunity for a detailed surface characterization by force microscopy imaging during the stages of the assembly process. This information will help to reveal individual features of layer organization of the protein-polyelectrolyte multilayer. Along with surface visualization, a general idea about the forces between the AFM tip and the surface, and thus the properties of the outer layer, can be obtained by measuring force-distance curves.

Here, in order to perform surface analysis, the protocol for cyt.c/PASA multilayer assembly on Au needle electrodes is transfered to planar gold electrodes with a nanometer-range roughness. Polyelectrolyte assemblies prepared on these electrodes show a linear increase in electrochemical response, similar to the needle electrodes, as illustrated in the cyclic voltammograms in Figure 4.9. However, the amount of deposited electroactive cyt.c for flat gold electrodes is substantially lower than that of the needle electrodes, which is attributed to a difference in micro-roughness: while arrangements of six PASA/cyt.*c* layers

on needle electrodes resulted in about 200 pmol cm^{-2}, the multilayers of the same composition formed on flat gold electrodes exhibit a value of about 30 pmol cm^{-2}.

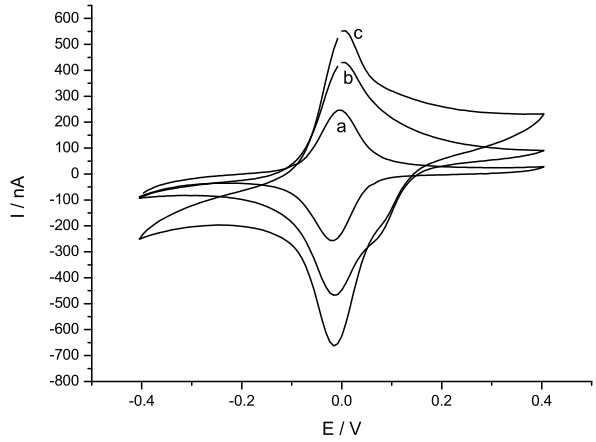

Figure 4.9. Cyclic voltammograms of modified flat gold electrodes: a) cyt.c monolayer; b)(PASA-cyt.c)$_3$; c) (PASA-cyt.c)$_6$. Scan rate 200 mVs^{-1}

Blank gold electrodes, separated from the wafer template showed a RMS roughness of 0.3 nm at a scan size of 1 μm^2 scanned both in dry state and in buffer 1. These values are in correspondence with the results reported for other template-stripped gold surfaces and allow investigation of the subsequently adsorbed polyelectrolyte-protein film (Wagner, Hegner et al. 1995). Force-distance curves of the unmodified electrodes indicate a solid surface and absence of electrostatic interaction between the AFM tip and the Au surface.

In order to estimate mechanical features of the MUA/MU layer, which was produced by chemisorption of the mixed alkanethiols from solution in ethanol, several AFM scans were measured with different force applied to the cantilever. First, the scanning was performed with a low force, just enough to resolve the relief of the surface (Figure 4.10.a). Here no characteristic gold surface features could be seen. The image obtained with increased force had a typical gold structure, Figure. 4.10.b. The third scan was performed at the same landing point as the two previous, again with a low force, indicating that the MUA/MU SAM was not totally removed by the AFM tip during scanning at high force (data not shown). Notably, by this step (scanning at low force second time) the surface became more uniform. The force-distance curve of the MUA/MU-modified gold showed the presence of a repulsive interaction between the AFM

tip and the surface (Figure 4.10.c), which can be explained by the negative charge at both the tip and the alkanethiol layer while measuring in buffer 1. It is also apparent from the force curve, that the surface is still solid.

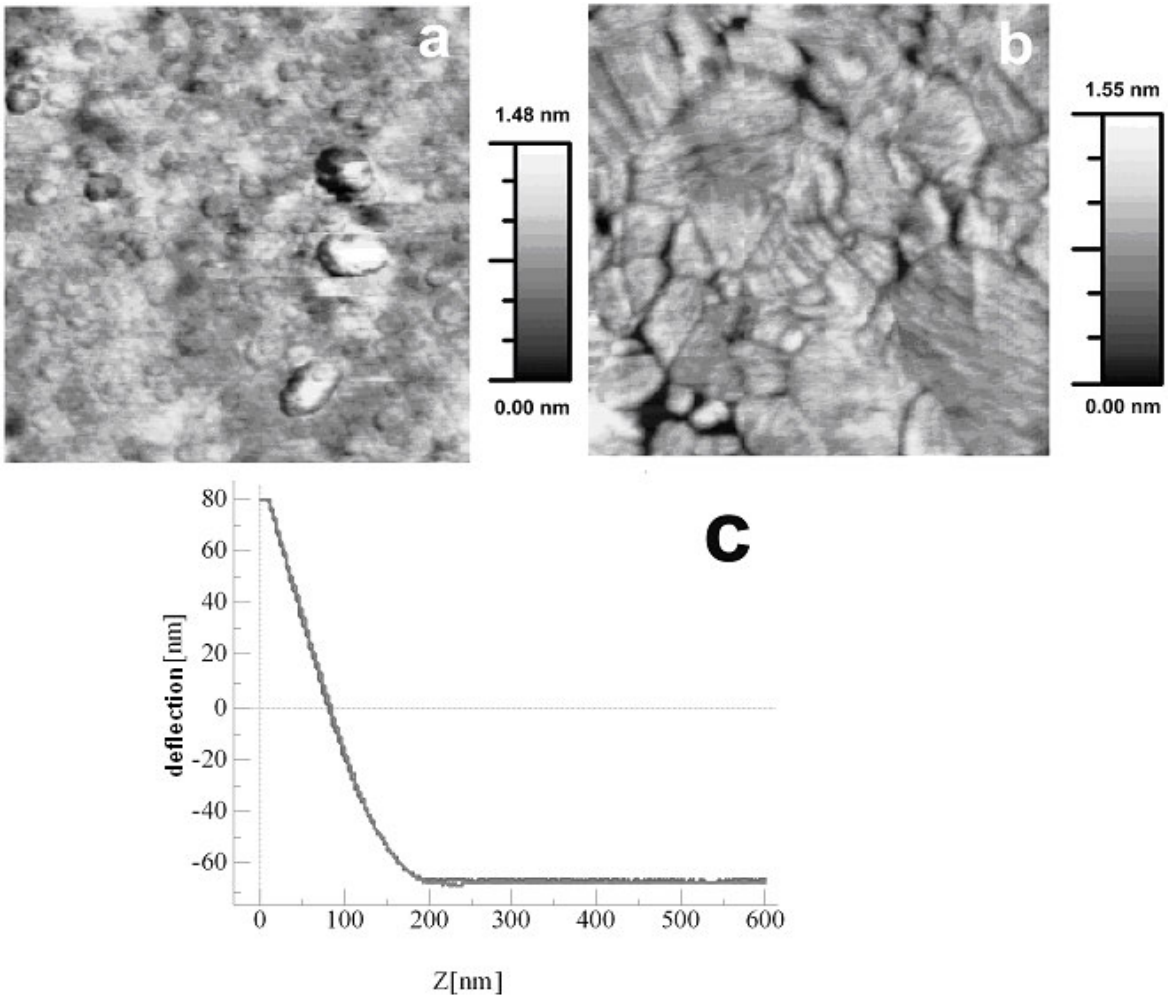

4.10. AFM (scan size 800x800 nm^2) of a MUA/MU-modified flat gold surface: a) topography measured at low force; b) topography measured at high force; c) force-distance curve. Measured in buffer1.

Subsequent adsorption of cyt.*c* onto the MUA/MU layer resulted in formation of a rather uniform protein layer (Figure 4.11.a). Topography images of this layer suggest that the adsorbed protein is bound to the promoter strong enough not to be swept away by the AFM tip in contact mode during measurements in liquid. This conclusion is also supported by the behavior of the force-distance curves, Figure 4.11.b. Here, the extension part of the

curve before and after the contact point has a linear form, showing no electrostatic repulsion between the tip and the cyt.*c* surface layer. Remarkably, the retraction curve after contact shows that the tip still remained attached to the surface until a critical pull-off force was reached. This effect can be due to the tip adhesion to the cyt.*c* layer.

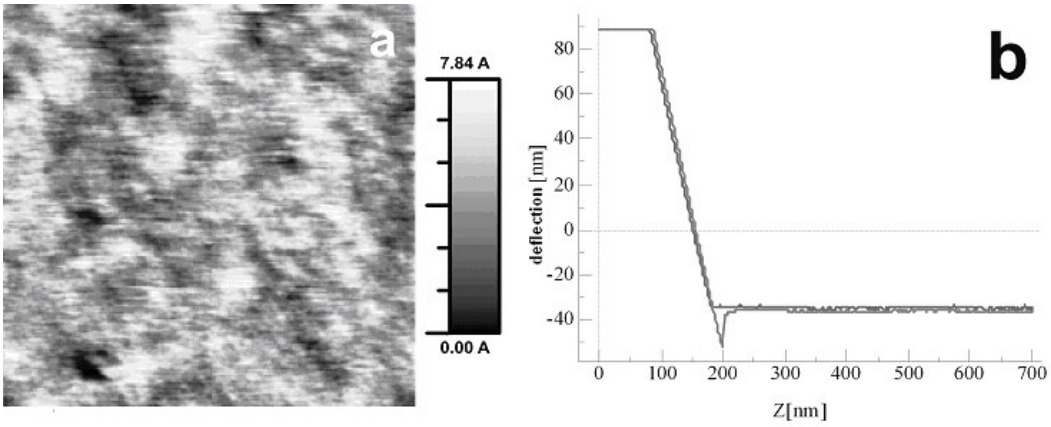

4.11. AFM (scan size 1x1 μm^2) of a cyt.c monolayer formed at the MUA/MU promoter-modified flat gold surface: a) topography scan; b) force-distance curve. Measured in buffer 1.

Further, a cyt.*c* monolayer electrode was incubated in a PASA solution and subsequently rinsed. As shown in Figure 4.12.a, the terminating PASA surface consists of a soft and loosely attached adhesive material, which at some points leads to tip contamination and appearance of stripe-like scanning artifacts. More insight into the PASA layer properties is provided by the force curve in Figure 4.12.b: whereas the extension segment shows electrostatic repulsion; the retraction part gives evidence for the presence of an adhesive soft material. Moreover, the fact that the approach segment has two slopes is an evidence for a very soft thin teminating layer.

After the second adsorption of cyt.c (Au-MUA/MU-cyt.c-PASA-cyt.c) the electrodes have rather similar topography as the cyt.c monolayer electrodes. However, with each further adsorption step, the surface becomes more heterogeneous and soft. The surface images and the force-distance curves of the next PASA and cyt.c deposition steps are almost identical to the results obtained in preceding immobilization steps.

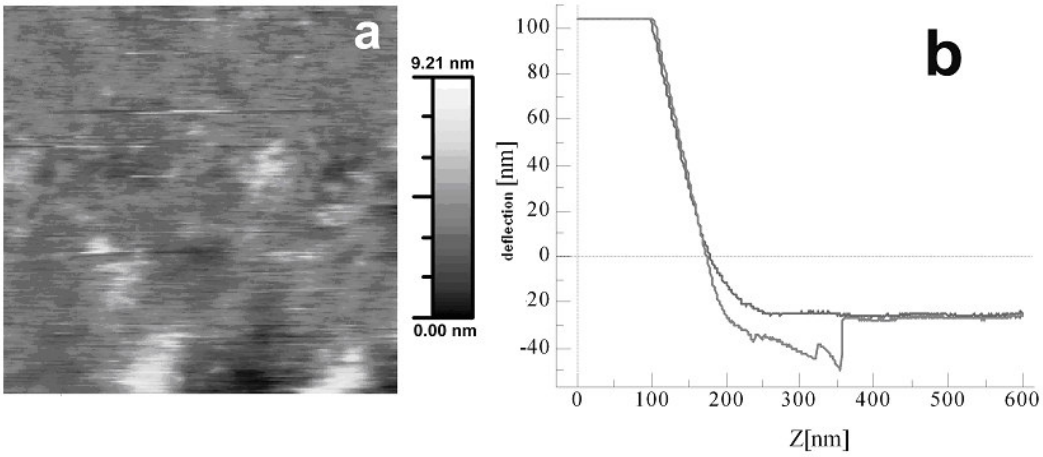

Figure 4.12. AFM (scan size 800x800 nm^2) of PASA adsorbed on cyt.c monolayer: a) topography scan with stripe-like scanning artifacts; b) force-distance curve. Measured in buffer1.

It can be therefore concluded that the properties of the terminating layer of the assembly correspond to the material adsorbed (cyt.c or PASA), which periodically alternates in each deposition cycle. The layers are formed as separate units rather than as a mixture of the two materials.

4.2 Bi-protein multilayers

4.2.1. Mediated electron transfer chains

As shown above, the cyt.c/PASA multilayer assembly exhibits a long-distance electron transfer within the film. Here another kind of electron transfer pathway is demonstrated, involving a second protein immobilized into a multilayer film.

4.2.1.1. Xanthine oxidase-cyt.c multilayer

Based on the cyt.c/PASA system, a two-protein multilayer assembly on gold electrodes has been developed in the current study in order to demonstrate the potential for an extension of applications of such protein/polyelectrolyte architectures. Here xanthine oxidase (XOD) has been combined with cyt. c. With this arrangement, a signal chain from hypoxanthine (HX) in solution via the two proteins towards the electrode could be established. Advantageously, the layer-by-layer deposition allows control over the physical characteristics of the assembly.

4.2.1.1.1. Concept

As a further development of the polyelectrolyte multilayer protein architecture, a system combining two proteins in order to construct a novel multicomponent signal chain is proposed. For this purpose, an arrangement combining multilayers of cyt.c with a multilayer assembly of XOD (Figure 4.13) was fabricated. The XOD/polyelectrolyte multilayer is located at the exterior part of the electrode and shall communicate both with the underlying cyt.c layers and with HX species in solution. XOD catalyzes the conversion of hypoxanthine to uric acid according to the following reaction scheme:

$$HX + O_2 \rightarrow UA + H_2O_2 \qquad (4.3)$$

Besides the two electron transfer to oxygen resulting in H_2O_2 there is also a one-electron pathway leading to the direct liberation of superoxide radicals (see the literature digest, chapter 2.2.2). On the other hand, XOD was shown to accept cyt.c as a reaction partner. Thus, in this study a special focus is given to the mechanism of charge transfer through such an assembly, which can be considered as a signal chain from HX via the two proteins towards the electrode.

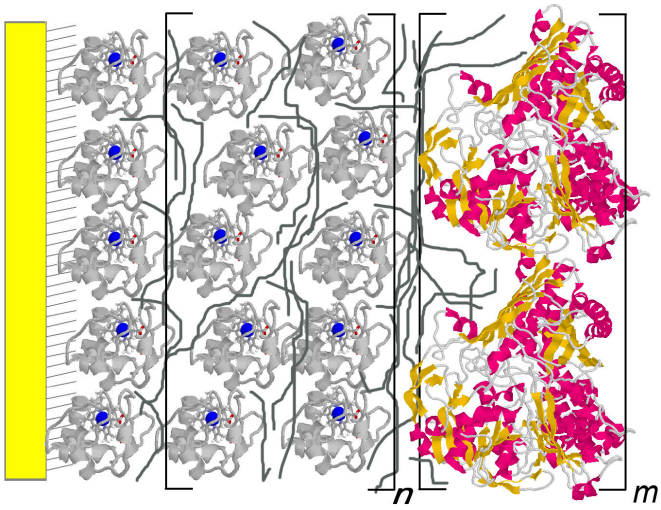

Figure 4.13. Scheme of the cyt.c/PASA-XOD/PEI multilayer assembly. A cyt.c monolayer is formed on MUA/MU (1:3) modified gold electrodes. The cyt.c multilayer is built by alternating incubations in PASA and cyt.c solutions. Finally, multilayers of PEI/XOD are assembled on the surface. (Preparation conditions: 0.2 mg/ml PEI and 3.5 μM XOD in 0.5 mM phosphate buffer pH 6.0, 10 min per each incubation step).

4.2.1.1.2. Assembly and electrochemical response

Xanthine oxidase is a slightly basic enzyme (pI = 5.1) therefore a cationic polyelectrolyte is necessary to perform the multilayer assembly (Xu, Xie et al. 1995). After preliminary experiments testing the formation process, poly(ethyleneimine) was chosen for this purpose.

However, after the immobilization of the first PEI layer onto PASA, the characteristic cyt.c redox peaks were hardly noticeable in cyclic voltammograms.

Amperometric measurements indicate that cyt.c is still electrochemically active in the polyelectrolyte multilayer after PEI immobilization, although cyt.c could not be addressed directly by CV. The electrode comprising cyt.c and XOD multilayers was polarized at a potential of +150 mV, and 10μM of HX was added into the measuring cell. The response curve of an electrode consisting of 3 PASA/cyt.c layers and 2 PEI/XOD layers is shown in Figure 4.14. The oxidation current reached 90 % of the response within 50 seconds.

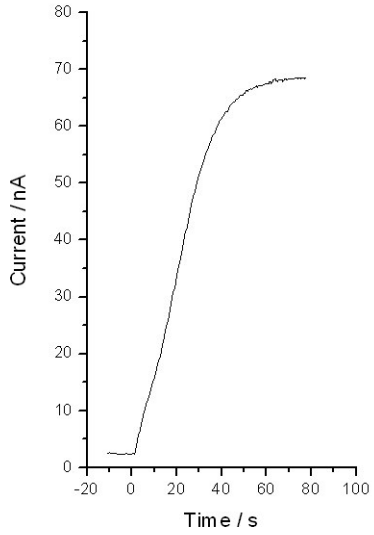

Figure 4.14. Amperometric response of an Au-MUAMU-cyt.c-(PASA-cyt.c)$_3$-PASA-(PEI-XOD)$_2$ electrode on addition of HX resulting in 10 μM concentration. (+150 mV, buffer 4, stirred solution).

As the control electrodes that had only PEI/XOD or PASA/cyt.c multilayers showed no response on addition of HX, this result clearly verifies that a signal chain from HX via the two proteins towards the electrode has been established. Thus, both structural components are essential for electron transport from HX to the electrode surface. Based on these results, a possible mechanism of the electron transfer will be discussed below.

4.2.1.1.3. Characterization of the multilayer formation

The formation of the polyelectrolyte multilayer arrangement consisting of cyt.c and XOD layers was proven by Surface Plasmon Resonance experiments.

In order to clarify whether XOD can be successfully immobilized in a polyelectrolyte network on top of cyt.c, different immobilization conditions have been tested.

Gold electrodes, modified with MUA/MU, were incubated in cyt.c and PASA solutions resulting in a negatively charged surface layer; then, adsorption of poly(ethyleneimine) rendered the surface positive thus facilitating the immobilization of anionic XOD (at pH 6.0). An example of PEI/XOD multilayer formation on cyt.c is given in Figure 4.15. Binding of both polyelectrolytes PASA and PEI was fast, whereas XOD showed a slower association behavior. Moreover, during adsorption of PEI to XOD some

XOD was removed from the electrode surface due to strong interaction with the polyelectrolyte in solution.

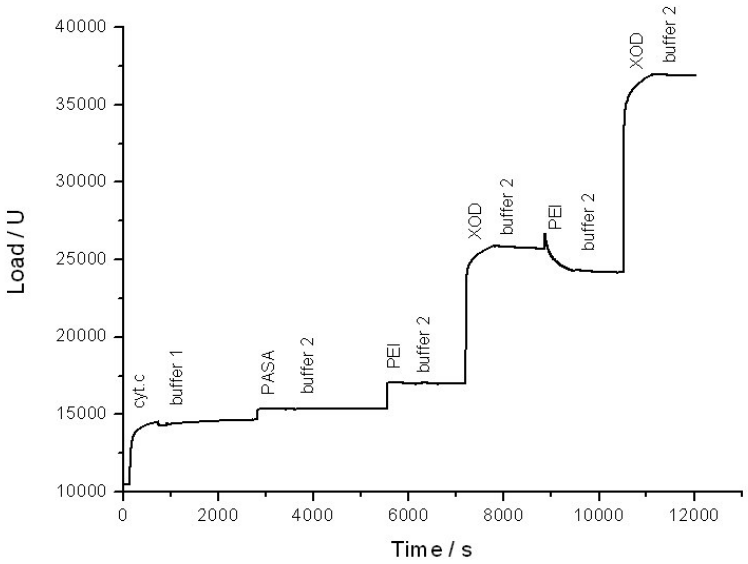

Figure 4.15. SPR experiment showing formation of XOD multilayers in a PEI matrix on a gold chip modified with MUA/MU, cyt.c and PASA. (Preparation conditions: 0.2 mg/ml PEI and 3.5 μM XOD in 0.5 mM phosphate buffer pH 6.0).

The combination of two oppositely charged polyelectrolytes (PASA and PEI) was chosen to form a bridging layer between the two parts of the assembly as no formation of XOD layer was observed directly on a cyt.c layer. The variation of the polyelectrolyte concentration and pH level of the solution showed optimum conditions for PEI/XOD multilayer formation: in contrast to the PASA/cyt.c multilayer, which was built at pH 5 (buffer 2), the formation of the PEI/XOD assembly showed best mass accumulation at pH 6.0 (buffer 3).

4.2.1.1.4. Electron transfer mechanism

In accordance with the results obtained by amperometric experiments, electrons could be transferred from HX molecules in solution to the electrode surface through the polyelectrolyte multilayer assembly of PASA/cyt.c and PEI/XOD if the electrode is polarized at a potential of +150 mV. Although both protein layers are necessary for a successful electron relay, it is reasonable to assume that the oxidation of HX occurs only

within the PEI/XOD layers where the enzymatic reaction can take place. Due to this reason, the cyt.c multilayers are responsible for relaying the electrons from XOD to the electrode surface. Two mechanisms for the signal transfer have to be taken into account. The electrons can be transferred directly from XOD to cyt.c and further to the electrode, or the electron transfer is mediated between the XOD and the electrode.

In an attempt to clarify the electron transfer mechanism within the multilayer arrangement an additional amperometric experiment was carried out: at a potential of +150 mV the influence of both main products of the enzymatic conversion, uric acid and hydrogen peroxide, can be neglected, Figure 4.16 (left).

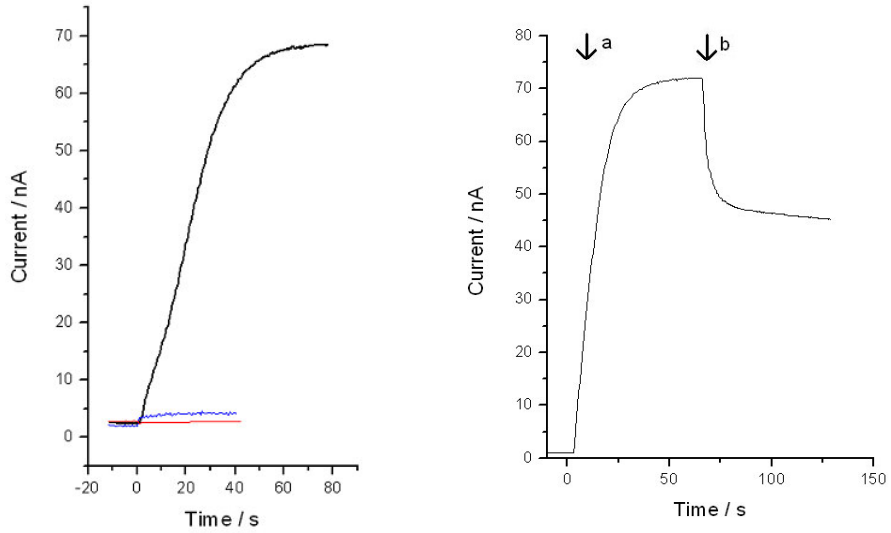

*Figure 4.16. Amperometric response of Au-MUAMU-cyt.c-(PASA-cyt.c)$_3$-PASA-(PEI-XOD)$_2$ electrodes on addition of 10 μM HX (black), 400 μM uric acid (blue), and 1 mM H_2O_2 (+150 mV, buffer 4, stirred solution), (**left**). Influence of a superoxide scavenger on the amperometric response of an Au-MUA/MU-cyt.c-(PASA-cyt.c)$_3$-PASA-(PEI-XOD)$_2$ electrode. The arrow **a** indicates addition of HX (10 μM) at 0 s; the arrow **b** - addition of 100 U/ml SOD at 60 s. (buffer 4, stirred solution), (**right**).*

The only reactive species capable for electron transport that should be taken into consideration are superoxide radicals. After addition of 10 μM HX into a measuring cell, an electrode consisting of 3 PASA/cyt.c layers and 2 PEI/XOD layers was subjected to the influence of SOD by addition of 100 U/ml SOD into the cell (Figure 4.16, right.). The response current upon addition of SOD showed a significant decrease. Since SOD is one of the most effective superoxide scavengers, the effect can be explained by conversion of superoxide produced in the PEI/XOD multilayer.

This demonstrates that superoxide radicals take active part in the electron transfer process within the multiprotein arrangement. Moreover, the loss of the response current without PASA/cyt.c multilayers indicates that this part of the assembly acts in a similar fashion as described for the cyt.c multilayer. However, the response current couldn't be totally suppressed as it was shown for cyt.c multilayer electrodes (Beissenhirtz, Scheller et al. 2004). This phenomenon can be explained by the electrode architecture: as SOD is a large protein, it cannot permeate the multilayer assembly. But it can destroy superoxide radicals, which diffuse in any direction from their place of origin within the XOD layers. Thus, a concentration gradient is established, resulting in a preferred diffusion out of the multilayer system. The steady state superoxide concentration within the system is therefore decreased in the presence of SOD and a lower current is detected at the electrode.

The partial suppression of the signal doesn't exclude the possibility of direct electron transfer from XOD to cyt.c. However, the superoxide mediated electron transfer from XOD via the cyt.c multilayers to the electrode is obviously the dominating mechanism. Further arguments for this hypothesis are inferred below by varying the layer composition of the structure.

4.2.1.1.5. Effect of the layer composition

In order to investigate the properties of the assembly, electrodes with a different number of cyt.c and XOD layers were studied. As shown in Figure 4.17, for Au-MUA/MU-cyt.c-(PASA-cyt.c)$_x$-PASA-(PEI-XOD)$_2$ electrodes the response current reached its maximum in the case of five PASA/cyt.c layers. This is quite close to the optimal composition found for the superoxide electrodes based on cyt.c multilayers (Beissenhirtz, Scheller et al. 2004). This fact underlines the importance of cyt.c within the assembly and supports the idea of a mediated electron transfer.

However, in the case of a further increase in numbers of cyt.c layers the electrodes showed a decrease in the response current (Figure 4.17) while only saturation was observed in the case of a cyt.c multilayer electrode in reaction with superoxide. This effect can be explained if one considers that every next layer of cyt.c has weaker interaction with its surrounding and the density of the polymer/cyt.c layers decreases. When large XOD molecules are attached at the interface the multilayer of cyt.c can be altered and some loosely bound protein is removed.

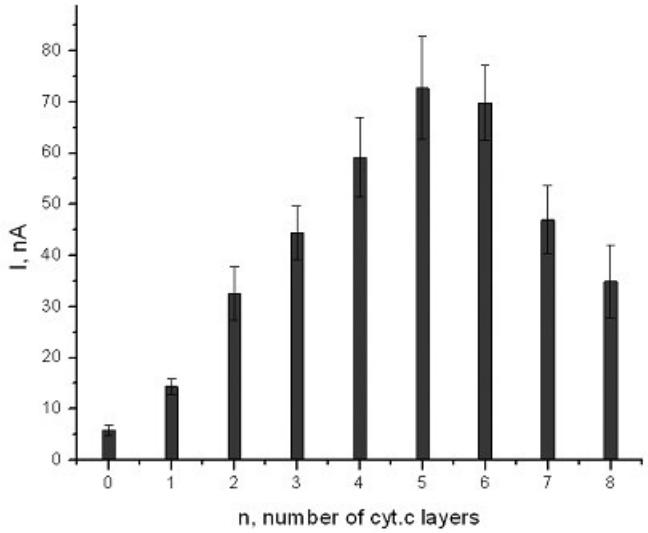

Figure 4.17. Dependence of the hypoxanthine response current of an Au-MUAMU-cyt.c-(PASA-cyt.c)$_n$-PASA-(PEI-XOD)$_2$-(PAA-PASA)$_2$ electrode on the number of cyt.c layers. Error bars were derived from 3 independent electrodes. (C_{HX}=100 μM, buffer 4, stirred solution).

This assumption is supported by the results obtained by UV-VIS spectrophotometry. ITO modified glass slides were incubated overnight in cyt.c solution to form a protein monolayer on the surface. After rinsing with buffer 1 and buffer 2, the electrode was alternately incubated in PASA and cyt.c solutions (see materials and methods 3.2.1.). Repeated incubation cycles yielded increasing absorption at 410 nm due to the deposition of cyt.c. However, after PEI/XOD incubation steps no increase of absorption was found. Instead, the absorption intensity at 410 nm decreased, which can be explained by removal of some loosely attached cyt.c from the outer layers by XOD or PEI molecules in solution, i.e. the interaction between XOD in solution and cyt.c in the last layer becomes stronger than the interaction between cyt.c and the polyelectrolyte matrix which results in cyt.c desorption from the electrode.

It was also found that the formation of the multilayer assembly depends on the initial monolayer quality: the coverage of cyt.c adsorbed on ITO electrodes was found to be significantly less than the one obtained for the MUA/MU modified gold surface, and thus a lower cyt.c loading in the following cyt.c/PASA layers was observed.

Variation of the number of XOD layers revealed an increase in the superoxide response up to 3 layers. With further increasing the number of XOD layers, the signal response remained approximately constant (Figure 4.18), which could be due to transport limitation of substrate or products through the XOD multilayers

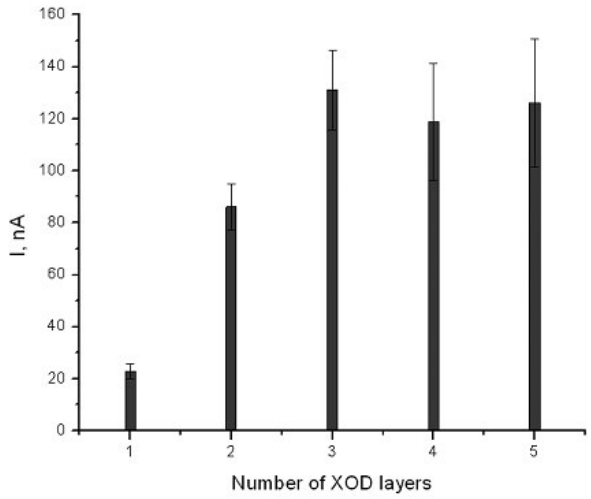

Figure 4.18. Dependence of the hypoxanthine response current of an Au-MUAMU-cyt.c-(PASA-cyt.c)$_5$-PASA-(PEI-XOD)$_m$-(PAA-PASA)$_2$ electrode on the number of XOD layers. Error bars were derived from 3 independent electrodes. (C_{HX}=100 μM, buffer 4 , stirred solution).

As shown above, antioxidants can influence the amperometric response of the multilayer electrode, since the electron transfer is mediated by superoxide radicals. In some cases, this phenomenon is to be avoided, e.g. in the application for HX sensing. The effect of superoxide scavengers on the electrode performance was tested for a number of antioxidants of different classes. SOD, one of the most efficient superoxide scavengers, reduces the electrode response current by about 20% at an Au-MUA/MU-cyt.c-(PASA-cyt.c)$_5$-PASA-(PEI-XOD)$_3$ electrode. Although SOD is not able to diffuse into the inner layers, it strongly affects the steady-state superoxide concentration within the assembly. Some small antioxidants, however, are able to diffuse into the structure of the electrode. In order to prevent contact between the electrode and superoxide scavengers in solution additional polyelectrolyte layers were built upon the last layer of XOD. Au-MUA/MU-cyt.c-(PASA-cyt.c)$_5$-PASA-(PEI-XOD)$_3$-(PEI-PASA)$_2$ electrodes showed practically no change in current on addition of 100 kU/ml of SOD into the measuring cell. The protective

layer was also able to block a number of smaller antioxidants, e.g. no change in current was observed on addition of epigallocatechin gallate and rutin in a concentration range up to 80 nM and 2.4 μM, respectively, where they show maximum activity in scavenging superoxide radicals (Ignatov, Shishniashvili et al. 2002). Introduction of additional $(PEI\text{-}PASA)_2$ protective layers entailed a longer response time of the electrode due to restriction of substrate diffusion. This effect, however, can be adjusted by selecting a composition of the polyelectrolyte membrane, e.g. using poly(allylamine) instead of PEI as a polycation reduced the response time without significant change in the protective properties. These examples illustrate the potential of the LbL technique in tailoring the relevant properties of the modified electrodes for specific applications.

4.2.1.1.6. XOD-cyt.c multilayer as amperometric sensor

Amperometric detection of hypoxanthine has been a subject of interest in recent years (Mulchandani, Luong et al. 1989; Park, Cho et al. 2000; Pei and Li 2000; Mao, Xu et al. 2001; Mello and Kubota 2002; Lu 2003; Watanabe, Tamada et al. 2005). The biosensor approach has received more attention due to the selectivity and sensitivity of xanthine oxidase towards hypoxanthine. It has to be mentioned that the sensor also responds to xanthine but for some applications such as fish freshness control it can be neglected due to low xanthine concentration.

The developed polyelectrolyte multilayer electrode was applied for quantification of HX. Standard solutions of different HX concentrations were injected into the measuring cell, and the corresponding amperometric curves were recorded for the optimized $Au\text{-}MUA/MU\text{-}cyt.c\text{-}(PASA\text{-}cyt.c)_5\text{-}PASA\text{-}(PEI\text{-}XOD)_3\text{-}(PAA\text{-}PASA)_2$ electrode. The t_{90} response time was 50 s. Linear dependence of the response current on HX concentration was found from 0.25 to 5 μM HX (Figure 4.19). Above that concentration, the ratio between the response current and substrate concentration decreased gradually. The electrode showed a sensitivity of 0.3 $A\cdot M^{-1}\cdot cm^{-2}$, that is more than one order of a magnitude higher than the value reported previously for amperometric biosensors based on XOD (0.028, 0.0218 $A\cdot M^{-1}\cdot cm^{-2}$) (Yao 1993; Nakatani, Vieira dos Santos et al. 2005). The proposed architecture also offers an advantage of using a potential of + 150 mV instead of + 600 mV for the earlier reported systems, which makes the electrode less susceptible to interfering substances and side reactions.

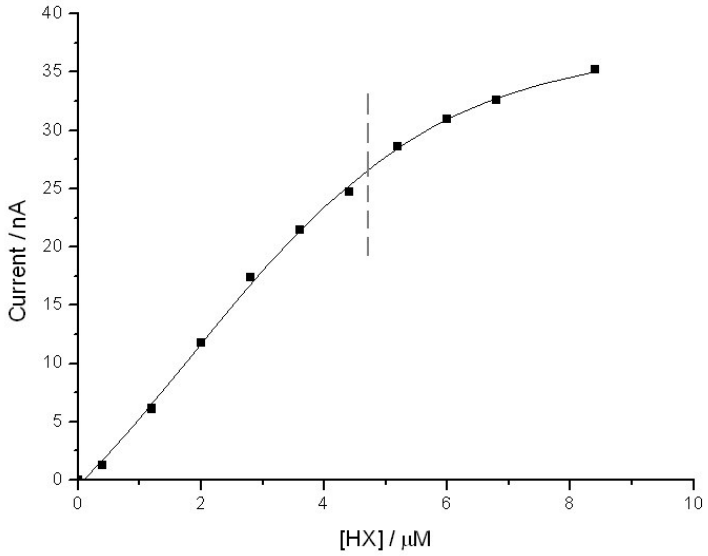

Figure 4.19. Calibration curve for an Au-MUA/MU-cyt.c-(PASA-cyt.c)$_5$-PASA-(PEI-XOD)$_3$-(PAA-PASA)$_2$ electrode towards hypoxanthine. (+150 mV vs. Ag/AgCl, 1 M KCl, buffer 4).

The considered polyelectrolyte multilayer arrangement is stabilized predominantly by electrostatic interactions. Therefore, the stability of protein multilayers is a question of great importance. In addition, the enzyme used in the assembly to govern selectivity for hypoxanthine, xanthine oxidase, is less stable than cyt.c and has a larger molecular weight. These factors resulted in unavoidable deterioration of the sensor performance during successive measurements or overnight storage, thus demanding stabilization.

Electrodes of different composition were studied with respect to stability. Stability of Au-MUA/MU-cyt.c-(PASA-cyt.c)$_5$-PASA-(PEI-XOD)$_3$ electrodes was compared to the ones with protective polyelectrolyte layers as discussed above. In addition, a strategy of exposing electrodes to higher temperature was used as an attempt to anneal the layers. As shown in Figure 4.20, the electrodes with two additional (PAA-PASA) layers showed much better stability than the ones without. Thermally treated electrodes also showed an improved stability. The stabilizing effect of thermal treatment on the polyelectrolyte multilayer films takes place due to annealing of structural defects (Steitz, Leiner et al. 2002; Antipov and Sukhorukov 2004). The structure undergoes irreversible changes resulting in the reinforcement of interactions between the components of the polyelectrolyte assembly.

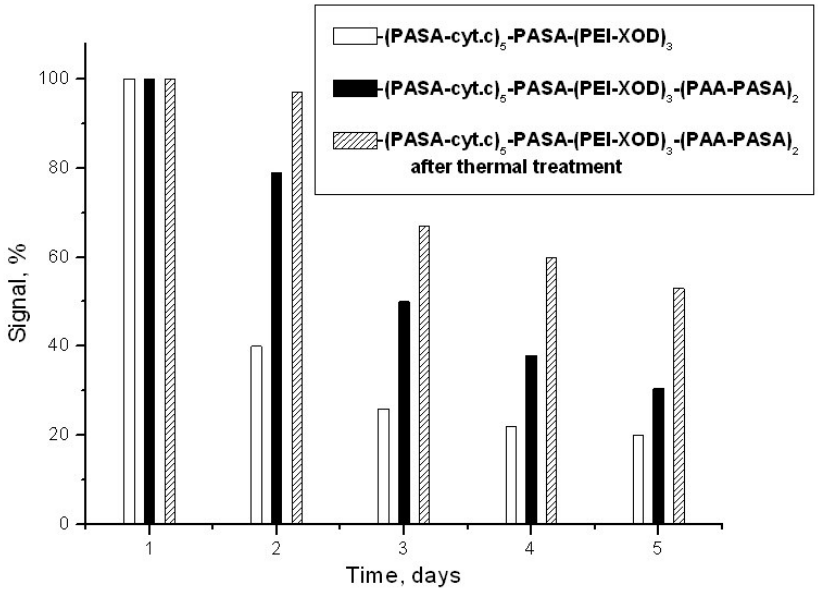

Figure 4.20. Stability of cyt.c-XOD multilayer electrodes of different composition. (After preparation and measurements, all electrodes were stored in buffer 2 at +4℃. Measurements were performed in buffer 4).

4.2.2. Redox signal chains based on direct electron transfer

4.2.2.1. Bilirubin oxidase-cyt.c multilayer

Here a new enzyme-protein-polyelectrolyte multilayer signal chain is introduced. It is designed by assembling proteins in complexes on electrodes in such a way that direct protein-protein electron transfer is feasible. This design does not need a redox mediator in analogy to natural protein communication. For this purpose, cyt.c and the enzyme bilirubin oxidase (BOD, EC 1.3.3.5) are co-immobilized in a self-assembled polyelectrolyte multilayer on gold electrodes. Although these two proteins are not natural reaction partners, the protein architecture facilitates an electron transfer from the electrode via multiple protein layers to molecular oxygen resulting in a significant catalytic reduction current.

4.2.2.1.1. Direct electron transfer of bilirubin oxidase on gold electrodes

In this and the following chapter direct and cyt.c mediated electron transfer between BOD and thiol-modified gold electrodes is established. It is also demonstrated that BOD exhibits catalytic activity towards oxygen reduction at gold electrodes without

the need of a redox mediator. This effect is studied as a function of pH. In addition, cyt.c in solution and in the adsorbed state is able to enhance electron transfer from the electrode to BOD thus acting as a biological mediator.

Direct electro-reduction of molecular oxygen by BOD was observed for the first time at promoter modified gold electrodes in absence of the enzyme substrate (bilirubin). Gold wire electrodes were modified with mercaptoundecanoic acid (MUA) and mercaptoundecanol (MU) forming a mixed self assembled monolayer. As shown in cyclic voltammograms in Figure 4.20, an electrocatalytic effect was observed in the presence of BOD and molecular oxygen in solution. Catalytic reduction started around +200 mV vs. Ag/AgCl although a minor activity at higher potentials can not be completely ruled out. The reduction current was found to depend on the oxygen concentration in solution. However, it was found that a catalytic current also occurred with very low oxygen concentrations as e.g. in an argon-purged buffer (Figure 4.20 see curve b) indicating a high enzyme activity on the surface. Compared to the electrocatatlytic oxygen reduction at carbon electrodes the current density is significantly smaller here and the start potential seems to be less positive (Shleev, El Kasmi et al. 2004; Tsujimura, Nakagawa et al. 2004).

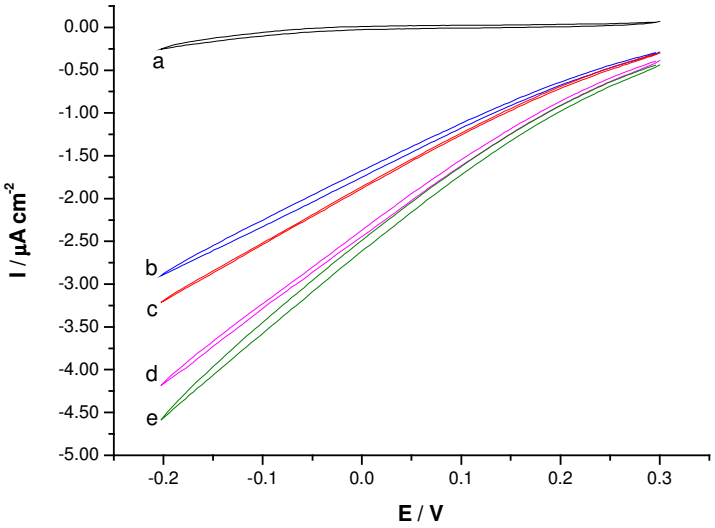

Figure 4.20. Cyclic voltammetry of MUA/MU modified gold electrode obtained in 5 mM citrate phosphate buffer 4.0, scan rate 20 mV/s. a) in air-saturated buffer; b) 1.5 µM BOD in argon-purged buffer; c) 1.5 µM BOD in 90% argon-purged buffer and 10% air-saturated buffer; d) 1.5 µM BOD in 50% argon-purged buffer and 50% air-saturated buffer; e) 1.5 µM BOD in air-saturated buffer.

From these experiments it can be concluded, that electron transfer from the electrode via BOD to oxygen occurs, however, with less efficiency compared to carbon nanotube-modified electrodes. In contrast to a naked gold electrode, the modification with the COOH/OH- terminated alkane thiols obviously prevents undesirable conformational changes of the enzyme thus allowing direct electron exchange (see the literature digest).

The enzymatic activity of BOD is strongly pH dependent. Thus, the effect of pH was also investigated for the electrocatalytic activity found at the modified gold electrodes. The diagram in Figure 4.21 illustrates the dependence of the catalytic current at a potential of –100 mV on the pH of the solution. At pH 4 efficient electro-reduction of oxygen takes place. However, at higher pH a gradual decrease in current was observed. At neutral pH the catalytic current becomes negligible. This behavior reflects to a large extent the activity of the enzyme in solution. However, since no catalytic activity was found in the neutral pH range, it is also likely that the increased negative charge density of the mixed thiol layer diminishes the productive interaction of the protein with the electrode.

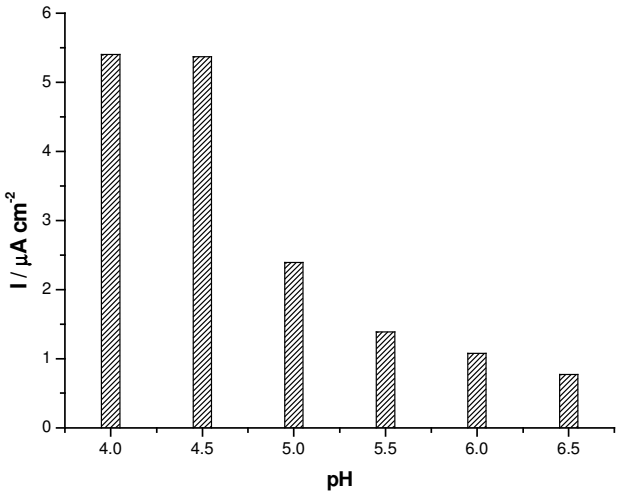

Figure 4.21. Catalytic reduction current at – 100 mV of MUA/MU modified gold electrode in 1.25 μM BOD in air-saturated 5 mM citrate-phosphate buffer versus pH.

For the interaction of BOD with carbon electrodes the T1 center has been proposed as the first electron acceptor in analogy to the interaction with the natural substrate. For carbon electrodes rather high potentials for the oxygen reduction have been found, corresponding to the redox potential of the T1 site (670-685 mV vs. NHE) (Christenson,

Shleev et al. 2006; Weigel, Tritscher et al. 2007). At the modified gold electrodes the oxygen reduction became visible at about 435 mV vs. NHE, which is rather far from the potential of the T1 site. This could serve as an indication for the involvement of another redox site in the case when the electron transfer is realized at the modified gold. However, it still must be clarified by additional investigations, since a direct cyclic voltammetric response of a copper site in the absence of substrate and co-substrate could not be verified in this study.

4.2.2.1.2. Interaction of bilirubin oxidase with cyt.c in solution

Although direct electron transfer between BOD and promoter-modified gold electrode was shown in acidic environment, the catalytic current steeply decreased at pH close to neutral. For neutral pH conditions mediators can be effectively used to enable the electron transfer. This was demonstrated e.g. with compounds, such as ferri-/ferrocyanide (Nakagawa, Tsujimura et al. 2003). Here it is shown that an electron transfer protein, cyt.c, can efficiently mediate the catalytic oxygen reduction of BOD on promoter-modified gold.

At neutral pH where the catalytic current did not substantially contribute to the measurable current, the presence of cyt.c resulted in a significant increase in the reduction current. The catalytic oxygen reduction became more efficient than in the case of DET of BOD at lower pH. Cyclic voltammograms of MUA/MU modified gold electrodes in presence of 0.4 mM cyt.c and different BOD concentrations in the cell, measured in air-saturated buffer, are shown in Figure 4.22. The enhanced reduction current with increasing BOD concentration can be explained by the higher density of conversion sites for oxygen. Obviously, cyt.c effectively replaces the natural substrate in delivering electrons to the enzyme for oxygen reduction and is present in sufficient excess avoiding “substrate” limitations.

Recent studies on blue copper enzymes suggest potential explanations for the electron transfer mechanism between BOD and the electrode (Shleev, El Kasmi et al. 2004; Zoppellaro, Sakurai et al. 2004; Shleev, Tkac et al. 2005). Maximum activity of BOD at pH 4.0 corresponds to an optimal conformation of the molecule, and the T1 center in particular, responsible for interaction with the substrate. While this process is efficient at low pH, the deficiency of activity at higher pH can be explained by unfavorable conformation of the T1 center and inability of electron transfer between the enzyme and

the electrode surface. Immobilisation of the enzyme on the electrode has been shown to be one approach to circumvent the strong decline in activity (Shleev, El Kasmi et al. 2004). But also the addition of cyt.c can drastically improve the catalytic turnover of oxygen (cyt.c itself shows no affinity towards oxygen). Thus, it is likely that at neutral pH cyt.c can replace the natural substrate at the T1 center, although interaction with the T2/T3 cluster can not be ruled out since the redox potential is sufficiently high to oxidize cyt.c, and structural simulations of BOD indicate accessibility of this redox center (Kataoka, Kitagawa et al. 2005).

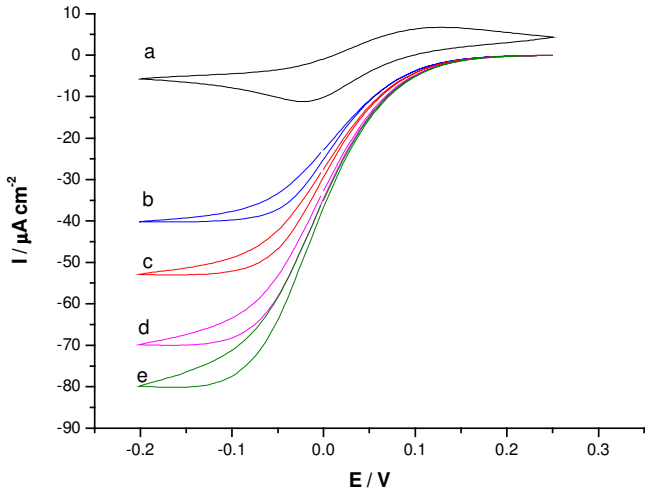

Figure 4.22. Cyclic voltammetry of MUA/MU modified gold electrode in air-saturated 5 mM phosphate buffer pH 7.0 in presence of 0.4 mM cyt.c, scan rate 10 mV/s. a) without BOD; b) 1.25 µM BOD; c) 2.5 µM BOD; d) 5 µM BOD; e) 7.5 µM BOD.

Pseudo first-order kinetic constants for the reaction of BOD with cyt.c (k_{cat}) were determined by the method of Nicholson and Shain (Nicholson and Shain 1965; Shain and Nicholson 1981). From this analysis the second order reaction rate constant for the homogeneous electron transfer reaction between BOD and cyt.c (k) has been calculated. Cyclic voltammograms of Au-MUA/MU electrodes were measured in the presence of 50 µM cyt.c and different BOD concentrations at different scan rates. The ratio between catalytic (I_{cat}) and diffusion-limited (I_{diff}) currents is proportional to the square root of k_{cat} (with v – scan rate of the voltammetric experiment).

$$(I_{cat}/I_{diff})^2 = \lambda = k_{cat}(RT/nF)/v \quad (4.4)$$

$$k_{cat} = k\,[BOD] \quad (4.5)$$

The value of the second order reaction rate constant calculated by this approach is $k=(15.3 \pm 1.9)\cdot 10^6\ M^{-1}s^{-1}$. Independently, the rate constant was also determined by spectrophotometric measurements to be $k=(12.6 \pm 1.3)\cdot 10^6\ M^{-1}s^{-1}$. The values found with both methods are in good agreement.

4.2.2.1.3. Reaction of BOD with the cyt.c monolayer electrode

Interaction of BOD with cyt.c also takes place in the case when the latter is adsorbed on the surface of the MUA/MU modified gold electrode. This is illustrated in Figure 4.23 by cyclic voltammograms of a cyt.c monolayer electrode in BOD-containing solution. In this case BOD molecules in solution accept electrons from a cyt.c monolayer formed by electrostatic adsorption with a coverage of about 13 ± 1 pmol cm^{-2}. It has to be noted here that the electron transfer of the immobilised cyt. c is quasi-reversible and rather fast ($k_s=75s^{-1}$) under these conditions. With the electrode-fixed redox protein the catalytic effect in bulk solution is inhibited (where only BOD is present without any redox mediators) and occurs at the surface of the cyt.c monolayer only.

The cyclic voltamogramms show that the catalytic current in this case also depends on the oxygen concentration. The fact that cyt.c in the adsorbed state reacts with BOD in solution may be due to its rotational flexibility at the MUA/MU promoter layer (Wei, Liu et al. 2002). This has already been observed in the interaction of cyt. c with NADPH cyt.c P450 reductase (Jin, Wollenberger et al. 1997).

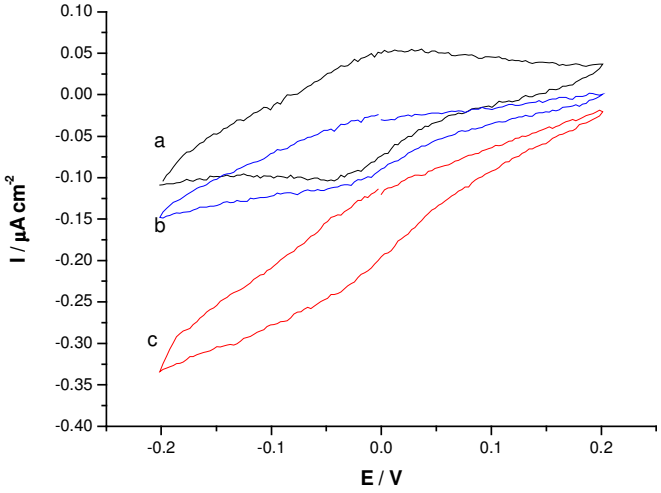

Figure 4.23. Cyclic voltammetry of Au-MUA/MU-cyt.c electrodes in 5mM phosphate air-saturated buffer pH 7.0, scan rate 10 mV/s (a); in presence of 1.25 μM BOD in N2-purged buffer (b); in presence of 1.25 μM BOD in air-saturated buffer (c).

4.2.2.1.4. BOD-cyt.c assembly and function

Here the reaction between cyt.c and BOD, described above, is confined to a surface and coupled with direct electron transfer of cyt.c to the transducing electrode.

Polyelectrolyte multilayers with embedded cyt.c, BOD and sulfonated polyaniline (PASA) as counter polyelectrolyte are assembled on a cyt.c monolayer electrode by alternating incubation of the electrode in solutions of PASA and a cyt.c/BOD mixture. The monolayer electrode consists of cyt.c adsorbed on a self-assembled mixed thiol-layer of mercaptoundecanoic acid (MUA) and mercaptoundecanol (MU). The design of the resulting multilayer is schematically shown in Figure 4.24. The formation of the assembly with cyt.c, BOD and PASA on the gold surface was confirmed by surface plasmon resonance experiments (Figure 4.25). Although the polyelectrolyte incubation steps caused singnificant loss of the protein mixture on the electrode surface, the assembly still could be carried out and the SPR signal increased after every adsorption cycle.

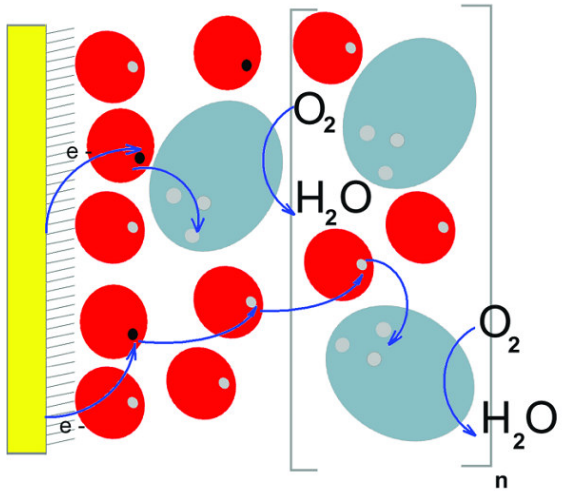

Figure 4.24. Schematic illustration of the redox chain in cyt.c/BOD multilayer coated electodes. Red circles - cyt.c protein, ellipses - BOD enzyme, arrows indicate electron transfer pathways between cyt.c and BOD within the polyelectrolyte network or the four-electron oxygen reduction process.

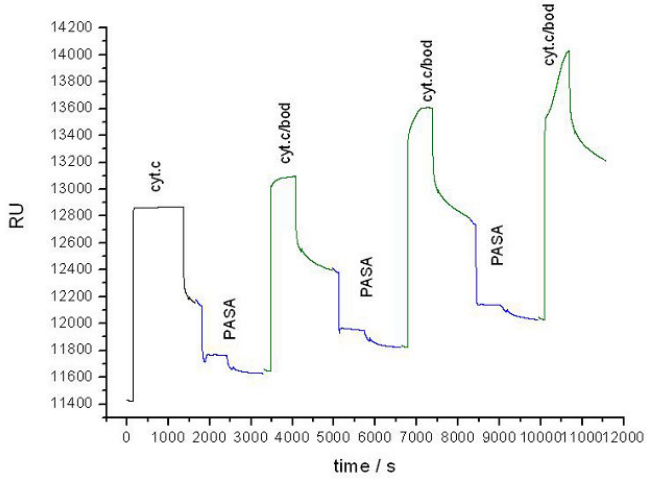

Figure 4.25. SPR experiment showing formation of BOD/cyt.c-PASA assembly on a gold chip modified with MUA/MU and cyt.c.

When the cyt.c/BOD multilayer electrode is exposed to an air saturated solution and a cathodic potential sweep is performed a substantial reduction current can be observed at neutral pH (Figure 4.26). The catalytic current results from reduction of cyt.c, most of which is in its ferric form due to oxidation by neighboring BOD molecules. Catalytic reduction of oxygen occurs at the BOD's tri-nuclear cluster, where electrons are transferred to molecular O_2 to produce water. Thus, a steady-state catalytic current is obtained. This cyclic voltammetry observation confirms the functioning of the signal

chain from the electrode via cyt.c to BOD and finally to O_2. Control experiments, where only one protein, either BOD or cyt.c, is immobilized in the multilayer, show no catalytic behavior.

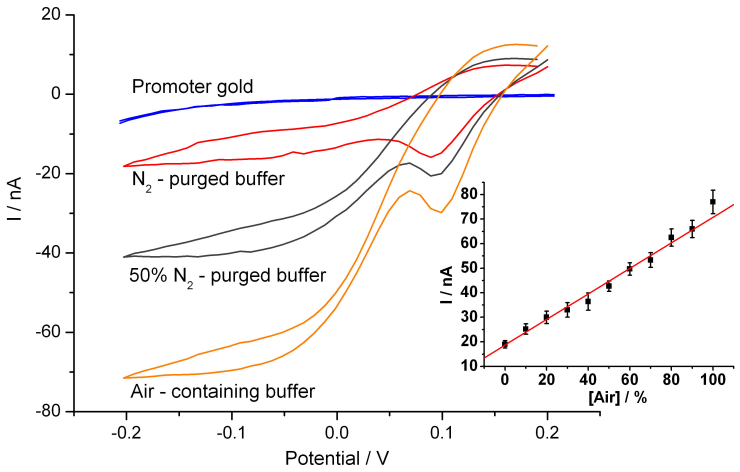

Figure 4.26. Cyclic voltammetry of an Au-MUA/MU-cyt.c-(PASA-cyt.c/BOD)$_3$ multilayer coated electrode measured at different oxygen concentrations; dependence of the catalytic current at - 0.2 V measured in N_2/air saturated buffers.

4.2.2.1.5. Electron transfer

In order to evaluate the rate-limiting step in the electron transfer chain, the multilayer assembly is analysed by cyclic voltammetry at different oxygen concentrations (Figure. 4.26). The experiments show a clear dependence of the reduction current on the oxygen content in solution. Such a dependence of the steady-state catalytic current at rather low scan rate (5 mVs^{-1}) suggests that here the overall current is limited by the catalytic reduction of oxygen at the enzyme BOD rather than by the reaction between cyt.c and BOD or cyt.c and the electrode (at least up to oxygen concentrations of about 250 µM found in air-saturated buffer). It has to be mentioned here that the additional peak, visible in the CV in Fig. 4.26 (E_f~130mV), results from the conversion of surface-bound PASA. This reaction occurs in parallel to the conversion of the protein molecules, however with a much slower kinetics. It is not interfering with the electron transfer towards BOD.

Since the reduction of O_2 at BOD is the rate limiting step in the electron transfer chain under nearly stationary conditions, more insight into the kinetics of the system can be obtained by a systematic variation of the scan rate. A result of such a variation is given in Figure 4.27. Whereas at low scan rates a pronounced catalytic current is observed at a

potential below 50 mV, it disappears at higher scan rates and the electrochemical signal of cyt.c becomes visible. In analogy to the reaction in solution, the electrochemical driving force above a certain scan rate changes faster than the catalytic reaction at the BOD can follow. So electrons are only exchanged with cyt.c and no catalytic reaction occurs at the enzyme. The arrangement shows a quasi reversible electron transfer with a formal potential –13±8 mV, which is in good agreement with data found for multilayers embedding only cyt.c.

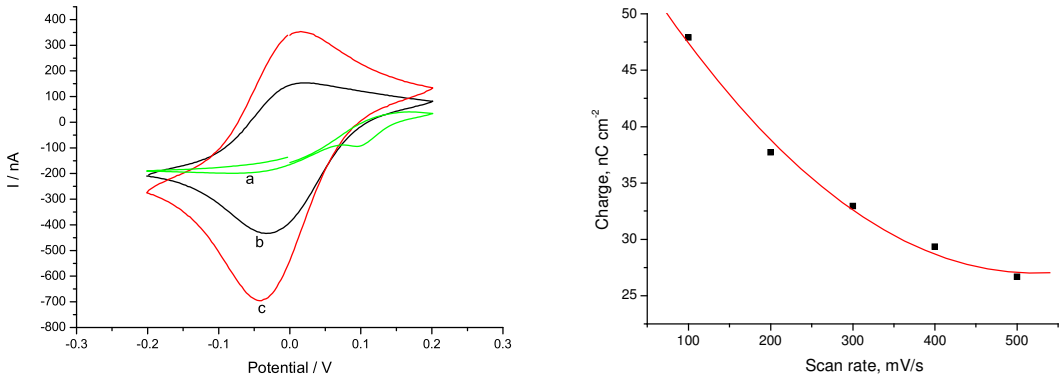

*Figure 4.27. Cyclic voltammograms of Au-MUA/MU-cyt.c-(PASA-cyt.c/BOD)$_6$ multilayer electrode at scan rates: a) 5 mV/s; b) 100 mV/s; c) 200 mV/s (**left**) Dependence of the charge transferred through 1 cm^2 of the Au-MUA/MU-cyt.c-(PASA-cyt.c/BOD)$_6$ during one scan on the scan rate (**right**).*

If the scan rate is further enhanced, it has to be noted that although the peak current is still increased the amount of the electrode-addressable cyt.c decreases. This means that now a scan rate is reached which is in the range of the cyt.c – cyt.c electron transfer rate so that not all cyt c molecules immobilised in the multilayers can be oxidized/reduced in the time period of a voltammetric sweep. Hence, the system behaves similar to a multilayer assembly with only cyt.c since protein-protein electron transfer is limiting. It has to be noted that the multilayer assembly is stable during these investigations: by decreasing the scan rate after the variation the same catalytic oxygen current is detected again.

4.2.2.1.6. Influence of composition and the number of layers

Within the assembly the proteins are arranged in stacked layers on the electrode – thus, rather thick layers can be prepared. To gain more insight into the electron transfer process the dependence of the electrocatalytic efficiency on the number of layers was analyzed. With this aim electrodes with different numbers of cyt.c/BOD layers have been prepared. CV data measured in air-saturated buffer at low scan rate are summarized in Figure 4.28. A proportional increase of the catalytic current with the layer numbers can be clearly seen. This means that by increasing the number of catalytic sites (BOD amount) the electrocatalytic conversion can be enhanced. This, however, also implies that all deposited BOD molecules are in electrical contact with the electrode. Since a large part of the enzymes is immobilized rather far from the electrode surface it can be concluded that cyt.c is providing the electrons for the enzymatic activity. This is supported by the fact that assemblies of BOD and PASA alone do not show a catalytic oxygen reduction.

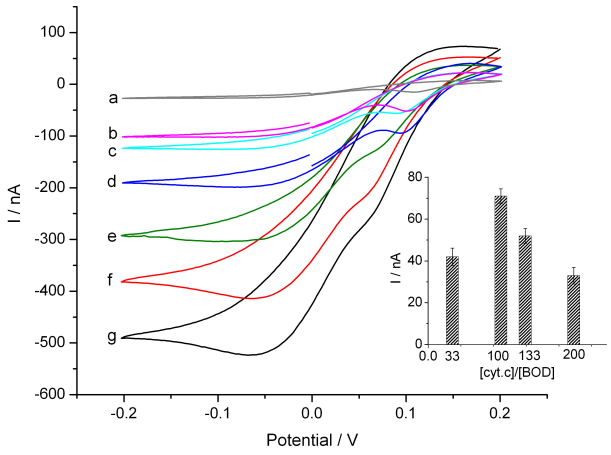

Figure 4.28. Cyclic voltammograms of cyt.c/BOD multilayer coated electrodes as a function of the (PASA-cyt.c/BOD)$_n$ layers: a) 1; b) 2; c) 4; d) 6; e) 8; f) 10; g) 12; inset: dependence of the catalytic current as a function of [BOD]/[cyt.c] ratio.

For applications of such protein/enzyme multilayer systems it is noted that the sensitivity towards the enzyme substrate (here oxygen) can be tuned to a large extent by the numbers of deposited layers without being limited by mediator diffusion or leakage.

It should be also mentioned that the electrode shows significant activity at neutral pH, however at pH 5 – the optimum pH for the enzyme – the oxygen reduction is further enhanced by a factor of ca. 3. This effect, again, illustrates an efficient electron supply for the BOD catalyzed reaction within the multilayer.

As discussed above, the two proteins have a different function within the layer assembly. Therefore, the relative amounts of BOD and cyt.c in each layer should have a profound effect on oxygen reduction if this hypothesis is correct. When the [cyt.c]/[BOD] ratio is decreased from 100 to 33 a 40% decrease in the catalytic response can be observed. This means although the amount of reaction sites for oxygen is increased (higher BOD amount), delivering of electrons to the enzyme becomes limiting and thus the activity is diminished. Since electrons are transferred from cyt.c to the enzyme, the proposed role of cyt.c as immobilized electron carrier is again supported. When high BOD concentrations are present, the electron pathway from cyt.c to cyt.c is hindered.

4.3. Multilayers formed by protein-protein interactions

Up till now, all of the reported polyelectrolyte multilayer arrangements with embedded proteins are stabilized by a polyelectrolyte matrix. Usually the scaffolding matrix is composed of an electrochemically inert polymer which stabilizes the arrangement (Lvov, Ariga et al. 1995; Jessel, Atalar et al. 2003). In a cyt.c/PASA multilayer arrangement the electron exchange between the cyt.c molecules was proposed as a dominating mechanism, but the role of the polymer in the electron transfer process has not been solved completely. Therefore, avoiding the use of a scaffolding polyelectrolyte can help to shed more light on the electron transfer mechanism within multi-protein arrangements.

4.3.1. Sulfite oxidase - cyt.c multilayer

Here a novel strategy for multi-protein LbL self-assembly combining cyt.*c* with the enzyme sulfite oxidase (SOx) without use of any additional polymer is described. Electrostatic interactions between these two proteins with rather separated isoelectric points during the assembly process from a low ionic strength buffer were found to be sufficient for layer-by-layer deposition of both components. Since these two proteins are natural redox partners and show efficient interaction in solution (see literature digest), it can also be anticipated that the inter-protein electron transfer can be preserved in the case when the two proteins are immobilized.

4.3.1.1. Assembly protocol

We assembled the horse heart cyt.*c* and human SOx (EC 1.8.3.1) by sequential incubation steps of a cyt.*c* monolayer electrode in solutions of SOx and cyt.*c* prepared in 0.5 mM potassium phosphate buffer pH 5.0 (Figure 4.29).

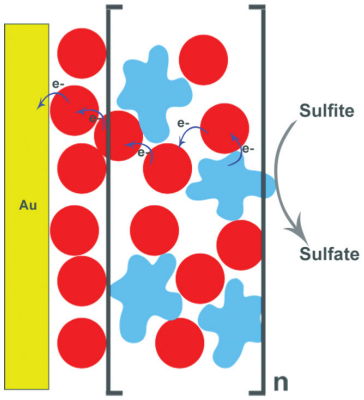

Figure 4.29. E*lectrode scheme: red circles = cyt.c, blue objects = SOx. Arrows denote substrate conversion and electron transfer processes.*

Preliminary experiments with SOx/cyt.c multilayers assembled from solutions of pure SOx (10 μM) and cyt.c (20 μM) showed deposition of these two proteins. Quartz crystal microbalance confirmed mass accumulation at the surface with each deposition cycle (Figure 4.30). Although SOx exceeds the mass of cyt.*c* by about a factor of 5, the enzyme still can bind to the cyt.*c* modified surface, and facilitate further adsorption of cyt.*c*.

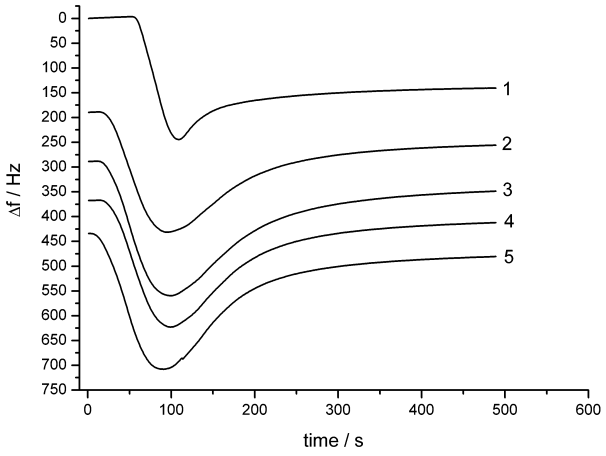

Figure 4.30. Deposition steps of SOx from a pure solution of 10 μM concentration against 20 μM cyt.c (not shown) measured by QCM. Numbers 1-5 denote adsorption cycles.

However, the voltammetric signal of cyt.c within the assemblies formed by sequential deposition shows practically no increase as a function of the number of layers. This behavior indicates that electron transfer between cyt.*c* in the monolayer and cyt.*c*

separated by a SOx layer is hindered. Assuming that the large enzyme molecules disrupt communication between different cyt.*c* layers, SOx shall be co-adsorbed together with cyt.*c* from a mixture in order to improve the electrochemical characteristics of the film.

In accordance with this method, SOx/cyt.*c* arrangements were built by alternating incubation of a cyt.*c* monolayer electrode into a SOx/cyt.*c* mixture and a pure cyt.*c* solution. QCM experiments showed an increase in the deposited protein mass after each incubation cycle (Figure 4.31).

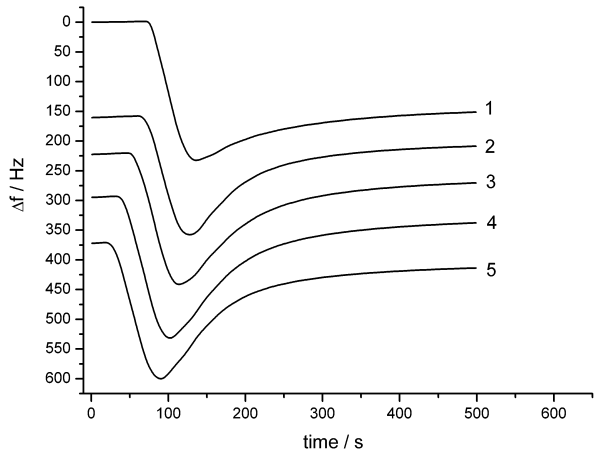

Figure 4.31. Deposition steps of SOx/cyt.c from a mixture containing 10 μM SOx and 1 μM cyt.c against 20 uM cyt.c (not shown) measured by QCM. Numbers 1-5 denote adsorption cycles.

4.3.1.2. Catalytic activity and electron transfer mechanism

The SOx/cyt.*c* arrangement prepared from the mixture containing 10 μM SOx and 1 μM cyt.*c* adsorbed against pure 20 μM cyt.*c* showed a pronounced electrocatalytic effect for oxidation of sodium sulfite. Figure 4.32 (left) demonstrates the electrode response upon addition of sulfite to the solution in the μmolar concentration range. Sulfite oxidation takes place at the SOx molecules, thus in the presence of the substrate most of the enzyme is reduced. A catalytic current is generated due to subsequent oxidation of SOx by cyt.*c* molecules, followed by the electron transfer towards the electrode via a long-range electron transfer process (*chapter 4.1.1.*). Here two possible mechanisms were considered: (i) electron transfer occurs by direct interaction between neighboring cyt.c molecules while the polyelectrolyte is responsible for stabilization of the arrangement; or (ii) cyt.c can be

wired by PASA, which under specific conditions can be a conductive polymer. However, in the current case long-range electron transfer is observed in a polymer-free system, which gives an additional strong argument for a face-to-face electron hopping between cyt.*c* molecules as a dominating electron transfer mechanism.

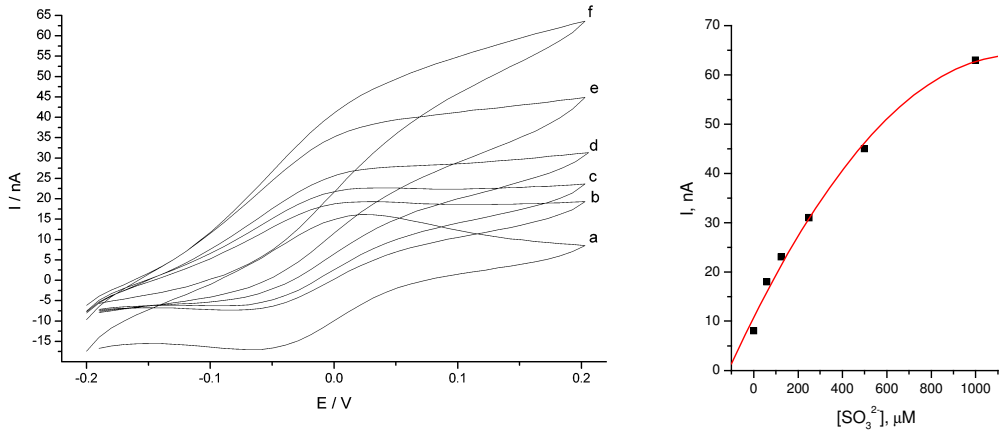

*Figure 4.32. Cyclic voltammograms of Au-MUA/MU-{(SOx/cyt.c-cyt.c)}$_8$-SOx/cyt.c electrode measured in a) absence of sulfite, b) 60 µM, c) 125 µM, d) 250 µM, e) 0.5 mM, f) 1 mM of Na_2SO_3, scan rate 100 mVs^{-1} (**left**). Dependence of the catalytic current at +200 mV for Au-MUA/MU-{(SOx/cyt.c-cyt.c)}$_8$-SOx/cyt.c electrode on Na_2SO_3 concentration in solution.*

Cyclic voltammograms of the assemblies containing a different number of layers (Figure 4.33, left), recorded in the presence of 1 mM sodium sulfite, show a linear increase of the catalytic current. This experiment not only confirms the QCM data for the film growth with each deposition cycle, but also indicates that the two proteins, that are natural reaction partners, are able to maintain efficient electronic communication being co-immobilized in multiple layers on the electrode. A ratio between the catalytic current (in presence 1 mM sulfite) to the non-catalytic one (without silfite) shows an increase of the relative contribution from the catalytic process as a function of the number of layers, at least up to 8 layers (Figure 4.33, right).

Since the system combines an electron transfer protein with an enzyme, it can be assumed that cyt.c within the arrangement is responsible for electron shuttling between the electrode, and the enzyme represents the sites where the catalytic reaction takes place. In this case, variation of the relative amount in the SOx/cyt.*c* mixture should have a profound effect on the electrochemical response of the arrangement.

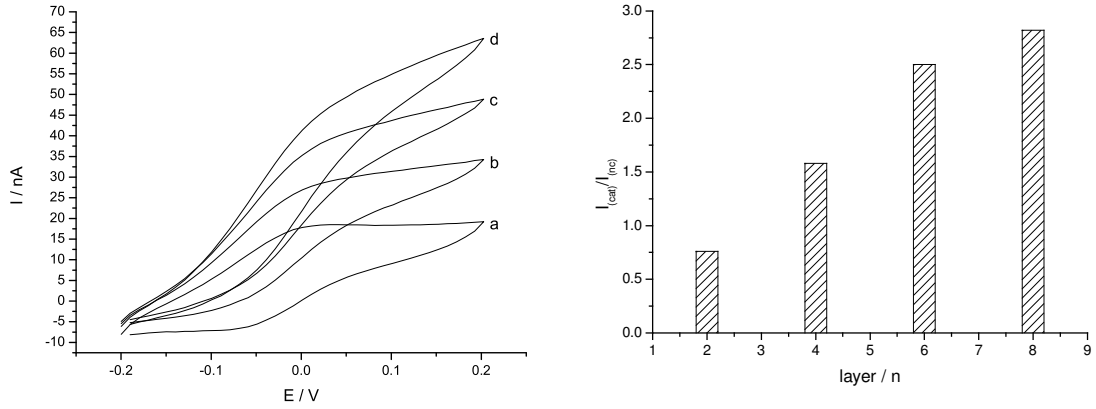

*Figure 4.33. Catalytic response of Au-MUA/MU-{(SOx/cyt.c-cyt.c)}$_n$-SOx/cyt.c electrode in 1 mM Na_2SO_3: a) n=2, b) n=4, c) n=6, d) n=8, scan rate 100 mVs^{-1}, pH 7.0 (**left**). Dependence of the ratio of oxidative catalytic and non-catalytic current on the number of deposited layers for an Au-MUA/MU-{(SOx/cyt.c-cyt.c)}$_n$-SOx/cyt.c electrode. Measured at a zero potential (**right**).*

Indeed, assemblies built up using a SOx/cyt.c mixture with lower enzyme concentration showed a smaller catalytic response (Figure 4.34, left). At the same time, electrodes prepared with a high relative amount of enzyme ([SOx]/[cyt.c]>25) also showed a low catalytic efficiency. Therefore, electrocatalytic performance of the arrangement requires (i) a sufficient SOx surface concentration in order to generate a catalytic current, and (ii) that the amount of cyt.*c* within the assembly is high enough to provide a long-range electron transfer to connect the enzyme to the electrode. Notably, the fast reaction of cyt.*c* with SOx in solution (k = 4.47±0.13 x 10^6 $M^{-1}s^{-1}$, pH 8.5) is preserved in the immobilized state since the catalytic effect can be observed even at scan rates up to 500 mVs^{-1} (Figure 4.34, right).

The catalytic current of the multilayer electrode follows the activity of SOx at different pH with a maximum response at pH 7, which is slightly shifted compared to the activity in solution (pH 8.5, see Figure 4.35). The current depends on the sulfite concentration in the range from 20 µM to 2 mM with an apparent Michaelis-Menten constant K_M of about 310 µM.

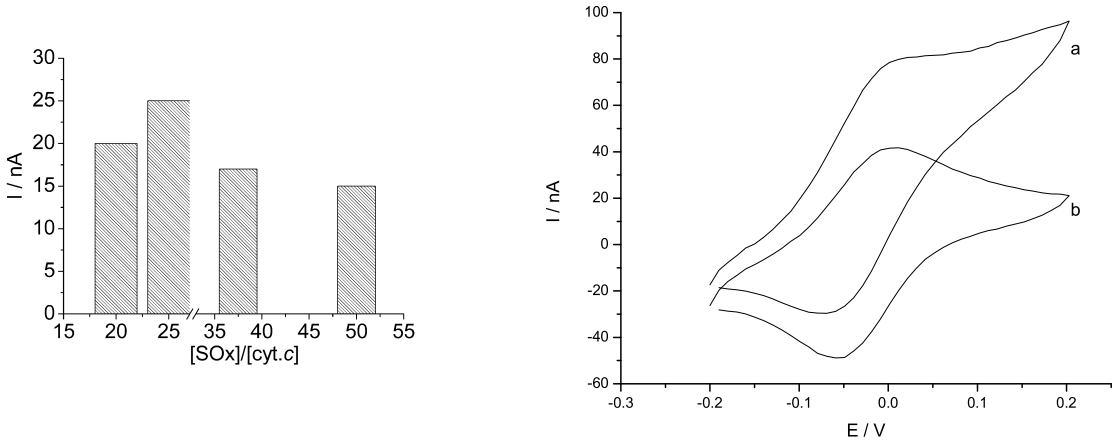

*Figure 4.34. Dependence of the catalytic current of Au-MUA/MU-{(SOx/cyt.c-cyt.c)}$_3$-SOx/cyt.c electrode on SOx/cyt.c ratio at a potential of +200 mV. Measurement performed at 5 mVs^{-1} in presence of 1 mM sulfite, pH 7.0 (**left**). Cyclic voltammograms showing catalytic response of Au-MUA/MU-{(SOx/cyt.c-cyt.c)}$_8$-SOx/cyt.c electrode scanned at 500 mVs^{-1} in 1 mM Na_2SO_3 (a) and absence of sulfite (b). Measurement performed at 5 mVs^{-1} in presence of 1 mM sulfite, pH 7.0 (**right**).*

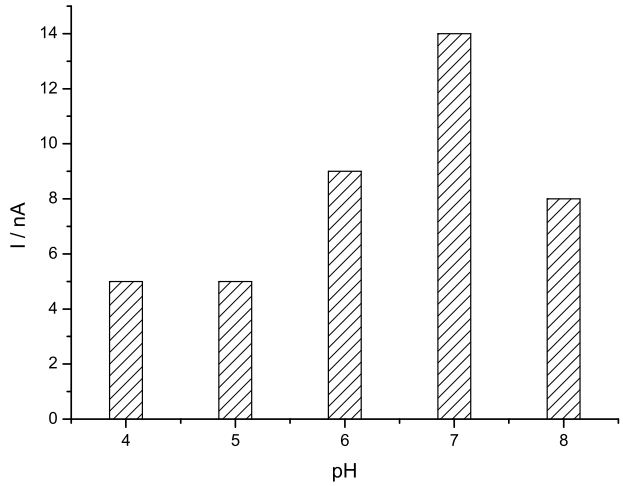

Figure 4.35. Catalytic current generated by Au-MUA/MU-{(SOx/cyt.c-cyt.c)}$_3$-SOx/cyt.c electrode at a potential of +200 mV at different pH. Measurement performed at 5 mVs^{-1} in presence of 1 mM sulfite.

In order to elucidate the rate-limiting step in this {SO_3^{2-} → SOx → (cyt.c …→ cyt.c)→ electrode}signal chain, one needs to take into account the behavior at high scan rates. A prominent catalytic current in the presence of SO_3^{2-} confirms that the electrons can still be transferred from the substrate in solution through the enzyme-catalyzed reaction to cyt.c, and then further to the electrode without limitation. This situation has been found to take place up to a scan rate of about 1 Vs^{-1}, at which the electron transfer from SOx to cyt.c becomes limiting.

4.4. Combination of LbL and S-layer techniques: hybrid protein multilayers

Isolated S-layer proteins are able to assemble into two-dimensional monocrystalline arrays at a large variety of supports. Here a strategy to combine a structurally well defined protein surface layer with a functional protein multilayer assembly is proposed. This approach was demonstrated on recrystallization of a bacterial cell-wall protein SbpA upon the PASA/cyt.c multilayer film.

4.4.1. Recrystallization of S-layer at cyt.c/PASA multilayer

As a preliminary experiment, recrystallization of SbpA on PASA- and cyt.c-terminated arrangements was performed. However, these results showed no S-layer formation on either cyt.c or PASA layers. Since S-layer protein SbpA was reported to recrystallize predominantly at negatively charged surfaces, it was not expected to recrystallize at a cyt.c layer. At the same time, the inability to crystallize at a PASA layer indicates that it is not only electrostatic interactions that determine the layer formation process.

Therefore, in order to obtain an S-layer an additional polyelectrolyte layer of PSS was used, deposited on top of the protein multilayer. This bridging layer is expected to promote recrystallization of the S-layer protein similar to a PSS/PAH arrangement, which was reported to efficiently facilitate SbpA crystalline layer formation (Toca-Herrera, Krastev et al. 2005).

As a test experiment, recrystallization of SbpA on ultra flat gold with a terminating PSS layer was carried out in a model system using promoter-modified electrodes with subsequently adsorbed PEI-PSS layers (Au-MUA/MU-PEI-PSS composition). The electrode was incubated in SbpA solution for 24 hours to ensure that the S-layer protein can be re-crystallized. Figure 4.36a shows an overview scan where the large flat areas of the crystallized protein (shown in light) cover about 90% of the whole area. On higher magnification scan a square S-layer lattice can easily be recognized, Figure 4.36b. Since recrystallization occurred from several nucleation points, it resulted in segments with different crystal orientation. Here the recrystallization front can be clearly seen, along with the areas of non-crystallized protein, amorphous layer of adsorbed polymer, and a segment of bare gold surface, which was produced prior to the scan by sweeping away the material from the surface with a higher force applied to the cantilever. Formation of the crystalline

surface layer was also confirmed by the force-distance curve measurement, showing an incompressible surface without significant electrostatic interactions between the tip and the surface during approach and retraction, Figure 4.36c.

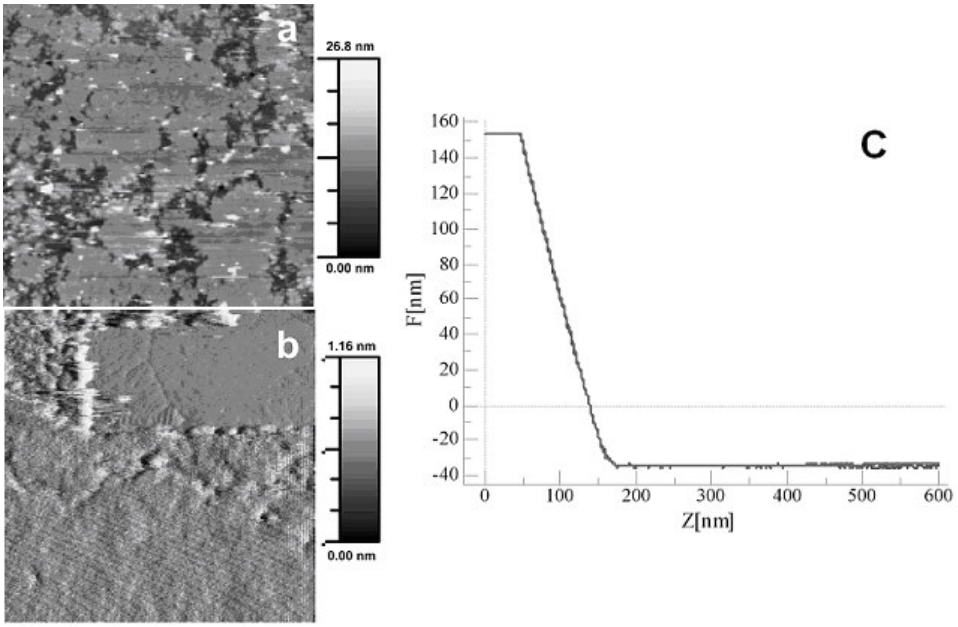

Figure 4.36. Characteristic AFM image of an SbpA layer crystallized on PEI-PSS-layer formed on a MUA/MU-modified flat gold: a) topography scan 10x10 μm^2; b) topography scan 800x800 nm^2, revealing a crystallization front, amorphous layer and a bare gold surface; c) force-distance curve. Measured in SbpA crystallization solution in buffer 6.

Further, recrystallization of SbpA on Au-MUA/MU-cyt.c-(PASA-cyt.c)$_3$-PSS electrodes was investigated. In contrast to the previous experiment, where only a partial coverage was observed on a 10x10 μm^2 scan, here, the surface is totally covered (figure not shown). In zoomed-in scans a characteristic S-layer lattice is also visible (see Figure 4.37a). The hysteretic form of the force-distance curve in Figure 4.37b, however, serves as an indication of a soft and compressible material underneath a crystalline surface layer. This conclusion is also supported by the comparison of the force curve slopes in Figure 4.37b and Figure 4.41c. A steeper slope in Figure 4.37b shows that an SbpA layer recrystallized on Au-MUA/MU-PEI-PSS promoter is more rigid than in the case of recrystallization upon cyt.c/PASA multilayer.

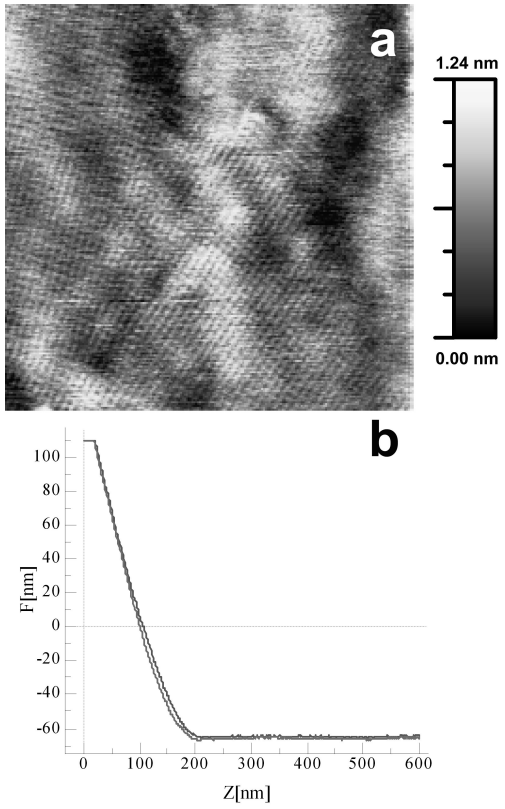

Figure 4.37. AFM image of SbpA layer crystallized flat Au-MUA/M-cyt.c(PASA-cyt.c)$_3$-PSS electrode: a) topography scan 800x800 nm^2; b) force-distance curve. Measured in buffer 1.

Similar results were obtained for an electrode with six intermediate (PASA-cyt.c) layers. In this case the surface roughness increased, which is a characteristic feature of polyelectrolyte protein films with increasing number of layers. Similar to the preceding case, an S-layer pattern is clearly seen (figure not shown). Notably, here the force-distance curve also points to a soft compressible material under the solid surface.

4.4.2. Electron transfer in cyt.c/PASA – SbpA hybrid multilayers

We have shown that formation of a S-layer membrane on a cyt.c/PASA multilayer is feasible, therefore not only the protein multilayer assemblies, but its combination with a crystalline S-layers can be used in design of functional bio-arrangements. However, it is necessary to assess maintenance of electroactivity of cyt.c within the multilayer after formation of the crystalline membrane.

The electrochemical response of the S-layer covered $(PASA\text{-}cyt.c)_6$ multilayer electrode is shown in Figure 4.38. Along with the relative decrease in oxidation and reduction peak heights, an additional reduction peak at about +90 mV appeared, which is attributed to electrochemical conversion of PASA (see Chapter 4.1.). This process was noted for PASA-containing arrangements and is more pronounced at scan rates below 50 mVs^{-1}. The total decrease in the amount of electrochemically active cyt.c after recrystallization of the S-layer on top of the standard $(PASA\text{-}cyt.c)_6$ electrode is about 50 %.

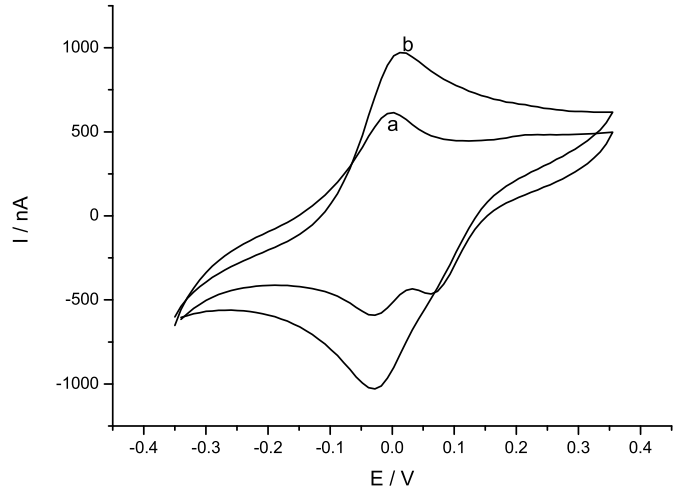

Figure 4.38. Cyclic voltammograms of flat Au-MUA/MU-cyt.c-$(PASA\text{-}cyt.c)_6$ multilayer electrodes: a) after recrystallization of SbpA; b) prior to crystallization of SbpA. Scan rate 200 mVs^{-1}.

A possible reason for the decrease of electroactivity can be seen in the bridging PSS layer, reported to influence cyt.c conformation (Weidinger, Murgida et al. 2006). Indeed, after adsorption of PSS a decrease in the amount of electroactive cyt.c by about 40 % was observed. Despite the fact that the PSS layer reduces the exchangeable charge, its use is necessary as it facilitates the S-layer recrystallization. SbpA envelope was electrochemically inactive in the potential range from -350 mV to +350 mV. Thus, SbpA-covered cyt.c/PASA multilayers are still electroactive with a response current corresponding to a supra-monolayer cyt.c surface concentration.

5. Conclusions.

In the current study a concept for the design of electroactive protein-polyelectrolyte multilayer assemblies, previously shown for the cyt.c/PASA system, was extended for arrangements containing two functional protein components coupled via redox interactions. The developed multilayer arrangements realize a redox chain between the electrode and the analyte in solution via multiple protein layers mimicking natural protein interaction via mediated and direct electron transfer. Special attention in this work is given to the electron transfer mechanism within such protein assemblies.

In the first part of the work the basic cyt.c/PASA system was analyzed with respect to the electron transfer mechanism and structure.

A mechanism for a long range electron transfer across cyt.c/PASA multilayers, proposed previously, suggests a direct electron exchange between cyt.c molecules as a principle electron pathway. Cyclic voltammograms of the cyt.c/PASA arrangements on promoter-modified gold, measured at high scan rates ($\geq$ 100 mVs^{-1}), show a quasi-reversible signal of cyt.c only. However, it was found that at low scan rates (< 20 mVs^{-1}) an additional peak appears, which corresponds to a PASA redox process. This result is an indication that PASA might also be involved in the electron transfer process. In order to obtain additional evidence about the electron transfer process and the state of both assembly components stationary and time-resolved surface-enhanced resonance Raman spectroelectrochemistry was applied to MUA/MU-cyt.c-PASA-cyt.c arrangements on roughened silver.

It was confirmed, that cyt.*c* immobilized in Ag-MUA/MU-cyt.c-PASA-cyt.c architecture retains its native structure. The protein is electroactive and exhibits a nearly ideal Nernst behavior. However on rough Ag electrodes, additional PASA/Cyt layers were found to be unstable and tend to desorb within the time scale of minutes.

It was also found that the polyelectrolyte (PASA) undergoes reversible potential-dependent changes as judged by SERR spectroscopy. Two spectrally different forms were identified, which differ in relative intensities, peak positions and absolute intensities.

Comparison of the redox equilibria and dynamics of cyt.c and PASA in Ag-MUA/MU-cyt.c-PASA-cyt.c and Ag-MUA/MU-apo.cyt.c-PASA-apo.cyt.c assemblies provides evidence for electron exchange between the protein and the polyelectrolyte. Therefore the polyelectrolyte – protein electron transfer may play an active role in

supporting long range electron transport within metal-MUA/MU-cyt.c-(PASA-cyt.c)$_n$ multilayer assemblies.

In the same part of the work the topography of the multilayer surface was analyzed throughout the assembly steps by AFM in liquid media. For this purpose, the assembly protocol for cyt.c/PASA multilayer arrangements on gold needle electrodes was transferred to ultra flat gold surfaces. It was found that the intermediate layers in a polyelectrolyte multilayer film of PASA/cyt.c assembled on ultra flat gold are formed as distinguishable units rather than as a mixed layer. All terminating layers of PASA or cyt.c have similar charge and adhesive properties throughout the multilayer film independent of the number of preceding layers (up to four PASA/cyt.*c* layers). However, the morphology of the film is changing during the build up process, as the surface roughness increases with the number of layers immobilized. These multilayers also show quasi-reversible electrochemistry of the surface-confined cyt.c with a transferred charge proportional to the number of immobilized layers, similar to the case of the arrangements constructed on gold needle electrodes

The second part of the work was focused on the development of polyelectrolyte-protein multilayers combining two functionally linked surface-confined proteins. Here, two systems were developed, representing two possible ways for inter-protein redox interaction: via mediated and direct electron transfer.

In the first case, cyt.c/PASA multilayer arrangement was combined with xanthine oxidase, also immobilized in a polyelectrolyte multilayer. The formation of the multilayer architecture has been studied by SPR, UV-vis spectroscopy and electrochemical methods. The electrode design relies on an internally mediated electron transfer from the exterior XOD layers, responsible for selective analyte conversion, towards the cyt.c core layers, where the signal is translated to a detectable current response. Hypoxanthine in solution reacting with XOD immobilized within the exterior of the multilayer arrangement is converted to uric acid, hydrogen peroxide, and superoxide. At a potential of +150 mV free superoxide radicals can be oxidized by cyt.c incorporated into underlying multilayers, with subsequent electron relay towards the electrode. It has been demonstrated that both cyt.c and XOD multilayers are necessary for successful signal transfer through the layer assembly.

The proposed architecture offers a good flexibility to adjust the properties of the assembly by tailoring the layer composition. In particular, susceptibility of the electrodes to a number of interfering agents can be controlled by the deposition of additional polyelectrolyte membrane with tunable permeability. Additionally, the electrode stability was examined and improved by thermal treatment.

A redox chain based on direct protein-protein communication was designed taking advantage of the interaction between cyt.c and bilirubin oxidase discovered in the course of this work. In this case cyt.c played a role of an electron transfer mediator between the electrode and the enzyme. BOD was found to accept cyt.c as a redox partner at around neutral pH with rather fast reaction kinetics. Further, this reaction was confined to a surface, and coupled with a direct electron transfer between the transducing electrode and cyt.c.

Direct electron transfer was established for the first time in a two-protein system immobilized within a polyelectrolyte multilayer architecture, combining cyt.c and BOD. Although these two proteins are not natural reaction partners, the electrode architecture facilitates the electron transfer from the electrode via multiple protein layers to molecular oxygen resulting in a catalytic reduction current. Sensitivity of the assembly towards the enzyme substrate (here oxygen) can be tuned to a large extent by the number of deposited layers without being limited by mediator diffusion or leakage.

The results are not only expected to have a considerable impact on the development of biofuel cells and biosensors, but also represent a significant advance in modeling biological signal transfer. For cyt.c as the electron carrier in the system other potential reaction partners might be used e.g. sulfite oxidase, laccase or nitrate reductase.

In the third part of the work it was shown, that the layer-by-layer assembly of globular proteins is feasible without use of polymers as counter-polyelectrolytes. The assembly is made by co-adsorption of cyt.c with sulfite oxidase. This arrangement shows a remarkable ability to transport electrons from the substrate in solution to the electrode over longer distances taking advantage of direct interaction between the two functional bio-components. Most importantly, the design does not require the use neither of additional redox mediators, nor a conventional polymer as a polyelectrolyte, which makes this approach interesting for the construction of third generation biosensors.

Avoiding the use of a scaffolding polyelectrolyte is one way to shed more light on the electron transfer mechanism within the PASA-based multi-protein arrangements. In every protein polyelectrolyte multilayer system reported in the first and the second part of this work, the cyt.c part of the arrangement was responsible for the long-range electron transfer across the multilayer film. Although the evidence that PASA undergoes redox conversion as judged by the CV and SERR spectroscopy would suggest that it may also take part in such long-range electron transfer, the presented results on the electron transfer within cyt.c/SOx arrangement gives a supporting evidence for the direct cyt.c-cyt.c electron exchange as a dominating mechanism.

Finally, in the last part of the work, S-layer recrystallization technique was demonstrated to be a complimentary assembly tool to the protein polyelectrolyte multilayer approach. The recrystallization of a protein surface layer of SbpA upon the PASA/cyt.c multilayer film was demonstrated in the case when a PSS bridging layer was immobilized before. Although immobilization of PSS entails a partial loss of the film electroactivity, the amount of retained electroactive protein is still enough for use of the assembly for analytical purposes. Notably, recrystallization of the S-layer has no considerable effect on the amount of electroactive cyt.*c* within the multilayer arrangement. Therefore, combination of self-assembled protein multilayers with S-layer recrystallization shall offer new advantages for construction of functional protein architectures.

We anticipate that the concepts described in this work will stimulate further progress in multilayer design of even more complex biomimetic signal cascades taking advantage of direct communication between proteins.

References

Abass, A. K., J. P. Hart, et al. (2000). "Development of an amperometric sulfite biosensor based on sulfite oxidase with cytochrome c, as electron acceptor, and a screen-printed transducer." Sensors and Actuators B-Chemical **62**(2): 148-153.

Allen, B. L., P. D. Kichambare, et al. (2007). "Carbon nanotube field-effect-transistor-based biosensors." Advanced Materials **19**(11): 1439-1451.

Allen, P. M., H. A. O. Hill, et al. (1984). "Surface Modifiers for the Promotion of Direct Electrochemistry of Cytochrome-C." Journal of Electroanalytical Chemistry **178**(1): 69-86.

Antipov, A. A. and G. B. Sukhorukov (2004). "Polyelectrolyte multilayer capsules as vehicles with tunable permeability." Advances in Colloid and Interface Science **111**(1-2): 49-61.

Anzai, J. and Y. Kobayashi (2000). "Construction of multilayer thin films of enzymes by means of sugar-lectin interactions." Langmuir **16**(6): 2851-2856.

Anzai, J., H. Takeshita, et al. (1998). "Layer-by-layer construction of enzyme multilayers on an electrode for the preparation of glucose and lactate sensors: Elimination of ascorbate interference by means of an ascorbate oxidase multilayer." Analytical Chemistry **70**(4): 811-817.

Armstrong, F. A., A. M. Bond, et al. (1989). "A Microscopic Model of Electron-Transfer at Electroactive Sites of Molecular Dimensions for Reduction of Cytochrome-C at Basal-Plane and Edge-Plane Graphite-Electrodes." Journal of Physical Chemistry **93**(17): 6485-6493.

Armstrong, F. A., H. A. Heering, et al. (1997). "Reactions of complex metalloproteins studied by protein-film voltammetry." Chemical Society Reviews **26**(3): 169-179.

Arys, X., A. Laschewsky, et al. (2001). "Ordered polyelectrolyte "multilayers". 1. Mechanisms of growth and structure formation: A comparison with classical fuzzy "multilayers"." Macromolecules **34**(10): 3318-3330.

Avila, A., B. W. Gregory, et al. (2000). "An electrochemical approach to investigate gated electron transfer using a physiological model system: Cytochrome c immobilized on carboxylic acid-terminated alkanethiol self-assembled monolayers on gold electrodes." Journal of Physical Chemistry B **104**(12): 2759-2766.

Balbinot, D., S. Atalick, et al. (2003). "Electrostatic assemblies of fullerene-porphyrin hybrids: Toward long-lived charge separation." Journal of Physical Chemistry B **107**(48): 13273-13279.

Bally, M., M. Halter, et al. (2006). "Optical microarray biosensing techniques." Surface and Interface Analysis **38**(11): 1442-1458.

Banci, L., I. Bertini, et al. (1997). "Solution structure of oxidized horse heart cytochrome c." Biochemistry **36**(32): 9867-9877.

Barbaro, A., C. Colapicchioni, et al. (1992). "Chemfet Devices for Biomedical and Environmental Applications." Advanced Materials **4**(6): 402-408.

Baur, J. W., M. F. Rubner, et al. (1999). "Forster energy transfer studies of polyelectrolyte heterostructures containing conjugated polymers: A means to estimate layer interpenetration." Langmuir **15**(19): 6460-6469.

Bayachou, M., L. Elkbir, et al. (2000). "Catalytic two-electron reductions of N2O and N-3(-) by myoglobin in surfactant films." Inorganic Chemistry **39**(2): 289-293.

Beissenhirtz, M. K., B. Kafka, et al. (2005). "Electrochemical quartz crystal microbalance studies on cytochrome c/polyelectrolyte multilayer assemblies on gold electrodes." Electroanalysis **17**(21): 1931-1937.

Beissenhirtz, M. K., F. W. Scheller, et al. (2004). "A superoxide sensor based on a multilayer cytochrome c electrode." Analytical Chemistry **76**(16): 4665-4671.

Beissenhirtz, M. K., F. W. Scheller, et al. (2004). "Electroactive cytochrome c multilayers within a polyelectrolyte assembly." Angewandte Chemie-International Edition **43**(33): 4357-4360.

Beveridge, T. J. (1994). "Bacterial S-Layers." Current Opinion in Structural Biology **4**(2): 204-212.

Bogue, R. (2005). "Developments in biosensors - where are tomorrow's markets?" Sensor Review **25**(3): 180-184.

Bourdillon, C., C. Demaille, et al. (1996). "From homogeneous electroenzymatic kinetics to antigen-antibody construction and characterization of spatially ordered catalytic enzyme assemblies on electrodes." Accounts of Chemical Research **29**(11): 529-535.

Boyer, M., S. Quillard, et al. (1997). "Oxidized model compounds of polyaniline studied by resonance Raman spectroscopy." Synthetic Metals **84**(1-3): 787-788.

Brautigan, D. L., S. Fergusonmiller, et al. (1978). "Definition of Cytochrome-C Binding Domains by Chemical Modification .1. Reaction with 4-Chloro-3,5-Dinitrobenzoate and Chromatographic-Separation of Singly Substituted Derivatives." Journal of Biological Chemistry **253**(1): 130-139.

Brautigan, D. L., S. Fergusonmiller, et al. (1978). "Definition of Cytochrome-C Binding Domains by Chemical Modification .2. Identification and Properties of Singly Substituted Carboxydinitrophenyl Cytochromes-C at Lysines 8, 13, 22, 27, 39, 60, 72, 87, and 99." Journal of Biological Chemistry **253**(1): 140-148.

Brody, M. S. and R. Hille (1999). "The kinetic behavior of chicken liver sulfite oxidase." Biochemistry **38**(20): 6668-6677.

BrowningKelley, M. E., K. WaduMesthrige, et al. (1997). "Atomic force microscopic study of specific antigen/antibody binding." Langmuir **13**(2): 343-350.

Calvo, E. J., C. Danilowicz, et al. (2002). "Molecular "wiring" enzymes in organized nanostructures." Journal of the American Chemical Society **124**(11): 2452-2453.

Calvo, E. J., C. B. Danilowicz, et al. (2005). "Supramolecular multilayer structures of wired redox enzyme electrodes." Physical Chemistry Chemical Physics **7**(8): 1800-1806.

Calvo, E. J., R. Etchenique, et al. (2001). "Layer-by-layer self-assembly of glucose oxidase and Os(Bpy)(2)ClPyCH2NH-poly(allylamine) bioelectrode." Analytical Chemistry **73**(6): 1161-1168.

Calvo, E. J. and A. Wolosiuk (2004). "Supramolecular architectures of electrostatic self-assembled glucose oxidase enzyme electrodes." Chemphyschem **5**(2): 235-239.

Caruso, F. and C. Schuler (2000). "Enzyme multilayers on colloid particles: Assembly, stability, and enzymatic activity." Langmuir **16**(24): 9595-9603.

Chan, Y. N. C., G. S. W. Craig, et al. (1992). "Synthesis of Palladium and Platinum Nanoclusters within Microphase-Separated Diblock Copolymers." Chemistry of Materials **4**(4): 885-894.

Chan, Y. N. C., R. R. Schrock, et al. (1992). "Synthesis of Silver and Gold Nanoclusters within Microphase-Separated Diblock Copolymers." Chemistry of Materials **4**(1): 24-27.

Chen, Q., Y. Kobayashi, et al. (1998). "Avidin-biotin system-based enzyme multilayer membranes for biosensor applications: Optimization of loading of choline esterase and choline oxidase in the bienzyme membrane for acetylcholine biosensors." Electroanalysis **10**(2): 94-97.

Chen, W. and T. J. McCarthy (1997). "Layer-by-layer deposition: A tool for polymer surface modification." Macromolecules **30**(1): 78-86.

Chiarelli, P. A., M. S. Johal, et al. (2001). "Controlled fabrication of polyelectrolyte multilayer thin films using spin-assembly." Advanced Materials **13**(15): 1167-+.

Choi, J. and M. F. Rubner (2005). "Influence of the degree of ionization on weak polyelectrolyte multilayer assembly." Macromolecules **38**(1): 116-124.

Christenson, A., N. Dimcheva, et al. (2004). "Direct electron transfer between ligninolytic redox enzymes and electrodes." Electroanalysis **16**(13-14): 1074-1092.

Christenson, A., S. Shleev, et al. (2006). "Redox potentials of the blue copper sites of bilirubin oxidases." Biochimica Et Biophysica Acta-Bioenergetics **1757**(12): 1634-1641.

Clark, L. C. and C. Lyons (1962). "Electrode Systems for Continuous Monitoring in Cardiovascular Surgery." Annals of the New York Academy of Sciences **102**(1): 29-&.

Coche-Guerente, L., J. Desbrieres, et al. (2005). "Physicochemical characterization of the layer-by-layer self-assembly of polyphenol oxidase and chitosan on glassy carbon electrode." Electrochimica Acta **50**(14): 2865-2877.

Colapicchioni, C., A. Barbaro, et al. (1992). "Fabrication and Characterization of Enfet Devices for Biomedical Applications and Environmental Monitoring." Sensors and Actuators B-Chemical **6**(1-3): 202-207.

Creutz, C. and N. Sutin (1973). "Mechanisms of Reactions of Cytochrome C .3. Reduction of Ferricytochrome C by Dithionite Ion - Electron-Transfer by Parallel Adjacent and Remote Pathways." Proceedings of the National Academy of Sciences of the United States of America **70**(6): 1701-1703.

Dammer, U., M. Hegner, et al. (1996). "Specific antigen/antibody interactions measured by force microscopy." Biophysical Journal **70**(5): 2437-2441.

Davis, J. J., R. J. Coles, et al. (1997). "Protein electrochemistry at carbon nanotube electrodes." Journal of Electroanalytical Chemistry **440**(1-2): 279-282.

Decher, G. (1997). "Fuzzy nanoassemblies: Toward layered polymeric multicomposites." Science **277**(5330): 1232-1237.

Decher, G., J. D. Hong, et al. (1992). "Buildup of Ultrathin Multilayer Films by a Self-Assembly Process .3. Consecutively Alternating Adsorption of Anionic and Cationic Polyelectrolytes on Charged Surfaces." Thin Solid Films **210**(1-2): 831-835.

Delcorte, A., P. Bertrand, et al. (1997). "Adsorption of polyelectrolyte multilayers on polymer surfaces." Langmuir **13**(19): 5125-5136.

Dellacorte, E. and F. Stirpe (1968). "Regulation of Xanthine Oxidase in Rat Liver - Modifications of Enzyme Activity of Rat Liver Supernatant on Storage at -20 Degrees." Biochemical Journal **108**(2): 349-&.

Dementiev, A. A., A. A. Baikov, et al. (2005). "Biological and polymeric self-assembled hybrid systems: Structure and properties of thylakoid/polyelectrolyte complexes." Biochimica Et Biophysica Acta-Biomembranes **1712**(1): 9-16.

Dieluweit, S., D. Pum, et al. (1998). "Formation of a gold superlattice on an S-layer with square lattice symmetry." Supramolecular Science **5**(1-2): 15-19.

Dopner, S., P. Hildebrandt, et al. (1996). "Analysis of vibrational spectra of multicomponent systems. Application to pH-dependent resonance Raman spectra of ferricytochrome c." Spectrochimica Acta Part a-Molecular and Biomolecular Spectroscopy **52**(5): 573-584.

Dopner, S., P. Hildebrandt, et al. (1999). "The structural and functional role of lysine residues in the binding domain of cytochrome c in the electron transfer to cytochrome c oxidase." European Journal of Biochemistry **261**(2): 379-391.

Dryhurst, G. and K. M. Kadish (1982). Bioelectrochemistry, New York, Academic Press.

Du, X. Y., J. Anzai, et al. (1996). "Amperometric alcohol sensors based on protein multilayers composed of avidin and biotin-labeled alcohol oxidase." Electroanalysis **8**(8-9): 813-816.

Dubas, S. T. and J. B. Schlenoff (1999). "Factors controlling the growth of polyelectrolyte multilayers." Macromolecules **32**(24): 8153-8160.

Dzyadevych, S. V., A. P. Soldatkin, et al. (2003). "Biosensors based on enzyme field-effect transistors for determination of some substrates and inhibitors." Analytical and Bioanalytical Chemistry **377**(3): 496-506.

Eddowes, M. J. and H. A. O. Hill (1977). "Novel Method for Investigation of Electrochemistry of Metalloproteins - Cytochrome-C." Journal of the Chemical Society-Chemical Communications(21): 771-772.

Eger, B. T., K. Okamoto, et al. (2000). "Purification, crystallization and preliminary X-ray diffraction studies of xanthine dehydrogenase and xanthine oxidase isolated from bovine milk." Acta Crystallographica Section D-Biological Crystallography **56**: 1656-1658.

Elbert, D. L., C. B. Herbert, et al. (1999). "Thin polymer layers formed by polyelectrolyte multilayer techniques on biological surfaces." Langmuir **15**(16): 5355-5362.

Elliott, S. J., A. E. McElhaney, et al. (2002). "A voltammetric study of interdomain electron transfer within sulfite oxidase." Journal of the American Chemical Society **124**(39): 11612-11613.

Epstein, J. R. and D. R. Walt (2003). "Fluorescence-based fibre optic arrays: a universal platform for sensing." Chemical Society Reviews **32**(4): 203-214.

Fan, C. H., G. X. Li, et al. (2000). "A reagentless nitric oxide biosensor based on hemoglobin-DNA films." Analytica Chimica Acta **423**(1): 95-100.

Farhat, T., G. Yassin, et al. (1999). "Water and ion pairing in polyelectrolyte multilayers." Langmuir **15**(20): 6621-6623.

Farooqi, M., M. Saleemuddin, et al. (1997). "Bioaffinity layering: A novel strategy for the immobilization of large quantities of glycoenzymes." Journal of Biotechnology **55**(3): 171-179.

Feng, C. J., R. V. Kedia, et al. (2002). "Effect of solution viscosity on intramolecular electron transfer in sulfite oxidase." Biochemistry **41**(18): 5816-5821.

Feng, Z. Q., S. Imabayashi, et al. (1997). "Long-range electron-transfer reaction rates to cytochrome c across long- and short-chain alkanethiol self-assembled monolayers: Electroreflectance studies." Journal of the Chemical Society-Faraday Transactions **93**(7): 1367-1370.

Ferapontova, E. E., T. Ruzgas, et al. (2003). "Direct electron transfer of heme- and molybdopterin cofactor-containing chicken liver sulfite oxidase on alkanethiol-modified gold electrodes." Analytical Chemistry **75**(18): 4841-4850.

Fergusonmiller, S., D. L. Brautigan, et al. (1978). "Definition of Cytochrome-C Binding Domains by Chemical Modification .3. Kinetics of Reaction of

Carboxydinitrophenyl Cytochromes-C with Cytochrome-C Oxidase." Journal of Biological Chemistry **253**(1): 149-159.
Florin, E. L., V. T. Moy, et al. (1994). "Adhesion Forces between Individual Ligand-Receptor Pairs." Science **264**(5157): 415-417.
Forzani, E. S., V. M. Solis, et al. (2000). "Electrochemical behavior of polyphenol oxidase immobilized in self-assembled structures layer by layer with cationic polyallylamine." Analytical Chemistry **72**(21): 5300-5307.
Freire, R. S., C. A. Pessoa, et al. (2003). "Direct electron transfer: An approach for electrochemical biosensors with higher selectivity and sensitivity." Journal of the Brazilian Chemical Society **14**(2): 230-243.
Frew, J. E. and H. A. O. Hill (1988). "Direct and Indirect Electron-Transfer between Electrodes and Redox Proteins." European Journal of Biochemistry **172**(2): 261-269.
Fried, R. (1971). "Oxidation of Vanillin by Cream Xanthine Oxidase and Its Inhibition by Allopurinol." Experientia **27**(2): 123-&.
Ge, B. and F. Lisdat (2002). "Superoxide sensor based on cytochrome c immobilized on mixed-thiol SAM with a new calibration method." Analytica Chimica Acta **454**(1): 53-64.
Gobi, K. V. and F. Mizutani (2001). "Layer-by-layer construction of an active multilayer enzyme electrode applicable for direct amperometric determination of cholesterol." Sensors and Actuators B-Chemical **80**(3): 272-277.
Gooding, J. J., R. Wibowo, et al. (2003). "Protein electrochemistry using aligned carbon nanotube arrays." Journal of the American Chemical Society **125**(30): 9006-9007.
Gorton, L. (1995). "Carbon-Paste Electrodes Modified with Enzymes, Tissues, and Cells." Electroanalysis **7**(1): 23-45.
Graul, T. W. and J. B. Schlenoff (1999). "Capillaries modified by polyelectrolyte multilayers for electrophoretic separations." Analytical Chemistry **71**(18): 4007-4013.
Gruger, A., A. Novak, et al. (1994). "Infrared and Raman-Study of Polyaniline .2. Influence of Ortho Substituents on Hydrogen-Bonding and Uv/Vis near-Ir Electron Charge-Transfer." Journal of Molecular Structure **328**: 153-167.
Gufler, P. C., D. Pum, et al. (2004). "Highly robust lipid membranes on crystalline S-layer supports investigated by electrochemical impedance spectroscopy." Biochimica Et Biophysica Acta-Biomembranes **1661**(2): 154-165.
Guilbaul.Gg and G. J. Lubrano (1973). "Enzyme Electrode for Amperometric Determination of Glucose." Analytica Chimica Acta **64**(3): 439-455.
Guo, J. A., X. X. Liang, et al. (1991). "Purification and Properties of Bilirubin Oxidase from Myrothecium-Verrucaria." Applied Biochemistry and Biotechnology **31**(2): 135-143.
Gupta, R. K. (1973). "Electron-Transfer in Cytochrome C Role of Polypeptide-Chain." Biochimica Et Biophysica Acta **292**(1): 291-295.
Gyorvary, E. S., O. Stein, et al. (2003). "Self-assembly and recrystallization of bacterial S-layer proteins at silicon supports imaged in real time by atomic force microscopy." Journal of Microscopy-Oxford **212**: 300-306.
Hammond, P. T. (1999). "Recent explorations in electrostatic multilayer thin film assembly." Current Opinion in Colloid & Interface Science **4**(6): 430-442.

Hart, J. P., A. K. Abass, et al. (2002). "Development of disposable amperometric sulfur dioxide biosensors based on screen printed electrodes." Biosensors & Bioelectronics **17**(5): 389-394.

Heptinstall, S., A. Johnson, et al. (2005). "Adenine nucleotide metabolism in human blood--important roles for leukocytes and erythrocytes." J Thromb Haemost **3**(10): 2331-9.

Hille, R. (1996). "The mononuclear molybdenum enzymes." Chemical Reviews **96**(7): 2757-2816.

Hinnen, C., R. Parsons, et al. (1983). "Electrochemical and Spectroreflectance Studies of the Adsorbed Horse Heart Cytochrome-C and Cytochrome-C3 from D-Vulgaris, Miyazaki Strain, at Gold Electrode." Journal of Electroanalytical Chemistry **147**(1-2): 329-337.

Hinterdorfer, P., W. Baumgartner, et al. (1996). "Detection and localization of individual antibody-antigen recognition events by atomic force microscopy." Proceedings of the National Academy of Sciences of the United States of America **93**(8): 3477-3481.

Hodak, J., R. Etchenique, et al. (1997). "Layer-by-layer self-assembly of glucose oxidase with a poly(allylamine)ferrocene redox mediator." Langmuir **13**(10): 2708-2716.

Hoogeveen, N. G., M. A. C. Stuart, et al. (1996). "Formation and stability of multilayers of polyelectrolytes." Langmuir **12**(15): 3675-3681.

Hoshi, T., J. Anzai, et al. (1995). "Controlled Deposition of Glucose-Oxidase on Platinum-Electrode Based on an Avidin-Biotin System for the Regulation of Output Current of Glucose Sensors." Analytical Chemistry **67**(4): 770-774.

Hoshi, T., T. Noguchi, et al. (2006). "The preparation of amperometric xanthine sensors based on multilayer thin films containing xanthine oxidase." Materials Science & Engineering C-Biomimetic and Supramolecular Systems **26**(1): 100-103.

Hoshi, T., H. Saiki, et al. (2003). "Amperometric uric acid sensors based on polyelectrolyte multilayer films." Talanta **61**(3): 363-368.

Hou, S. F., H. Q. Fang, et al. (1997). "An amperometric enzyme electrode for glucose using immobilized glucose oxidase in a ferrocene attached poly(4-vinylpyridine) multilayer film." Analytical Letters **30**(9): 1631-1641.

Hu, S. Z., I. K. Morris, et al. (1993). "Complete Assignment of Cytochrome-C Resonance Raman-Spectra Via Enzymatic Reconstitution with Isotopically Labeled Hemes." Journal of the American Chemical Society **115**(26): 12446-12458.

Huang, W. S., B. D. Humphrey, et al. (1986). "Polyaniline, a Novel Conducting Polymer - Morphology and Chemistry of Its Oxidation and Reduction in Aqueous-Electrolytes." Journal of the Chemical Society-Faraday Transactions I **82**: 2385-&.

Hugotlegoff, A. and M. C. Bernard (1993). "Protonation and Oxidation Processes in Polyaniline Thin-Films Studied by Optical Multichannel Analysis and in-Situ Raman-Spectroscopy." Synthetic Metals **60**(2): 115-131.

Ignatov, S., D. Shishniashvili, et al. (2002). "Amperometric biosensor based on a functionalized gold electrode for the detection of antioxidants." Biosens Bioelectron **17**(3): 191-9.

Ilk, N., C. Vollenkle, et al. (2002). "Molecular characterization of the S-layer gene, sbpA, of Bacillus sphaericus CCM 2177 and production of a functional S-layer fusion protein with the ability to recrystallize in a defined orientation while presenting the fused allergen." Applied and Environmental Microbiology **68**(7): 3251-3260.

Jaber, J. A., P. B. Chase, et al. (2003). "Actomyosin-driven motility on patterned polyelectrolyte mono- and multilayers." Nano Letters **3**(11): 1505-1509.

Jessel, N., F. Atalar, et al. (2003). "Bioactive coatings based on a polyelectrolyte multilayer architecture functionalized by embedded proteins." Advanced Materials **15**(9): 692-695.

Jin, W., F. Bier, et al. (1995). "Construction and Characterization of a Multilayer Enzyme Electrode - Covalent Binding of Quinoprotein Glucose-Dehydrogenase onto Gold Electrodes." Biosensors & Bioelectronics **10**(9-10): 823-829.

Jin, W., U. Wollenberger, et al. (1997). "Electrochemical investigations of the intermolecular electron transfer between cytochrome c and NADPH-cytochrome P450-reductase." Journal of Electroanalytical Chemistry **8**(15): 135-139.

Jisr, R. M., H. H. Rmaile, et al. (2005). "Hydrophobic and ultrahydrophobic multilayer thin films from perfluorinated polyelectrolytes." Angewandte Chemie-International Edition **44**(5): 782-785.

Kang, C. H., D. L. Brautigan, et al. (1978). "Definition of Cytochrome-C Binding Domains by Chemical Modification - Reaction of Carboxydinitrophenyl-Cytochromes-C and Trinitrophenyl-Cytochromes-C with Bakers-Yeast Cytochrome-C Peroxidase." Journal of Biological Chemistry **253**(18): 6502-6510.

Karakas, E., H. L. Wilson, et al. (2005). "Structural insights into sulfite oxidase deficiency." Journal of Biological Chemistry **280**(39): 33506-33515.

Kaschak, D. M., S. A. Johnson, et al. (1999). "Artificial photosynthesis in lamellar assemblies of metal poly(pyridyl) complexes and metalloporphyrins." Coordination Chemistry Reviews **186**: 403-416.

Kataoka, K., R. Kitagawa, et al. (2005). "Point mutations at the type I Cu ligands, Cys457 and Met467, and at the putative proton donor, Asp105, in Myrothecium verrucaria bilirubin oxidase and reactions with dioxygen." Biochemistry **44**(18): 7004-12.

Kellogg, G. J., A. M. Mayes, et al. (1996). "Neutron reflectivity investigations of self-assembled conjugated polyion multilayers." Langmuir **12**(21): 5109-5113.

Kisker, C., H. Schindelin, et al. (1997). "Molybdenum-cofactor-containing enzymes: Structure and mechanism." Annual Review of Biochemistry **66**: 233-267.

Kobayashi, Y. and J. Anzai (2001). "Preparation and optimization of bienzyme multilayer films using lectin and glyco-enzymes for biosensor applications." Journal of Electroanalytical Chemistry **507**(1-2): 250-255.

Korell, U. and R. B. Lennox (1993). "A Sulfite Biosensor - Coupling of Sulfite Oxidase (Ec 1.8.3.1) to a Ttftcnq Electrode." Journal of Electroanalytical Chemistry **351**(1-2): 137-143.

Kupcu, S., M. Sara, et al. (1995). "Liposomes Coated with Crystalline Bacterial-Cell Surface Protein (S-Layer) as Immobilization Structures for Macromolecules." Biochimica Et Biophysica Acta-Biomembranes **1235**(2): 263-269.

Kuswandi, B., R. Andres, et al. (2001). "Optical fibre biosensors based on immobilised enzymes." Analyst **126**(8): 1469-1491.

Lee, G. U., D. A. Kidwell, et al. (1994). "Sensing Discrete Streptavidin Biotin Interactions with Atomic-Force Microscopy." Langmuir **10**(2): 354-357.

Lee, S. S., J. D. Hong, et al. (2001). "Layer-by-layer deposited multilayer assemblies of ionene-type polyelectrolytes based on the spin-coating method." Macromolecules **34**(16): 5358-5360.

Li, Q. W., G. A. Luo, et al. (2001). "Direct electron transfer for heme proteins assembled on nanocrystalline TiO2 film." Electroanalysis **13**(5): 359-363.

Li, W. J., Z. Wang, et al. (2000). "Fabrication of multilayer films containing horseradish peroxidase and polycation-bearing Os complex by means of electrostatic layer-by-layer adsorption and its application as a hydrogen peroxide sensor." Analytica Chimica Acta **418**(2): 225-232.

Li, Z. and N. F. Hu (2003). "Direct electrochemistry of heme proteins in their layer-by-layer films with clay nanoparticles." Journal of Electroanalytical Chemistry **558**: 155-165.

Lindholm-Sethson, B., J. C. Gonzalez, et al. (1998). "Electron transfer to a gold electrode from cytochrome oxidase in a biomembrane via a polyelectrolyte film." Langmuir **14**(23): 6705-6708.

Lisdat, F., B. Ge, et al. (1999). "Superoxide dismutase activity measurement using cytochrome c modified electrode." Analytical Chemistry **71**(7): 1359-1365.

Lisdat, F., B. Ge, et al. (1999). "An electrochemical method for quantification of the radical scavenging activity of SOD." Fresenius Journal of Analytical Chemistry **365**(6): 494-498.

Liu, X. J., W. L. Peng, et al. (2005). "DNA facilitating electron transfer reaction of xanthine oxidase." Electrochemistry Communications **7**(5): 562-566.

Loew, N., F. W. Scheller, et al. (2004). "Characterization of self-assembling of glucose dehydrogenase in mono- and multilayers on gold electrodes." Electroanalysis **16**(13-14): 1149-1154.

Lu, H. Y., J. Yang, et al. (2006). "Vapor-surface sol-gel deposition of titania alternated with protein adsorption for assembly of electroactive, enzyme-active films." Electroanalysis **18**(4): 379-390.

Lu, S. (2003). "A multi-wall carbon nanotubes-dicetyl phosphate electrode for the determination of hypoxanthine in fish." Anal Sci **19**(9): 1309-12.

Lvov, Y., K. Ariga, et al. (1995). "Assembly of Multicomponent Protein Films by Means of Electrostatic Layer-by-Layer Adsorption." Journal of the American Chemical Society **117**(22): 6117-6123.

Lvov, Y., G. Decher, et al. (1993). "Assembly, Structural Characterization, and Thermal-Behavior of Layer-by-Layer Deposited Ultrathin Films of Poly(Vinyl Sulfate) and Poly(Allylamine)." Langmuir **9**(2): 481-486.

Lvov, Y., B. Munge, et al. (2000). "Films of manganese oxide nanoparticles with polycations or myoglobin from alternate-layer adsorption." Langmuir **16**(23): 8850-8857.

Ma, H. Y., N. F. Hu, et al. (2000). "Electroactive myoglobin films grown layer-by-layer with poly(styrenesulfonate) on pyrolytic graphite electrodes." Langmuir **16**(11): 4969-4975.

Macdiarmid, A. G., L. S. Yang, et al. (1987). "Polyaniline - Electrochemistry and Application to Rechargeable Batteries." Synthetic Metals **18**(1-3): 393-398.

Mader, C., S. Kupcu, et al. (1999). "Stabilizing effect of an S-layer on liposomes towards thermal or mechanical stress." Biochimica Et Biophysica Acta-Biomembranes **1418**(1): 106-116.

Mano, N., F. Mao, et al. (2003). "Characteristics of a miniature compartment-less glucose-O-2 biofuel cell and its operation in a living plant." Journal of the American Chemical Society **125**(21): 6588-6594.

Mao, L. Q., F. Xu, et al. (2001). "Miniaturized amperometric biosensor based on xanthine oxidase for monitoring hypoxanthine in cell culture media." Analytical Biochemistry **292**(1): 94-101.

Marazuela, M. D. and M. C. Moreno-Bondi (2002). "Fiber-optic biosensors - an overview." Analytical and Bioanalytical Chemistry **372**(5-6): 664-682.
Marcus, R. A. (1993). "Electron-Transfer Reactions in Chemistry - Theory and Experiment (Nobel Lecture)." Angewandte Chemie-International Edition in English **32**(8): 1111-1121.
Marcus, R. A. and N. Sutin (1985). "Electron Transfers in Chemistry and Biology." Biochimica Et Biophysica Acta **811**(3): 265-322.
Massey, V., L. M. Schopfer, et al. (1989). "Differences in Protein-Structure of Xanthine Dehydrogenase and Xanthine-Oxidase Revealed by Reconstitution with Flavin Active-Site Probes." Journal of Biological Chemistry **264**(18): 10567-10573.
Mello, L. D. and L. T. Kubota (2002). "Review of the use of biosensors as analytical tools in the food and drink industries." Food Chemistry **77**(2): 237-256.
Michaels, A. S. and R. G. Miekka (1961). "Polycation-Polyanion Complexes - Preparation and Properties of Poly-(Vinylbenzyltrimethylammonium) Poly-(Styrenesulfonate)." Journal of Physical Chemistry **65**(10): 1765-&.
MindBranch, I. (2004). ""US and Worldwide Biosensor Market, R&D and Commercial Implication"." Fuji-Keizai USA, Inc.
Mizutani, F., Y. Sato, et al. (1996). "Enzyme ultra-thin layer electrode prepared by the co-adsorption of poly-L-lysine and glucose oxidase onto a mercaptopropionic acid-modified gold surface." Chemistry Letters(4): 251-252.
Monk, D. J. and D. R. Walt (2004). "Optical fiber-based biosensors." Analytical and Bioanalytical Chemistry **379**(7-8): 931-945.
Mugweru, A., B. Q. Wang, et al. (2004). "Voltammetric sensor for oxidized DNA using ultrathin films of osmium and ruthenium metallopolymers." Analytical Chemistry **76**(18): 5557-5563.
Mulchandani, A., C. A. Groom, et al. (1991). "Determination of Sulfite in Food-Products by an Enzyme Electrode." Journal of Biotechnology **18**(1-2): 93-102.
Mulchandani, A., J. H. T. Luong, et al. (1989). "Development and Application of a Biosensor for Hypoxanthine in Fish Extract." Analytica Chimica Acta **221**(2): 215-222.
Munge, B., S. K. Das, et al. (2003). "Electron transfer reactions of redox cofactors in spinach Photosystem I reaction center protein in lipid films on electrodes." Journal of the American Chemical Society **125**(41): 12457-12463.
Murgida, D. H. and P. Hildebrandt (2001). "Heterogeneous electron transfer of cytochrome c on coated silver electrodes. Electric field effects on structure and redox potential." Journal of Physical Chemistry B **105**(8): 1578-1586.
Murphy, L. (2006). "Biosensors and bioelectrochemistry." Current Opinion in Chemical Biology **10**(2): 177-184.
Nader, P. A., S. S. Vives, et al. (1990). "Studies with a Sulfite Oxidase-Modified Carbon Paste Electrode for Detection Determination of Sulfite Ion and So2(G) in Continuous-Flow Systems." Journal of Electroanalytical Chemistry **284**(2): 323-333.
Nadzhafova, O. Y., V. N. Zaitsev, et al. (2004). "Heme proteins sequestered in silica sol-gels using surfactants feature direct electron transfer and peroxidase activity." Electrochemistry Communications **6**(2): 205-209.
Nagasawa, M., T. Murase, et al. (1965). "Potentiometric Titration of Stereoregular Polyelectrolytes." Journal of Physical Chemistry **69**(11): 4005-&.

Nakagawa, T., S. Tsujimura, et al. (2003). "Bilirubin oxidase and [Fe(CN)(6)](3-/4-) modified electrode allowing diffusion-controlled reduction of O-2 to water at pH 7.0." Chemistry Letters **32**(1): 54-55.

Nakatani, H. S., L. Vieira dos Santos, et al. (2005). "Biosensor Based on Xanthine Oxidase for Monitoring Hypoxanthine in Fish Meat." Am. J. Biochem. & Biotech **1**(2): 85-89.

Narvaez, A., G. Suarez, et al. (2000). "Reagentless biosensors based on self-deposited redox polyelectrolyte-oxidoreductases architectures." Biosensors & Bioelectronics **15**(1-2): 43-52.

Navati, M. S., A. Ray, et al. (2004). "Probing solvation-shell hydrogen binding in glassy and sol-gel matrixes through vibronic sideband luminescence spectroscopy." Journal of Physical Chemistry B **108**(4): 1321-1327.

Neubauer, A., C. Hodl, et al. (1994). "A Multistep Enzyme Sensor for Sucrose Based on S-Layer Microparticles as Immobilization Matrix." Analytical Letters **27**(5): 849-865.

Neubauer, A., D. Pum, et al. (1993). "An Amperometric Glucose Sensor-Based on Isoporous Crystalline Protein Membranes as Immobilization Matrix." Analytical Letters **26**(7): 1347-1360.

Nguyen, Q. T., Z. H. Ping, et al. (2003). "Simple method for immobilization of bio-macromolecules onto membranes of different types." Journal of Membrane Science **213**(1-2): 85-95.

Nicholson, R. and I. Shain (1965). "Theory of Stationary Electrode Polarography for a Chemical Reaction Coupled between 2 Charge Transfers." Analytical Chemistry **37**(2): 178-&.

Niki, K., W. R. Hardy, et al. (2003). "Coupling to lysine-13 promotes electron tunneling through carboxylate-terminated alkanethiol self-assembled monolayers to cytochrome c." Journal of Physical Chemistry B **107**(37): 9947-9949.

Nishino, T., T. Nishino, et al. (1989). "The Reactivity of Chicken Liver Xanthine Dehydrogenase with Molecular-Oxygen." Journal of Biological Chemistry **264**(5): 2518-2527.

NIST Standard Reference Database 74 **http://xpdb.nist.gov/enzyme_thermodynamics**.

Nocek, J. M., S. L. Hatch, et al. (2002). "Interprotein electron transfer in a confined space: Uncoupling protein dynamics from electron transfer by sol-gel encapsulation." Journal of the American Chemical Society **124**(32): 9404-9411.

Olson, J. S., D. P. Ballou, et al. (1974). "Mechanism of Action of Xanthine-Oxidase." Journal of Biological Chemistry **249**(14): 4363-4382.

Olson, J. S., D. P. Ballou, et al. (1974). "Reaction of Xanthine-Oxidase with Molecular-Oxygen." Journal of Biological Chemistry **249**(14): 4350-4362.

Park, I. S., Y. J. Cho, et al. (2000). "Characterization and meat freshness application of a serial three-enzyme reactor system measuring ATP-degradative compounds." Analytica Chimica Acta **404**(1): 75-81.

Park, S. Y., C. J. Barrett, et al. (2001). "Anomalous adsorption of polyelectrolyte layers." Macromolecules **34**(10): 3384-3388.

Pei, J. H. and X. Y. Li (2000). "Xanthine and hypoxanthine sensors based on xanthine oxidase immobilized on a CuPtCl6 chemically modified electrode and liquid chromatography electrochemical detection." Analytica Chimica Acta **414**(1-2): 205-213.

Phuvanartnuruks, V. and T. J. McCarthy (1998). "Stepwise polymer surface modification: Chemistry-layer-by-layer deposition." Macromolecules **31**(6): 1906-1914.

Pick, F. M., Mcgartol.Ma, et al. (1971). "Reaction of Formaldehyde and of Methanol with Xanthine Oxidase." European Journal of Biochemistry **18**(1): 65-&.

Porras, A. G., J. S. Olson, et al. (1981). "The Reaction of Reduced Xanthine-Oxidase with Oxygen - Kinetics of Peroxide and Superoxide Formation." Journal of Biological Chemistry **256**(17): 9096-9103.

Pranitis, D. M., M. Teltingdiaz, et al. (1992). "Potentiometric Ion-Selective, Gas-Selective, and Bioselective Membrane Electrodes." Critical Reviews in Analytical Chemistry **23**(3): 163-186.

Pum, D., G. Stangl, et al. (1997). "Deep UV patterning of monolayers of crystalline S layer protein on silicon surfaces." Colloids and Surfaces B-Biointerfaces **8**(3): 157-162.

Qu, F. L., M. H. Yang, et al. (2005). "Amperometric biosensor for choline based on layer-by-layer assembled functionalized carbon nanotube and polyaniline multilayer film." Analytical Biochemistry **344**(1): 108-114.

Raiteri, R., M. Grattarola, et al. (2001). "Micromechanical cantilever-based biosensors." Sensors and Actuators B-Chemical **79**(2-3): 115-126.

Ram, M. K., M. Adami, et al. (2000). "Nano-assembly of glucose oxidase on the in situ self-assembled films of polypyrrole and its optical, surface and electrochemical characterizations." Nanotechnology **11**(2): 112-119.

Ram, M. K., P. Bertoncello, et al. (2001). "Cholesterol biosensors prepared by layer-by-layer technique." Biosensors & Bioelectronics **16**(9-12): 849-856.

Ramanathan, K., B. R. Jonsson, et al. (2001). "Sol-gel based thermal biosensor for glucose." Analytica Chimica Acta **427**(1): 1-10.

Ray, A., M. L. Feng, et al. (2005). "Direct electrochemistry and Raman spectroscopy of sol-gel-encapsulated myoglobin." Langmuir **21**(16): 7456-7460.

Reed, D. E. and F. M. Hawkridge (1987). "Direct Electron-Transfer Reactions of Cytochrome-C at Silver Electrodes." Analytical Chemistry **59**(19): 2334-2339.

Riklin, A. and I. Willner (1995). "Glucose and Acetylcholine Sensing Multilayer Enzyme Electrodes of Controlled Enzyme Layer Thickness." Analytical Chemistry **67**(22): 4118-4126.

Rodrigues, C. G., A. G. Wedd, et al. (1991). "Electrochemistry of Xanthine-Oxidase at Glassy-Carbon and Mercury-Electrodes." Journal of Electroanalytical Chemistry **312**(1-2): 131-140.

Rodriguez, J., M. Gomez, et al. (2000). "Reactively sputter-deposited titanium oxide coatings with parallel penniform microstructure." Advanced Materials **12**(5): 341-+.

Ropp, P. A. and H. H. Thorp (1999). "Site-selective electron transfer from purines to electrocatalysts: voltammetric detection of a biologically relevant deletion in hybridized DNA duplexes." Chemistry & Biology **6**(9): 599-605.

Ros, R., F. Schwesinger, et al. (1998). "Antigen binding forces of individually addressed single-chain Fv antibody molecules." Proceedings of the National Academy of Sciences of the United States of America **95**(13): 7402-7405.

Rosca, V. and I. C. Popescu (2002). "Kinetic analysis of horseradish peroxidase "wiring" in redox polyelectrolyte-peroxidase multilayer assemblies." Electrochemistry Communications **4**(11): 904-911.

Salimi, A., E. Sharifi, et al. (2007). "Direct electrochemistry and electrocatalytic activity of catalase immobilized onto electrodeposited nano-scale islands of nickel oxide." Biophysical Chemistry **125**(2-3): 540-548.

Samuni, U., D. Dantsker, et al. (2002). "Spectroscopically and kinetically distinct conformational populations of sol-gel-encapsulated carbonmonoxy myoglobin - A comparison with hemoglobin." Journal of Biological Chemistry **277**(28): 25783-25790.

Sandifer, J. R. and J. J. Voycheck (1999). "A review of biosensor and industrial applications of pH-ISFETs and an evaluation of Honeywell's "DuraFET"." Mikrochimica Acta **131**(1-2): 91-98.

Sangribsub, S., P. Tangboriboonrat, et al. (2005). "Hydrophobization of multilayered film containing layer-by-layer assembled nanoparticle by Nafion adsorption." Polymer Bulletin **53**(5-6): 425-434.

Sara, M. and U. B. Sleytr (1987). "Molecular-Sieving through S-Layers of Bacillus-Stearothermophilus Strains." Journal of Bacteriology **169**(9): 4092-4098.

Sara, M. and U. B. Sleytr (1996). "Biotechnology and biomimetic with crystalline bacterial cell surface layers (S-layers)." Micron **27**(2): 141-156.

Sariciftci, N. S. and H. Kuzmany (1987). "Optical Spectroscopy and Resonance Raman-Scattering of Polyaniline During Electrochemical Oxidation and Reduction." Synthetic Metals **21**(2): 157-162.

Scheller, F. W., U. Wollenberger, et al. (2001). "Research and development in biosensors." Current Opinion in Biotechnology **12**(1): 35-40.

Scheller, W., W. Jin, et al. (1999). "Cytochrome C based superoxide sensor for in vivo application." Electroanalysis **11**(10-11): 703-706.

Schlenoff, J. B., S. T. Dubas, et al. (2000). "Sprayed polyelectrolyte multilayers." Langmuir **16**(26): 9968-9969.

Schmitt, J., T. Grunewald, et al. (1993). "Internal Structure of Layer-by-Layer Adsorbed Polyelectrolyte Films - a Neutron and X-Ray Reflectivity Study." Macromolecules **26**(25): 7058-7063.

Schultze-Lam, S., G. Harauz, et al. (1992). "Participation of a Cyanobacterial-S Layer in Fine-Grain Mineral Formation." Journal of Bacteriology **174**(24): 7971-7981.

Schuster, B., P. C. Gufler, et al. (2004). "S-layer proteins as supporting scaffoldings for functional lipid membranes." Ieee Transactions on Nanobioscience **3**(1): 16-21.

Schuster, B., D. Pum, et al. (1998). "Self-assembled alpha-hemolysin pores in an S-layer-supported lipid bilayer." Biochimica Et Biophysica Acta-Biomembranes **1370**(2): 280-288.

Schuster, B., D. Pum, et al. (2001). "S-layer ultrafiltration membranes: A new support for stabilizing functionalized lipid membranes." Langmuir **17**(2): 499-503.

Schuster, B., D. Pum, et al. (2006). "S-layer proteins as key components of a versatile molecular construction kit for biomedical nanotechnology." Mini-Reviews in Medicinal Chemistry **6**(8): 909-920.

Scott, R. A. and A. G. Mauk (1995). Cytochrome c: A multidiscelinary approach. Sausalito, CA, University science books.

Shain, I. and R. S. Nicholson (1981). "Citation Classic - Theory of Stationary Electrode Polarography - Single Scan and Cyclic Methods Applied to Reversible, Irreversible, and Kinetic Systems." Current Contents/Physical Chemical & Earth Sciences(6): 18-18.

Shen, H., J. E. Mark, et al. (1997). "Blocking behavior of self-assembled monolayers on gold electrodes." Journal of Solid State Electrochemistry **1**(2): 148-154.

Shenton, W., D. Pum, et al. (1997). "Synthesis of cadmium sulphide superlattices using self-assembled bacterial S-layers." Nature **389**(6651): 585-587.

Shi, H. B., Z. Song, et al. (2005). "Effects of the type of polycation in the coating films prepared by a layer-by-layer deposition technique on the properties of amperometric choline sensors." Sensors and Actuators B-Chemical **109**(2): 341-347.

Shi, L. X., Y. X. Lu, et al. (2003). "Site-selective lateral multilayer assembly of bienzyme with polyelectrolyte on ITO electrode based on electric field-induced directly layer-by-layer deposition." Biomacromolecules **4**(5): 1161-1167.

Shimizu, A., J. H. Kwon, et al. (1999). "Myrothecium verrucaria bilirubin oxidase and its mutants for potential copper ligands." Biochemistry **38**(10): 3034-3042.

Shiratori, S. S. and M. F. Rubner (2000). "pH-dependent thickness behavior of sequentially adsorbed layers of weak polyelectrolytes." Macromolecules **33**(11): 4213-4219.

Shleev, S., A. El Kasmi, et al. (2004). "Direct heterogeneous electron transfer reactions of bilirubin oxidase at a spectrographic graphite electrode." Electrochemistry Communications **6**(9): 934-939.

Shleev, S., J. Tkac, et al. (2005). "Direct electron transfer between copper-containing proteins and electrodes." Biosensors & Bioelectronics **20**(12): 2517-2554.

Shoham, B., Y. Migron, et al. (1995). "A Bilirubin Biosensor Based on a Multilayer Network Enzyme Electrode." Biosensors & Bioelectronics **10**(3-4): 341-352.

Shulga, A. A., M. Koudelkahep, et al. (1995). "The Effect of Divalent Metal-Ions on the Performance of a Glucose-Sensitive Enfet Using Potassium Ferricyanide as an Oxidizing Substrate." Sensors and Actuators B-Chemical **27**(1-3): 432-435.

Simonian, A. L., A. Revzin, et al. (2002). "Characterization of oxidoreductase-redox polymer electrostatic film assembly on gold by surface plasmon resonance spectroscopy and Fourier transform infrared-external reflection spectroscopy." Analytica Chimica Acta **466**(2): 201-212.

Sirkar, K., A. Revzin, et al. (2000). "Glucose and lactate biosensors based on redox polymer/oxidoreductase nanocomposite thin films." Analytical Chemistry **72**(13): 2930-2936.

Skladal, P. (2003). "Piezoelectric quartz crystal sensors applied for bioanalytical assays and characterization of affinity interactions." Journal of the Brazilian Chemical Society **14**(4): 491-502.

Sleytr, U. B. (2004). Self-assembly protein systems. Biopolymers. A. Steinbuchel, WILEY-VCH.

Sleytr, U. B., H. Bayley, et al. (1997). "Applications of S-layers." Fems Microbiology Reviews **20**(1-2): 151-175.

Sleytr, U. B. and T. J. Beveridge (1999). "Bacterial S-layers." Trends in Microbiology **7**(6): 253-260.

Sleytr, U. B., E. M. Egelseer, et al. (2007). "S-Layers as a basic building block in a molecular construction kit." Febs Journal **274**(2): 323-334.

Sleytr, U. B. and P. Messner (1983). "Crystalline Surface-Layers on Bacteria." Annual Review of Microbiology **37**: 311-339.

Soeno, T., K. Inokuchi, et al. (2004). "Ultra-water-repellent surface: fabrication of complicated structure Of SiO2 nanoparticles by electrostatic self-assembled films." Applied Surface Science **237**(1-4): 543-547.

Song, S., R. A. Clark, et al. (1993). "Characterization of Cytochrome-C Alkanethiolate Structures Prepared by Self-Assembly on Gold." Journal of Physical Chemistry **97**(24): 6564-6572.

Song, Y. H., L. Wang, et al. (2006). "A novel hydrogen peroxide sensor based on horseradish peroxidase immobilized in DNA films on a gold electrode." Sensors and Actuators B-Chemical **114**(2): 1001-1006.

Spink, C. and I. Wadso (1976). "Calorimetry as an analytical tool in biochemistry and biology." Methods Biochem Anal. **23**: 1–159.

Steitz, R., V. Leiner, et al. (2002). "Temperature-induced changes in polyelectrolyte films at the solid-liquid interface." Applied Physics a-Materials Science & Processing **74**: S519-S521.

Stellwagen, E. and R. D. Cass (1975). "Complexation of Iron Hexacyanides by Cytochrome-C - Evidence for Electron Exchange at Exposed Heme Edge." Journal of Biological Chemistry **250**(6): 2095-2098.

Stellwagen, E., R. Rysavy, et al. (1972). "Conformation of Horse Heart Apocytochrome-C." Journal of Biological Chemistry **247**(24): 8074-8077.

Sullivan, E. P., J. T. Hazzard, et al. (1993). "Electron-Transfer in Sulfite Oxidase - Effects of Ph and Anions on Transient Kinetics." Biochemistry **32**(46): 12465-12470.

Sun, C. Q., W. J. Li, et al. (1999). "Fabrication of multilayer films containing horseradish peroxidase based on electrostatic interaction and their application as a hydrogen peroxide sensor." Electrochimica Acta **44**(19): 3401-3407.

Suye, S., H. T. Zheng, et al. (2005). "Assembly of alternating polymerized mediator, polymerized coenzyme, and enzyme modified electrode by layer-by-layer adsorption technique." Sensors and Actuators B-Chemical **108**(1-2): 671-675.

Suzuki, I., K. Murakami, et al. (1998). "Preparation and molecular recognition of cyclodextrin monolayers with different cavity size on a gold wire electrode." Materials Science & Engineering C-Biomimetic Materials Sensors and Systems **6**(1): 19-25.

Tang, D. P., R. Yuan, et al. (2005). "New amperometric and potentiometric immunosensors based on gold nanoparticles/tris(2,2 '-bipyridyl)cobalt(III) multilayer films for hepatitis B surface antigen determinations." Biosensors & Bioelectronics **21**(4): 539-548.

Taniguchi, I., T. Murakami, et al. (1982). "Cyclic Voltammetric Behavior of Horse Heart Cytochrome-C at a Platinum-Electrode in the Presence of 4,4'-Bipyridine." Journal of Electroanalytical Chemistry **131**(JAN): 397-401.

Taniguchi, I., K. Toyosawa, et al. (1982). "Reversible Electrochemical Reduction and Oxidation of Cytochrome-C at a Bis(4-Pyridyl) Disulfide-Modified Gold Electrode." Journal of the Chemical Society-Chemical Communications(18): 1032-1033.

Taniguchi, I., K. Toyosawa, et al. (1982). "Voltammetric Response of Horse Heart Cytochrome-C at a Gold Electrode in the Presence of Sulfur Bridged Bipyridines." Journal of Electroanalytical Chemistry **140**(1): 187-193.

Tarabia, M., H. Hong, et al. (1998). "Neutron and x-ray reflectivity studies of self-assembled heterostructures based on conjugated polymers." Journal of Applied Physics **83**(2): 725-732.

Tarlov, M. J. and E. F. Bowden (1991). "Electron-Transfer Reaction of Cytochrome-C Adsorbed on Carboxylic-Acid Terminated Alkanethiol Monolayer Electrodes." Journal of the American Chemical Society **113**(5): 1847-1849.

Tarr, H. L. A. (1966). "Post-Mortem Changes in Glycogen Nucleotides Sugar Phosphates and Sugars in Fish Muscles - a Review." Journal of Food Science **31**(6): 846-&.

Temple, C. A., T. N. Graf, et al. (2000). "Optimization of expression of human sulfite oxidase and its molybdenum domain." Archives of Biochemistry and Biophysics **383**(2): 281-287.

Thevenot, D. R., K. Toth, et al. (2001). "Electrochemical biosensors: recommended definitions and classification." Biosensors & Bioelectronics **16**(1-2): 121-131.

Toca-Herrera, J. L., R. Krastev, et al. (2005). "Recrystallization of bacterial S-layers on flat polyelectrolyte surfaces and hollow polyelectrolyte capsutes." Small **1**(3): 339-348.

Topoglidis, E., C. J. Campbell, et al. (2001). "Factors that affect protein adsorption on nanostructured titania films. A novel spectroelectrochemical application to sensing." Langmuir **17**(25): 7899-7906.

Trau, D. and R. Renneberg (2003). "Encapsulation of glucose oxidase microparticles within a nanoscale layer-by-layer film: immobilization and biosensor applications." Biosensors & Bioelectronics **18**(12): 1491-1499.

Tsujimura, S., K. Kano, et al. (2005). "Bilirubin oxidase in multiple layers catalyzes four-electron reduction of dioxygen to water without redox mediators." Journal of Electroanalytical Chemistry **576**(1): 113-120.

Tsujimura, S., M. Kawaharada, et al. (2003). "Mediated bioelectrocatalytic O-2 reduction to water at highly positive electrode potentials near neutral pH." Electrochemistry Communications **5**(2): 138-141.

Tsujimura, S., T. Nakagawa, et al. (2004). "Kinetic study of direct bioelectrocatalysis of dioxygen reduction with bilirubin oxidase at carbon electrodes." Electrochemistry **72**(6): 437-439.

Tsujimura, S., A. Wadano, et al. (2001). "Photosynthetic bioelectrochemical cell utilizing cyanobacteria and water-generating oxidase." Enzyme and Microbial Technology **29**(4-5): 225-231.

Ulman, A. (1996). "Formation and structure of self-assembled monolayers." Chemical Reviews **96**(4): 1533-1554.

Updike, S. J. and G. P. Hicks (1967). "Enzyme Electrode." Nature **214**(5092): 986-&.

Updike, S. J. and G. P. Hicks (1967). "Reagentless Substrate Analysis with Immobilized Enzymes." Science **158**(3798): 270-&.

Vadillo-Rodriguez, V., H. J. Busscher, et al. (2005). "Role of lactobacillus cell surface hydrophobicity as probed by AFM in adhesion to surfaces at low and high ionic strength." Colloids and Surfaces B-Biointerfaces **41**(1): 33-41.

Valette, G. and A. Hamelin (1973). "Structure and Properties of Electrochemical Double Film on Interphase of Aqueous Sodium-Fluoride Solutions and Silver." Journal of Electroanalytical Chemistry **45**(2): 301-319.

Valincius, G. (1998). "Elastic electrocapillary properties of polycrystalline gold." Langmuir **14**(21): 6307-6319.

Venugopal, V. (2002). "Biosensors in fish production and quality control." Biosens Bioelectron **17**(3): 147-57.

Wagner, P., M. Hegner, et al. (1995). "Formation and in-Situ Modification of Monolayers Chemisorbed on Ultraflat Template-Stripped Gold Surfaces." Langmuir **11**(10): 3867-3875.

Wanekaya, A. K., W. Chen, et al. (2006). "Nanowire-based electrochemical biosensors." Electroanalysis **18**(6): 533-550.

Wang, B. Q. and J. F. Rusling (2003). "Voltammetric sensor for chemical toxicity using [Ru(bpy)(2)poly(4-vinylpyridine)(10)Cl)](+) as catalyst in ultrathin films. DNA

damage from methylating agents and an enzyme-generated epoxide." Analytical Chemistry **75**(16): 4229-4235.
Wang, F. C., R. Yuan, et al. (2007). "Probing traces of hydrogen peroxide by use of a biosensor based on mediator-free DNA and horseradish peroxidase immobilized on silver nanoparticles." Analytical and Bioanalytical Chemistry **387**(2): 709-717.
Wang, G., J. J. Xu, et al. (2002). "Interfacing cytochrome c to electrodes with a DNA - carbon nanotube composite film." Electrochemistry Communications **4**(6): 506-509.
Wang, J. X., M. X. Li, et al. (2002). "Investigation of the electrocatalytic behavior of single-wall carbon nanotube films on an Au electrode." Microchemical Journal **73**(3): 325-333.
Wang, L. and Z. B. Yuan (2004). "Direct electrochemistry of xanthine oxidase at a gold electrode modified with single-wall carbon nanotubes." Analytical Sciences **20**(4): 635-638.
Wang, S. G., Q. Zhang, et al. (2003). "A novel multi-walled carbon nanotube-based biosensor for glucose detection." Biochemical and Biophysical Research Communications **311**(3): 572-576.
Watanabe, E., Y. Tamada, et al. (2005). "Development of quality evaluation sensor for fish freshness control based on KI value." Biosens Bioelectron **21**(3): 534-8.
Waud, W. R. and K. V. Rajagopalan (1976). "Mechanism of Conversion of Rat-Liver Xanthine Dehydrogenase from an Nad+-Dependent Form (Type D) to an O-2-Dependent Form (Type O)." Archives of Biochemistry and Biophysics **172**(2): 365-379.
We, X., M. G. Zhang, et al. (2003). "Coupling the lactate oxidase to electrodes by ionotropic gelation of biopolymer." Analytical Chemistry **75**(9): 2060-2064.
Wei, J. J., H. Y. Liu, et al. (2002). "Direct wiring of cytochrome c's heme unit to an electrode: Electrochemical studies." Journal of the American Chemical Society **124**(32): 9591-9599.
Wei, J. J., H. Y. Liu, et al. (2004). "Probing electron tunneling pathways: Electrochemical study of rat heart cytochrome c and its mutant on pyridine-terminated SAMs." Journal of Physical Chemistry B **108**(43): 16912-16917.
Weidinger, I. M., D. H. Murgida, et al. (2006). "Redox processes of cytochrome c immobilized on solid supported polyelectrolyte multilayers." Journal of Physical Chemistry B **110**(1): 522-529.
Weigel, M. C., E. Tritscher, et al. (2007). "Direct electrochemical conversion of bilirubin oxidase at carbon nanotube-modified glassy carbon electrodes." Electrochemistry Communications **9**(4): 689-693.
Wetzer, B., A. Pfandler, et al. (1998). "S-layer reconstitution at phospholipid monolayers." Langmuir **14**(24): 6899-6906.
Willner, I. (2002). "Biomaterials for sensors, fuel cells, and circuitry." Science **298**(5602): 2407-2408.
Willner, I., E. Katz, et al. (1992). "Mediated Electron-Transfer in Glutathione-Reductase Organized in Self-Assembled Monolayers on Au Electrodes." Journal of the American Chemical Society **114**(27): 10965-10966.
Willner, I., M. Liondagan, et al. (1995). "Bioelectrocatalyzed Amperometric Transduction of Recorded Optical Signals Using Monolayer-Modified Au-Electrodes." Journal of the American Chemical Society **117**(24): 6581-6592.

Wink, T., S. J. vanZuilen, et al. (1997). "Self-assembled monolayers for biosensors." Analyst **122**(4): R43-R50.

Wolfbeis, O. S. (2002). "Fiber-optic chemical sensors and biosensors." Analytical Chemistry **74**(12): 2663-2677.

Xie, B., K. Ramanathan, et al. (2000). "Mini/micro thermal biosensors and other related devices for biochemical/clinical analysis and monitoring." Trac-Trends in Analytical Chemistry **19**(5): 340-349.

Xie, Y. W. and S. J. Dong (1992). "Effect of Ph on the Electron-Transfer of Cytochrome-C on a Gold Electrode Modified with Bis(4-Pyridyl)Disulphide." Bioelectrochemistry and Bioenergetics **29**(1): 71-79.

Xu, F., W. S. Shin, et al. (1996). "A study of a series of recombinant fungal laccases and bilirubin oxidase that exhibit significant differences in redox potential, substrate specificity, and stability." Biochimica Et Biophysica Acta-Protein Structure and Molecular Enzymology **1292**(2): 303-311.

Xu, F., L. Wang, et al. (2002). "Amperometric determination of glutathione and cysteine on a Pd-IrO2 modified electrode with high performance liquid chromatography in rat brain microdialysate." Analytical and Bioanalytical Chemistry **372**(7-8): 791-794.

Xu, J. J., W. Zhao, et al. (2005). "A sensitive biosensor for lactate based on layer-by-layer assembling MnO2 nanoparticles and lactate oxidase on ion-sensitive field-effect transistors." Chemical Communications(6): 792-794.

Xu, Y. J., Q. J. Xie, et al. (1995). "Simultaneous Uv-Visible Spectroelectrochemical and Quartz-Crystal Microgravimetric Measurements During the Growth of Poly(1-Naphthylamine) Film." Journal of Electroanalytical Chemistry **389**(1-2): 85-90.

Yang, M. H., Y. Yang, et al. (2006). "Layer-by-layer self-assembled multilayer films of carbon nanotubes and platinum nanoparticles with polyelectrolyte for the fabrication of biosensors." Biomaterials **27**(2): 246-255.

Yao, T. (1993). "Enzyme Electrode for the Successive Detection of Hypoxanthine and Inosine." Analytica Chimica Acta **281**(2): 323-326.

Yoo, D., S. S. Shiratori, et al. (1998). "Controlling bilayer composition and surface wettability of sequentially adsorbed multilayers of weak polyelectrolytes." Macromolecules **31**(13): 4309-4318.

Yoon, H. C., M. Y. Hong, et al. (2000). "Functionalization of a poly(amidoamine) dendrimer with ferrocenyls and its application to the construction of a reagentless enzyme electrode." Analytical Chemistry **72**(18): 4420-4427.

Yu, A. M. and F. Caruso (2003). "Thin films of polyelectrolyte-encapsulated catalase microcrystals for biosensing." Analytical Chemistry **75**(13): 3031-3037.

Zhang, S. X., W. W. Yang, et al. (2004). "Multilayered construction of glucose oxidase and poly(allylamine)ferrocene on gold electrodes by means of layer-by-layer covalent attachment." Sensors and Actuators B-Chemical **101**(3): 387-393.

Zhang, X., F. Shi, et al. (2004). "Polyelectrolyte multilayer as matrix for electrochemical deposition of gold clusters: toward super-hydrophobic surface." Journal of the American Chemical Society **126**(10): 3064-3065.

Zhang, Y., P. L. He, et al. (2004). "Horseradish peroxidase immobilized in TiO2 nanoparticle films on pyrolytic graphite electrodes: direct electrochemistry and bioelectrocatalysis." Electrochimica Acta **49**(12): 1981-1988.

Zhao, J. G., R. W. Henkens, et al. (1992). "Direct Electron-Transfer at Horseradish-Peroxidase Colloidal Gold Modified Electrodes." Journal of Electroanalytical Chemistry **327**(1-2): 109-119.

Zhao, N., F. Shi, et al. (2005). "Combining layer-by-layer assembly with electrodeposition of silver aggregates for fabricating superhydrophobic surfaces." Langmuir **21**(10): 4713-4716.

Zhao, W., J. J. Xu, et al. (2006). "Electrochemical biosensors based on layer-by-layer assemblies." Electroanalysis **18**(18): 1737-1748.

Zheng, H., H. Okada, et al. (2004). "Layer-by-layer assembly of enzymes and polymerized mediator on electrode surface by electrostatic adsorption." Science and Technology of Advanced Materials **5**(3): 371-376.

Zhou, H., Y. Xu, et al. (2006). "Electrochemistry of xanthine oxidase and its interaction with nitric oxide." Analytical Sciences **22**(2): 337-340.

Zhou, Y. L., N. F. Hu, et al. (2002). "Heme protein-clay films: Direct electrochemistry and electrochemical catalysis." Langmuir **18**(1): 211-219.

Zhou, Y. L., Z. Li, et al. (2002). "Layer-by-layer assembly of ultrathin films of hemoglobin and clay nanoparticles with electrochemical and catalytic activity." Langmuir **18**(22): 8573-8579.

Zilbermann, I., A. Lin, et al. (2004). "Electrostatically arranged cytochrome c-fullerene photoelectrodes." Chemical Communications(1): 96-97.

Zoppellaro, G., N. Sakurai, et al. (2004). "The reversible change in the redox state of type I Cu in Myrothecium verrucaria bilirubin oxidase depending on pH." Biosci Biotechnol Biochem **68**(9): 1998-2000.